NOAA Technical Report NOS CS 40

NOS COOK INLET OPERATIONAL FORECAST SYSTEM: MODEL DEVELOPMENT AND HINDCAST SKILL ASSESSMENT

Silver Spring, Maryland
September 2020

noaa National Oceanic and Atmospheric Administration

U.S. DEPARTMENT OF COMMERCE
National Ocean Service
Coast Survey Development Laboratory

Office of Coast Survey
National Ocean Service
National Oceanic and Atmospheric Administration
U.S. Department of Commerce

The Office of Coast Survey (OCS) is the Nation's only official chartmaker. As the oldest United States scientific organization, dating from 1807, this office has a long history. Today it promotes safe navigation by managing the National Oceanic and Atmospheric Administration's (NOAA) nautical chart and oceanographic data collection and information programs.

There are four components of OCS:

The Coast Survey Development Laboratory develops new and efficient techniques to accomplish Coast Survey missions and to produce new and improved products and services for the maritime community and other coastal users.

The Marine Chart Division acquires marine navigational data to construct and maintain nautical charts, Coast Pilots, and related marine products for the United States.

The Hydrographic Surveys Division directs programs for ship and shore-based hydrographic survey units and conducts general hydrographic survey operations.

The Navigational Services Division is the focal point for Coast Survey customer service activities, concentrating predominately on charting issues, fast-response hydrographic surveys, and Coast Pilot updates.

NOAA Technical Report NOS CS 40

NOS COOK INLET OPERATIONAL FORECAST SYSTEM: MODEL DEVELOPMENT AND HINDCAST SKILL ASSESSMENT

Lei Shi[1], Lyon Lanerolle[1,2], Yi Chen[1,2], Degui Cao[3], Richard Patchen[1], Aijun Zhang[3], and Edward P. Myers[1]

1 Coast Survey Development Laboratory, National Oceanic and Atmospheric Administration, Silver Spring, MD
2 Earth Resources Technology, Laurel, MD
3 Center for Operational Oceanographic Products and Services, National Oceanic and Atmospheric Administration, Silver Spring, MD

Corresponding Author: Lei Shi, 1315 East West Highway, Silver Spring, MD 20910; email: L.Shi@noaa.gov; tel: 240-847-8259

September 2020

noaa National Oceanic and Atmospheric Administration

U. S. DEPARTMENT OF COMMERCE
Wilbur Louis Ross Jr.
Secretary

National Oceanic and Atmospheric Administration
Dr. Neil Jacobs
Acting Under Secretary

National Ocean Service
Nicole LeBoeuf,
Acting Assistant Administrator

Office of Coast Survey
Capt. Richard Brennan
Acting Director

Coast Survey Development Laboratory
Dr. Shachak Pe'eri
Division Chief

NOTICE

Mention of a commercial company or product does not constitute an endorsement by NOAA. Use for publicity or advertising purposes of information from this publication concerning proprietary products or the tests of such products is not authorized.

TABLE OF CONTENTS

LIST OF FIGURES

LIST OF TABLES

EXECUTIVE SUMMARY

The National Ocean Service (NOS) of the National Oceanic and Atmospheric Administration (NOAA) has developed a three-dimensional hydrodynamic ocean model-based Cook Inlet Operational Forecast System (CIOFS) for Cook Inlet region of Alaska. The primary purpose of this model is to provide navigational mariners with water surface elevation (water level) and current forecast guidance, but in addition, it also generates temperature and salinity predictions which could be used to support oil spill, marine environment, ecological and ecosystem forecasting in the region.

CIOFS is based on Rutgers University's Regional Ocean Modeling System (ROMS) numerical ocean model. The model domain covers all of Cook Inlet and the waters leading to Cook Inlet around the Kodiak Archipelago, including Shelikof Strait to the south, and Stevenson Entrance, Kennedy Entrance and Chugach Passage to the southeast.

Three numerical simulations have been performed based on the availability of observed data sets. One tidal only simulation and two hindcast simulations were conducted. Ten tidal constituents (K_1, O_1, P_1, Q_1, M_2, S_2, N_2, K_2, M_4, and M_6) are used to force the tides and tidal currents in the CIOFS. Of two hindcast simulations, the first hindcast simulation (Hindcast 1) was from 1/1/2012 to 9/15/2012, which coincided with summer 2012 current meter deployments in Cook Inlet. The second hindcast simulation (Hindcast 2) lasted two years from 8/15/2013 to 9/15/2015. The skill assessments based on these simulations and corresponding observations were performed. The water level prediction performed very well for both hindcasts. Central Frequency (CF) was more than 95% from all water level stations. The major finding of the water level skill assessment is that the RMSE increased towards the upper Cook Inlet (Anchorage) where it is shallow, muddy, and tidal range can be 8-9 meters high.

For temperature skill assessment, the CF was usually more than 98%, with the exception of Anchorage where CF was 88.3% in Hindcast 2. In the upper Cook Inlet (Anchorage), the model temperature, especially during the summer, usually had a warm bias. With gradual improvement of weather models, the surface forcing bias should be able to be reduced along with improvement of the hydrodynamic model results.

For current skill assessment, the current direction was simulated well. At 8 out of 9 current observation locations, CF of current direction was above 90%. At one station near south Fire Island, CF of current direction was 87.0%. For current speed, 6 out of 9 stations had a CF value above 90%. Three current stations had a CF of current speed less than 90%. These three stations are Southwest of Pt. Pogishi, Point Possession, and North Fire Island. The corresponding CF values were 74.3%, 86.4%, and 65.2% respectively.

In summary, the CIOFS development and performance verification have been completed. NOS has implemented the hindcast setup in the NOS standard HPC-COMF environment. CIOFS has undergone pre-operational test runs on the National Centers for Environmental Prediction (NCEP) high-performance computer systems. The system has been in full operation since July, 2019.

1. INTRODUCTION

The Cook Inlet region of Alaska (Figure 1) is heavily trafficked by shipping and contains the major ports of Homer, Nikiski and Anchorage. Ships enter Cook Inlet via the Shelikof Strait to the South and the Gulf of Alaska (Stevenson Entrance, Kennedy Entrance and Chugach Passage) to the Southeast and travel upwards towards these ports. NOAA's National Ocean Service (NOS) has developed a hydrodynamic ocean model-based Operational Forecast System (OFS) for this geographic region to provide guidance to marine navigators. This report describes the development, calibration and skill assessment of such a hydrodynamic model,named Cook Inlet Operational Forecast System (CIOFS). The primary purpose of CIOFS is to provide navigational mariners with water surface elevation (water level) and current predictions, but in addition, it also generates temperature and salinity predictions which could be used to support ecological and ecosystem forecasting in the region.

CIOFS is based on Rutgers University's Regional Ocean Modeling System (ROMS) numerical ocean model (Haidvogel et al., 2000; Shchepetkin and McWilliams, 2003, 2005; Warner et al., 2005). ROMS is a split-explicit model which computes on structured, orthogonal curvilinear grids in the horizontal and on terrain-following coordinates in the vertical. Additional details on the attributes of the model can be found on myroms.org (Shchepetkin and McWilliams, 2003, 2005; Warner et al., 2005) and the particular features of the model key to CIOFS will be elaborated further here. As CIOFS was partly designed as an inundation model with flooding and drying over the tidal cycle, the ROMS wetting-drying algorithm was employed and both bathymetry and topography are present in the model. ROMS has three options for specifying the bottom stress – quadratic, logarithmic and linear formulations. The logarithmic formulation generated the most accurate water level predictions (online communication in ROMS forum, myroms.org/forum/) and hence it was employed. A special algorithmic option in ROMS was employed to prevent the abrupt reversal of the sign of the bottom stress during the drying cycle, without which computations in wetting-drying cycles would be rendered numerically unstable (online communication in ROMS forum, myroms.org/forum/). ROMS has a suite of eddy-viscosity models which characterize vertical mixing in the water column and after testing several of these options, the Mellor-Yamada level-2.5 turbulence closure scheme (Mellor and Yamada, 1982) was found to be as effective as any of the others which is attributed to the well mixed nature of the water column due to the strong actions of the tides; furthermore, this algebraic model is computationally cheaper than using a General Length Scale (GLS) (Umlauf and Burchard, 2003) model which is inherently expensive as a result of having to solve additional partial differential equations for the turbulence variables (Warner et al., 2005). At the ocean surface, ROMS allows the wind stresses and the net heat flux to be specified in two ways: directly, using known fields, or indirectly, using the TOGA-COARE Bulk Flux formulation (Fairall et al., 1996; Fairall et al., 2003) which needs the wind velocity components, air temperature, relative humidity, air pressure, net shortwave radiation flux and downward longwave radiation flux. In CIOFS, the latter approach was adopted as sufficiently accurate surface stress and heat fluxes were not available and the model surface forcing was augmented by imposing atmospheric pressure onto sea surface to account for the effects of the air pressure on the water surface elevations. It is known in upper Cook Inlet that there is massive sediment transport and deposition especially during the spring time, and during the winter months, broken ice is present throughout Cook Inlet. However, in the current version of CIOFS, due to the

lack of reliable sediment and ice forecast capabilities in ROMS, sediment and ice dynamics are not included in the model. Due to computational time limits on supercomputing platforms, long simulations often need to be broken up into smaller segments; this was also the case with CIOFS, and the ROMS perfect restart algorithms were employed to carry out the full simulations in a seamless and continuous fashion.

The model domain was defined to include the whole of Cook Inlet (lower, middle and upper Cook Inlet) and also the adjacent waters of Kodiak Archipelago (Kodiak Shelikof Strait and western Gulf of Alaska) due to the ship traffic passing through it. This ensured that the ports of Homer, Nikiski and Anchorage were contained in the computational domain. Ship traffic enters Cook Inlet via the entrances from the Gulf of Alaska (Stevenson Entrance, Kennedy Entrance and Chugach Passage) too and hence a segment of the Gulf of Alaska was included. In upper Cook Inlet, both the Knik and Turnagain Arms were present so as to incorporate the shipping routes and the shallow tidal mudflats. Another reason for including the full Cook Inlet estuary including the tidal flood-drying regions (e.g. mudflats, etc.) and some topography was to ensure that the full volume of the domain was accounted for so as to ensure the hydrodynamic balance of fluid flow in shallow regions.

CIOFS was developed in two stages. In the first stage, the computational domain was truncated at the boundary between Cook Inlet and the Gulf of Alaska and at the entrance to Shelikof Strait from the open ocean (Lanerolle et al., 2012). The model consisted of a parent grid covering the full domain and two higher resolution nests – one for the Kachemak Bay region and the other for the upper Cook Inlet region both of which are significant for navigation (ports of Homer and Anchorage are encompassed in these nests). First the parent grid was run and using the predictions from that as boundary conditions, the nested grids were forced and run. Hence, the nesting was one-way only. Simulations with this setup showed that the discrepancies of the model predictions relative to observations in the water levels grew significantly when moving up the domain (towards Anchorage) and were "locked" and could not be diminished (or controlled) with the prescription of various bottom stress formulations or coefficient strengths. Furthermore, a single simulation involved running three separate computational domains which was triple the effort. Additionally, the model predictions from the nests were not a significant improvement over those from the parent grid. These shortcomings motivated the designing of a single grid for CIOFS which had similar grid resolutions as the nested grids in Kachemak Bay and upper Cook Inlet. In addition, the open boundary was extended farther out (beyond the outside of Kodiak Island) and the topography was extended up to 15 m elevation above Mean Sea Level (MSL), thus allowing the action of tidal flooding-drying to occur unimpeded and in a natural way. The extension of the open boundary and the topography enabled the water level model discrepancies to be controlled more effectively and generate significantly improved water level predictions. The single grid configuration also resulted in a simpler CIOFS set-up where only a single domain was necessary to be run as opposed to three separate domains as in the nested configuration. In this CIOFS technical report only the second stage development is represented. For first stage nested grid one-way coupling approach, the results can be referred to the Oceans '12 tidal kinetic energy paper (Lanerolle et al., 2012).

Three simulations were conducted using the single grid CIOFS configuration: a tidal simulation to evaluate the accuracy of the water level and current predictions and to calibrate the tides to achieve the most accurate model predictions; an 8-month summer 2012 synoptic hindcast simulation to

evaluate the model predicted water levels, currents, temperature and salinity against field survey observations; and a multi-year (25-month) synoptic hindcast simulation covering the August 2013 – September 2015 time period again to evaluate these model predicted variables and also examine the response of the model to the springtime river discharges, summertime tidal mudflat heating, and wintertime oceanic and atmospheric conditions (due to the lack of an ice module, etc.).

This report is organized as follows. Section 2 will provide information about model configuration, development and calibration of CIOFS. Section 3 gives details of the three simulations conducted; model results and skill assessment of the single grid CIOFS configuration against observed data will be discussed. In Section 4, a summary, set of conclusions and recommendations will be stated.

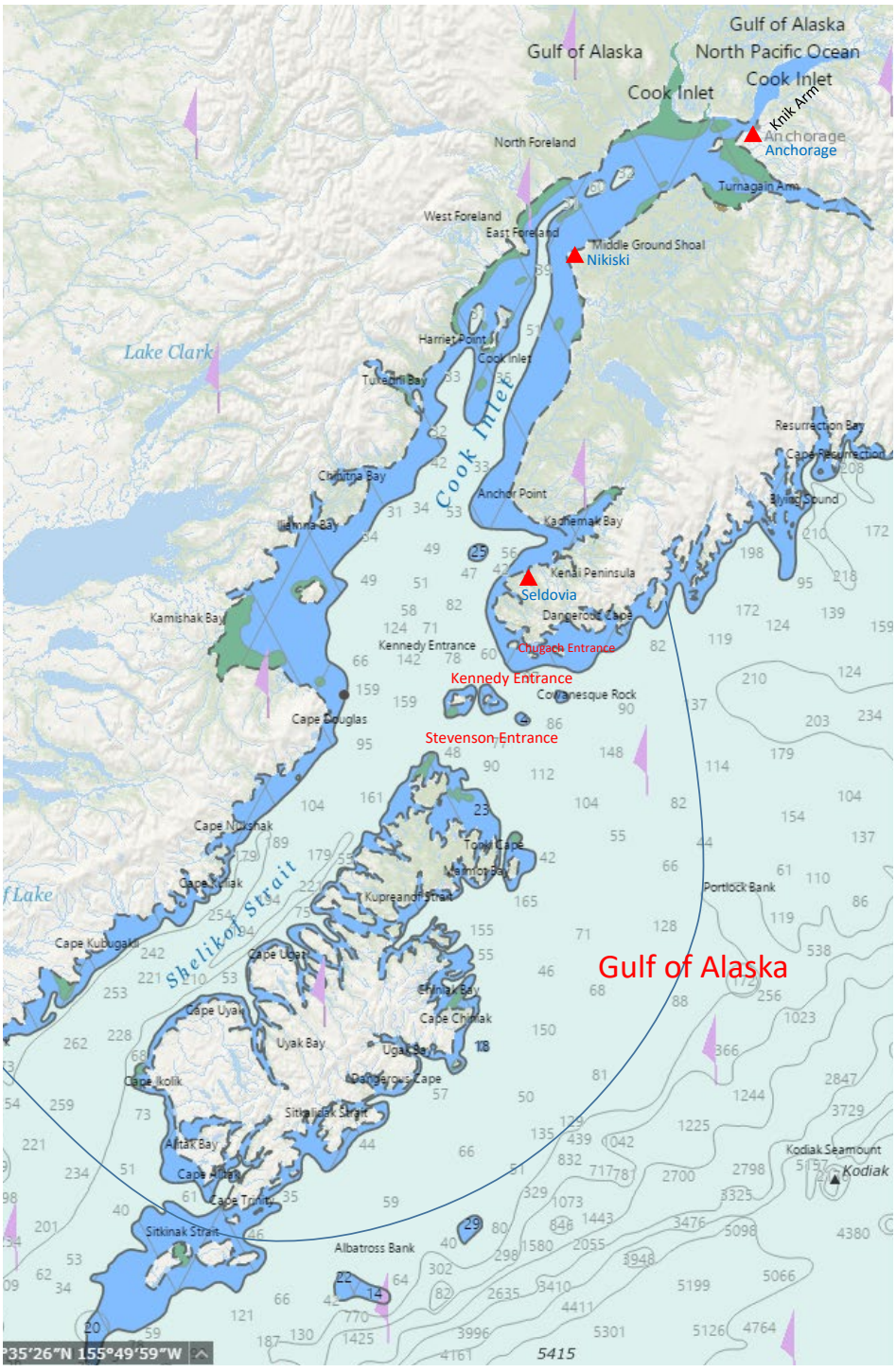

Figure 1. Cook Inlet Operational Forecast System (CIOFS) domain. The blue curve is the CIOFS open water boundary. There are three main long term water level stations (red triangles) in the domain: from north to south, Anchorage, Nikiski, and Seldovia. Black dashed line is the MHW shoreline, black solid line is 50 foot depth contour, and green patch is tidal flat between MLLW and MHW.

2. CIOFS MODEL CONFIGURATION

In this Section the CIOFS model development will be described by elaborating on its various components.

2.1 Model Domains and Curvilinear Mesh Grids

The model domain is shown in Figure 1. The domain covers the full Cook Inlet region (lower, middle and upper Cook Inlet) and extends to the north of Anchorage, AK. It also includes Knik Arm, Turnagain Arm in the upper Cook Inlet, Kachemak Bay in the middle Cook Inlet, the Shelikof Strait, Stevenson Entrance, Kennedy Entrance and Chugach Passage to the south which is important navigationally.

The model grid was of a structured, orthogonal quadrilateral type. The model grid was extended into the topography up to the 15 m contour above mean sea level. The adjustment was to ensure that the full flooding-drying zone was incorporated in the model so as to ensure that the true volume of the hydrodynamic basin would be accounted for. The single, high resolution grid was generated in seven individual pieces and pasted together (and orthogonalized) using Delft3D grid generator (Deltares, 2014). It is shown in Figure 2.

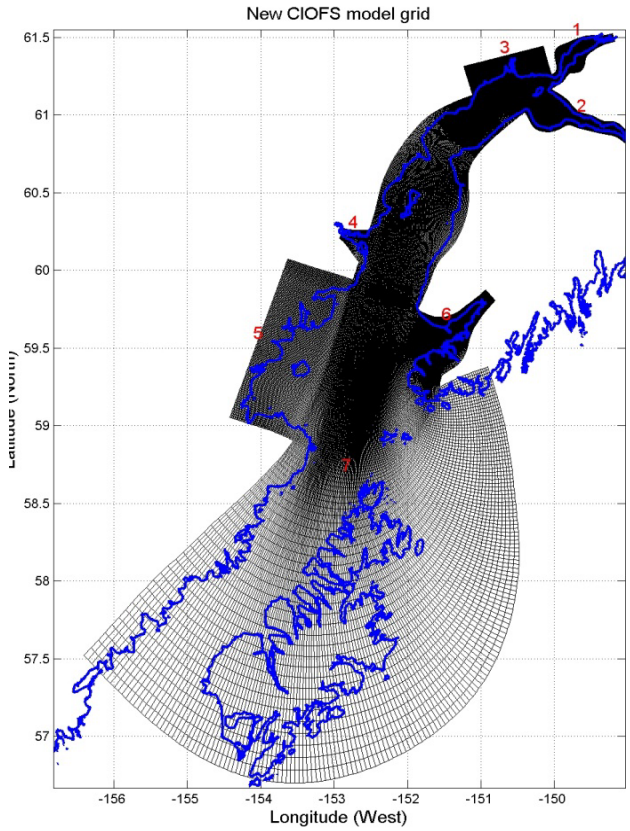

Figure 2. The single high resolution CIOFS grid and the individual grid segments. 1. Knik Arm, 2. Turnagain Arm, 3. Susitna River delta, 4. Tuxedni Bay (River), 5. Kamishak Bay, 6. Kachemak Bay, 7. Cook Inlet main stem, Shelikof Strait, Kodiak Archipelago, and entrances from Gulf of Alaska to Cook Inlet.

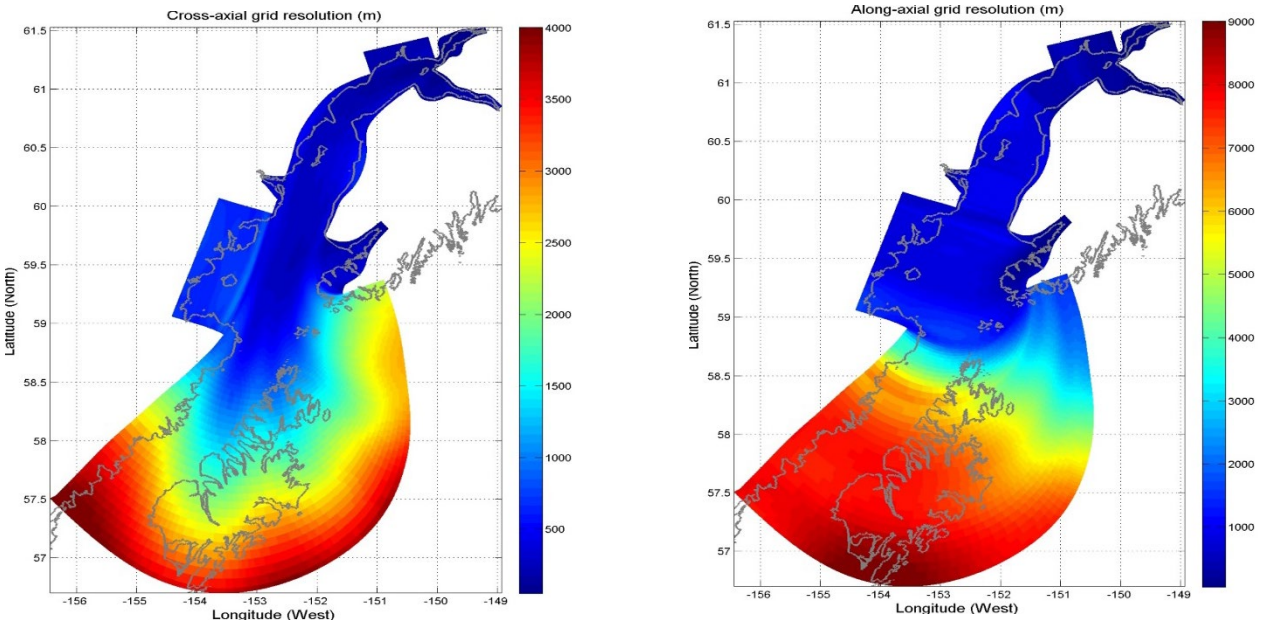

Figure 3. Cross-axial grid resolution and along-axial grid resolution of CIOFS curvilinear mesh grid.

Figure 3 shows the model grid resolutions in the cross-axial and the along-axial directions. It shows the refinement that has been added to the regions within Cook Inlet and in particular Kachemak Bay and upper Cook Inlet. The grid had 744 x 1024 grid points in the horizontal and 30 vertical terrain-following sigma grid levels were specified. The maximum horizontal spatial resolution is around 8000-9000 meters along the open boundary, and the minimum resolution is about 50 meters around upper Cook Inlet.

2.2 Bathymetry and Topography

Due to flooding and drying (i.e. wetting and drying), the model domains require both bathymetry and topography. As CIOFS is not built to simulate tsunamis, the topography is truncated at a 15m elevation above mean sea level.

The bathymetry-topography needs to be seamless without any discontinuities. It is generated by interpolation from a Digital Elevation Model (DEM) built by combining (i) bathymetric sounding data, (ii) shoreline data and (iii) land topography data in a seamless fashion. One of the challenges in developing the DEM is to account for the different vertical datums associated with (i), (ii) and (iii) in a consistent manner.

The bathymetric soundings used were from NOAA/National Ocean Service (NOS) surveys of the Shelikof Strait – Cook Inlet region covering the 1907-2004 and 2008-2009 time periods. The soundings have been quality controlled and the data files in Bathymetry Attributed Grid (BAG) format where first converted to ASCII format before being used. The native vertical datum of the bathymetry was Mean Lower Low Water (MLLW). Soundings were interpolated to the CIOFS model grids in a supersession sequence beginning with the year 2009 and ending with 1907. The

interpolation covered the wet-point grid delineated by the MLLW shoreline. The interpolation method was an inverse-square algorithm with the radius of influence being determined by the encompassing grid size.

The above interpolated bathymetry, MLLW and Mean High Water (MHW) shorelines are used to fill the area between MLLW and MHW with bathymetric values by adopting a MLLW reference frame where the MLLW shoreline is assumed to have a bathymetric value of zero as illustrated in Figure 4. The filling is carried out using a bilinear interpolation algorithm.

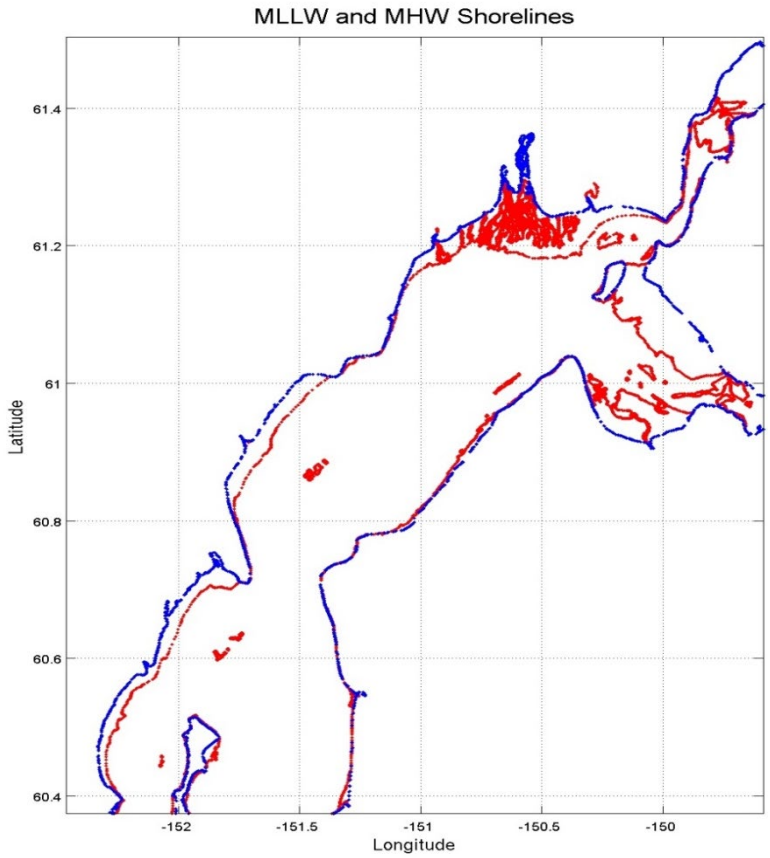

Figure 4. MHW (blue) and MLLW (red) shorelines for upper and middle Cook Inlet.

The topography above the MHW shoreline is filled by interpolating gridded/digitized land topography from the US Geological Survey (USGS) and from a DEM of Kachemak Bay produced by NOAA/National Centers for Environmental Information (NCEI). The USGS digitized data has spatial resolutions of 1/9", 1/3", 1" and 2" and the NCEI DEM was of a 1/3" spatial resolution. When interpolating the topography, the finest resolution was employed first and thereafter, progressively coarser resolutions were used. The topography was assumed to be on a MHW vertical datum and the interpolation was carried out using the same algorithm as for the bathymetry (for consistency).

The bathymetric soundings are on a MLLW datum, the two shorelines are on a MLLW and a MHW datum and the topography is on a MHW datum. When carrying out the numerical interpolations, the interpolating fields must all be on the same datum. Furthermore, the final

bathymetry-topography needs to be on a Mean Sea Level (MSL) datum as the NOS OFSs are run on this datum and hence, the CIOFS model grid's bathymetry-topography also needs to be on a MSL datum. The vertical datum transformational fields (to go from one datum to another) were formed by interpolating the discrete values derived and published by NOS/Center for Operational Oceanographic Products and Services (CO-OPS) to cover the full Shelikof Strait – Cook Inlet domain. In addition to interpolation, some extrapolation was also required and this process in turn required the specification of extended pseudo-points of data. The interpolated bathymetry-topography was clipped at 15m above MSL.

Figure 5 shows the bathymetry-topography on the single grid with zoom-ins for Cook Inlet, upper Cook Inlet and Kachemak Bay. The plots show the deep, narrow channels present in both upper Cook Inlet and Kachemak Bay and also the bathymetry-topography interface.

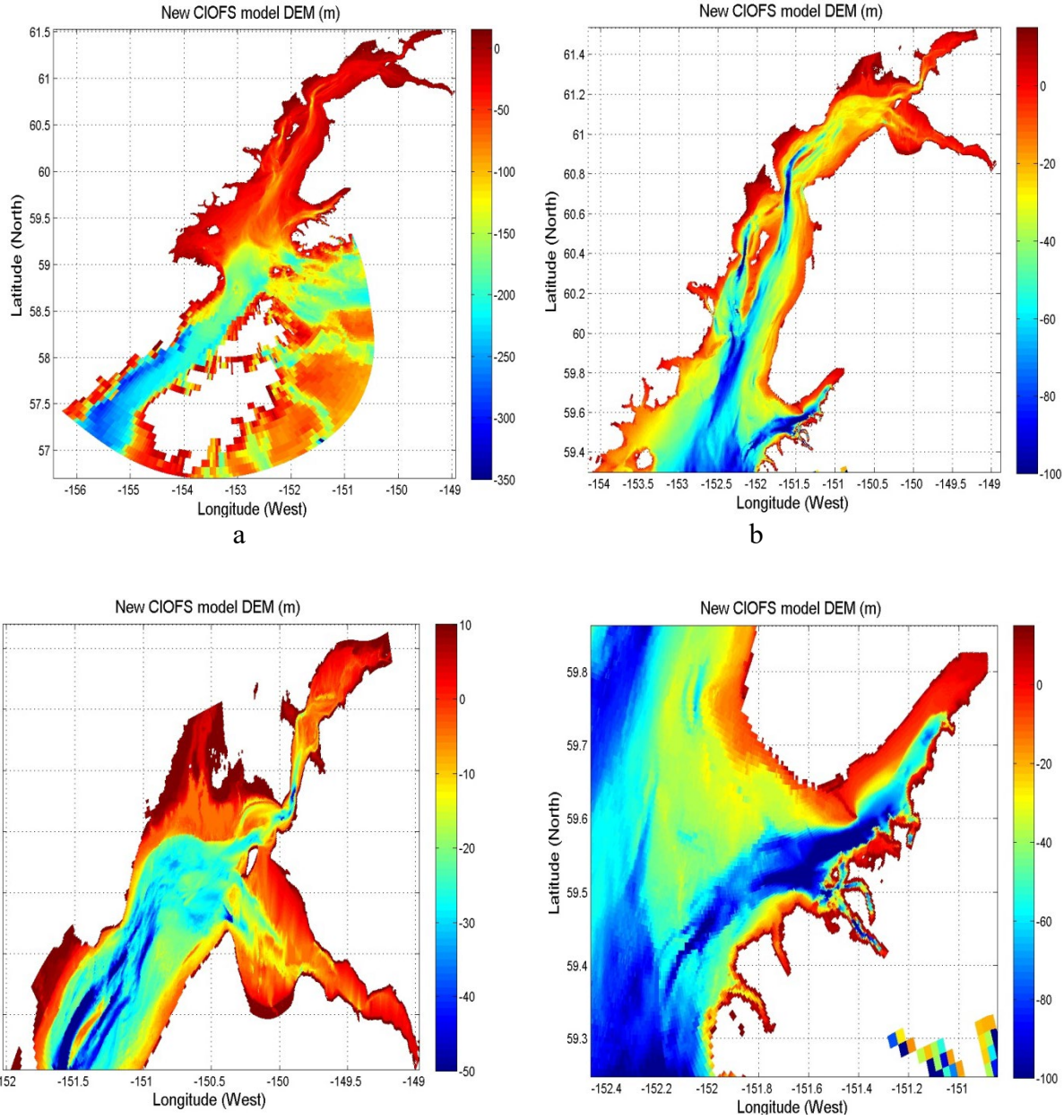

c d

Figure 5. Bathymetry-topography of Cook Inlet Operational Forecast System (CIOFS). a, CIOFS model domain. b, Cook Inlet. c, upper Cook Inlet, Susitna River delta, Knik Arm and Turnagain Arm. d, Kachemak Bay.

2.3 Tidal Forcing at Open Boundary

In ROMS, tides are forced by predicted tidal water level and predicted tidal currents at the open boundary, which consists of 10 tidal harmonic constituents, namely K_1, O_1, P_1, Q_1, M_2, S_2, N_2, K_2, M_4, and M_6. The individual tidal constituents are interpolated from an Advanced Circulation (ADCIRC) tidal model-generated tidal database for that region (Spargo et al., 2003).

2.4 River Input

Figure 6 shows the catchment area of Cook Inlet. The total drainage area is about 50,000 km^2. It can be divided into 4 major subdomains: Kenai Peninsula, Anchorage/Matanuska Area, Susitna Area, and West Cook Inlet Area (Table 1). The Susitna Area is the major drainage area with more than 50% of Cook Inlet catchment area.

Table 1. Cook Inlet 4 drainage areas.

Percentage\area	Kenai Peninsula	Anchorage/Matanuska Area	Susitna Area	West Cook Inlet Area
Percentage of total Cook Inlet drainage area	17%	12%	53%	18%

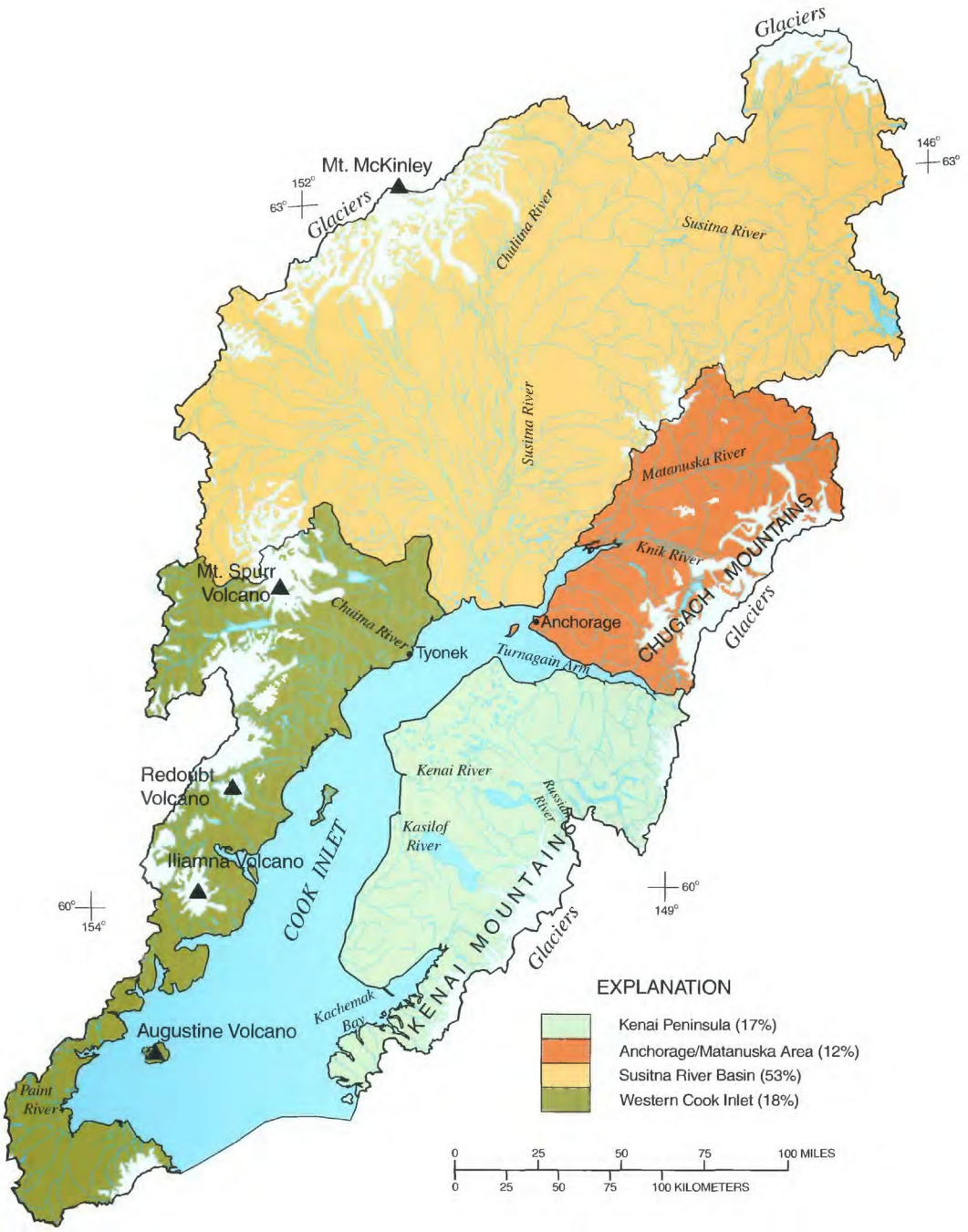

Figure 6. Major drainage areas of the Cook Inlet Basin, Alaska. (from USGS Water-Resources Investigations Report 99-4025 (Brabets et al., 1999))

The model includes 12 major river systems in the drainage basin (Table 2; Figure 7); each has real-time discharge available.

Table 2. Minimum river discharge Q_min (m^3), maximum river discharge Q_max (m^3), and mean river discharge Q_mean (m^3) of USGS river stations where real-time discharges are available.

	Station Number	Q_min (m^3)	Q_max (m^3)	Q_mean (m^3)	River_Station_Name
1	15295700	0	136.20	8.48	Terror River at mouth near Kodiak, AK
2	15239070	0	98.87	3.15	Bradley River near Tidewater near Homer, AK
3	15239900	0	134.84	5.93	Anchor River near Anchor Point, AK
4	15266300	0	1172.80	170.00	Kenai River at Soldotna, AK
5	15271000	0	214.45	25.21	Sixmile Creek near Hope, AK
6	15274600	0	35.41	1.92	Campbell Creek near Spendard, AK
7	15275100	0	9.77	0.61	Chester Canal at Arctic Boulevard at Anchorage, AK
8	15276000	0	59.21	4.12	Ship Canal near Anchorage, AK
9	15281000	0	1699.00	205.00	Knik River near Palmer, AK
10	15284000	0	1153.00	111.68	Matanuska River near Palmer, AK
11	15290000	0	154.39	5.86	Little Susitna River near Palmer, AK
12	15292780	0	5487.81	697.91	Susitna River at Sunshine, AK

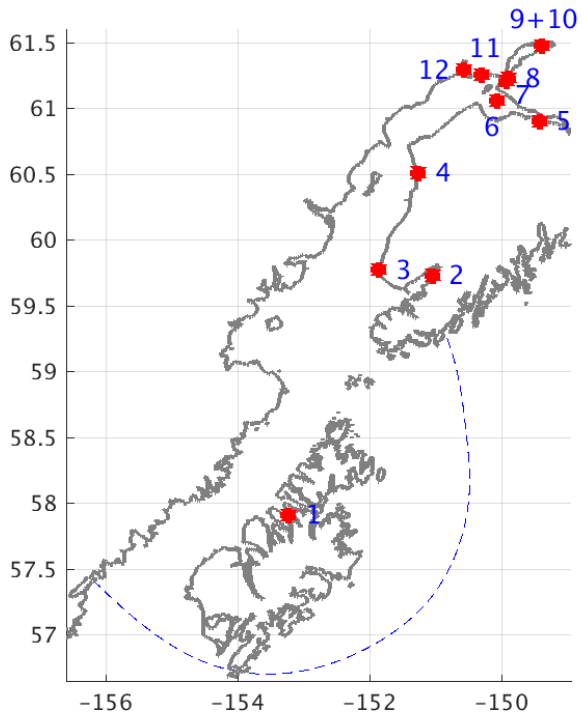

1. Terror River
2. Bradley River
3. Anchor River
4. Kenai River
5. Sixmile Creek
6. Campbell Creek
7. Chester Canal
8. Ship Canal
9. Knik River
10. Matanuska River
11. Little Sustina River
12. Sustina River

Figure 7. The spatial distribution of the twelve rivers and corresponding input points (red crosses) in the CIOFS. Blue dashed line is CIOFS ocean boundary.

The temperature of the river influx that flows into the Cook Inlet was assigned the ambient water temperature at the location where the river discharge data was available.

2.5 Initial Condition

There are two sets of data used for the temperature and salinity initial condition when hindcast run is first initialized and needs to be spun up (cold start). One is to use the World Ocean Atlas for the temperature and salinity field (applied to both hindcast runs), and another alternative is to use Global Real-Time Ocean Forecast System (G-RTOFS) to initialize the temperature and salinity field. In the tides only simulation, the temperature and salinity are set to a constant without surface boundary fluxes. The initial condition for velocity was set to zero, and water level was set to model zero as well. In a cold start, the model always had some spin up period (for days, months and even years dependent on the variables and physical dimension of the model) to eliminate the impact of the initial condition on the model results.

2.6 Open Boundary Condition

In the tidal only simulation, the temperature and salinity at open boundary are set to a constant (the same value as the initial condition). The open boundary was forced by the prescribed tidal water level and tidal currents without non-tidal water level and velocity. For Hindcast 1, the open boundary condition was provided by G-RTOFS for non-tidal water level and velocity in addition to the prescribed tidal water level and tidal currents, and temperature, and salinity open boundary condition was provided by World Ocean Atlas. For Hindcast 2, the open boundary condition was provided by G-RTOFS for temperature, salinity, non-tidal water level and velocity in addition to the prescribed tidal water level and tidal currents.

2.7 Model Sea Surface Condition, Heat and Water Exchange

In the tides only run, there is no heat and water exchange on the sea surface. For the hindcast runs, the exchange is formulated using the bulk flux formulation (Fairall et al., 1996; Fairall et al., 2003). All meteorological parameters are provided using the North American Mesoscale (NAM) (DiMego, 2012) 6 kilometer resolution Alaska nest hourly products.

3. MODEL TESTS AND SKILL ASSESSMENT

In the development of CIOFS, three numerical tests were performed under different scenarios:

1) Tides only simulation. Test the tide forcing boundary inputs and the response of the model to the tidal forcing.
2) Hindcast 1 model simulation from 1/1/2012 to 9/15/2012. Test the model performance during the testing time period, especially the currents using the observed currents data.
3) Hindcast 2 model simulation from 8/15/2013 to 9/15/2015. Test the model performance under multiple year simulation.

3.1 NOS Standards for Skill Assessment

Skill assessment is a key component of OFSs development. It provides unified measures to ensure the quality and performance of OFSs against certain criteria for output state variables, e.g. water level, current, temperature and salinity. The skill assessment will follow NOS Standards for Evaluating Operational Nowcast and Forecast Hydrodynamic Model Systems (Hess et al., 2003). The skill assessment will be conducted using the skill assessment software package developed by Zhang et al. (2010).

The main measure of the skill assessment is the central frequency CF(X), which is the fraction (percentage) of errors that lie within the limits ±X, where X is the acceptable error magnitude. Table 3 provides the default acceptable error magnitude (X_0) for water level, current direction, current speed, temperature and salinity. In an area where there is high water level and current diurnal/semidiurnal variability, the acceptable error magnitude X should be an adjustable parameter that is proportional to the diurnal range of the variable being assessed. That is X= max(X_0 , 10% range), where X_0 is the default acceptable error magnitude. For velocity, the speed range is the diurnal range of the observed current velocity projected into the Principle Current Direction (PCD).

Beside Central Frequency CF(X), the NOS standard skill assessment software also computes some major additional statistical parameters: Root Mean Square Error (RMSE), Positive Outlier Frequency (POF), and Negative Outlier Frequency (NOF). The NOS standard criteria are greater than 90% for CF and less than 1% for NOF and POF. More detailed definitions of the above parameters can be found in Hess et al. (2003).

For Hindcast 1 simulation, in additional to current skill assessment, we performed harmonic analysis for both observed and modeled currents, and made comparison of tidal constituent amplitudes and epochs for tidal currents in PCD and cross PCD. PCD and values of R (ratio of variance of cross PCD current and variance of PCD current) are also calculated from harmonic analysis of currents. Standard and implementation of harmonic analysis of current for model evaluation purpose can be found in Hess et al. (2003) and Zhang et al. (2010).

Table 3. Criteria for skill assessment acceptable error magnitude X, and default acceptable error magnitude X_0.

X_0,X\value\variable	Water level	Current direction	Current speed	Temperature	Salinity
X_0	15 cm	22.5 degrees	26 cm/s	3 degree Celsius	3.5 PSU
X	max(X_0 , 10% range)	22.5 degrees	max(X_0 , 10% range	3 degree Celsius	3.5 PSU

Since our main purpose of CIOFS is to provide forecast guidance to the mariner, and also because of lack of data, we will not perform skill assessment for salinity in this report.

3.2 Tidal Simulation and Calibration

Tidal signal is the most dominant component of water level and current in Cook Inlet. Therefore, in order to calibrate the tides, a simulation in which the density was held constant (temperature at 15 ºC and salinity at 35 PSU) was carried out. The calibration was done with water levels, currents, the quadratic and logarithmic bottom stress formulations, and various levels associated with them were tried together with the modulation of the tidal harmonic constituent amplitudes and phases.

The tidal calibration process showed that the best water level predictions were accomplished with the logarithmic bottom stress formulation, and the quadratic formulation was ignored. Bottom roughness coefficients ranging from 0.0075 m to 0.024 m were tried out with various open boundary conditions and with phase and amplitude adjustments to the boundary forcing tidal harmonic constituents. The best results were achieved with no modulation of tidal constituent amplitude but with a phase adjustment of 5 minutes. The optimal bottom roughness coefficient was 0.01 m. Using larger coefficients did not impact the water levels significantly, but was seen to inflict noticeable damping in the current model predictions. Unlike the nested grid configuration, here in addition to attempting to get the best water level predictions, it was also attempted to achieve the best possible current predictions from the model. The currents used for the comparison in this exercise were the Principal Current Direction (PCD) components (Preisendorfer, 1988). The metrics used to measure the model prediction accuracy were the amplitude and phase error, calculated via an autocorrelation method as described in Lanerolle et al. (2011). The outcome of the calibration exercise is summarized in Table 4.

Table 4. Water level amplitude and phase error, PCD currents amplitude and phase error. Amplitude error computed with raw time series and demeaned time series separated with slash /. Demeaning does not affect phase error.

	Seldovia	Nikiski	Anchorage
Water level amplitude error (cm)	15.9/16.4	20.9/18.9	40.6/32.0
Water level phase error (min)	1.0	-2.0	2.0
PCD current amplitude error (cm/s)	3.2/3.2	30.3/28.5	42.8/36.0

	Seldovia	Nikiski	Anchorage
PCD current phase error (min)	35.0	4.0	-15.0

The model is seen to exhibit excellent phase accuracy in the water level predictions, and the phase errors of the currents are larger in the current predictions. The amplitude error for both water levels and currents is seen to decrease with the demeaning process as seen before. Also, the amplitude error is seen to grow when moving up Cook Inlet whereas the phase error does not show any geographical bias.

3.3 Synoptic Hindcast 1 (Summer 2012) Simulation and Skill Assessment

In the summer of 2012, NOS/CO-OPS conducted a field survey in Cook Inlet which involved the deployment of current meters. This survey resulted in high spatio-temporal resolution current measurements at 9 locations in Cook Inlet which included Kachemak Bay and lower, middle and upper Cook Inlet (Table 5). This dataset was in addition to NOS' 6-minute water level measurements at Seldovia (Kachemak Bay), Nikiski and Anchorage. This field survey provided the motivation to carry out a synoptic hindcast simulation covering the summer of 2012 to assess the accuracy and robustness of the CIOFS model set-up.

Table 5. Locations of the NOS/CO-OPS Summer 2012 current survey.

Station	Longitude	Latitude	Name	Depth of skill assessment results presented (m)
COI1201	-151.40	59.59	Homer Spit	6.4
COI1202	-151.92	59.42	Pt. Pogishi, SW of	4.6
COI1203	-152.03	59.74	Anchor Point, W of	5.8
COI1204	-151.08	62.06	North Forelands	6
COI1205	-151.71	60.47	Kalgin Island	5.5
COI1207	-150.36	61.06	Point Possession	5.7
COI1208	-150.26	61.10	Fire Island, South	6.2
COI1209	-150.20	61.18	Fire Island, North	5.9
COI1210	-151.23	60.89	Middle Ground Shoal	5.2

As ocean models take time to spin-up from rest, it was decided to begin the synoptic hindcast simulation on January 01, 2012 and run it through September 15, 2012. This would allow at least a few months spin-up which was thought to be sufficient. Due to the unavailability of sufficiently accurate water level and current fields, it was decided to spin-up the model from rest so that the currents would develop in response to the density field. The initialization and open boundary temperature and salinity fields were generated from NOAA's World Ocean Atlas (WOA) gridded monthly climatology. The tides were ramped linearly over a 5-day period to ensure a numerically stable spin-up where the currents would grow gradually in time. The river forcing data was from the USGS data sources (both volume discharge and temperature) and the Bradley River temperatures were used for all of the rivers after finding out that the river temperatures over the Cook Inlet domain did not show a strong variation geographically. The Susitna River has two

contributions which needed to be combined – the discharge measured at the Susitna station and that measured at Sunshine station. The gauge at Sunshine has been discontinued and a historical analysis showed that the combined discharge was roughly twice the discharge from the Susitna station. Hence, the Susitna River volume discharge was estimated as being twice that measured at Susitna and this discharge level was used in the numerical simulations. River forcing too was ramped-up in time linearly over a 5-day time period.

Along the open ocean boundary, tidal forcing was provided by harmonic constituents for the water levels and the barotropic velocities which were obtained by interpolating from an ADCIRC model-generated tidal harmonics database (Spargo et al., 2003). The water level tidal signal was augmented by adding a sub-tidal component from the Global Real Time Ocean Forecast System (G-RTOFS) model product. The sub-tidal forcing too was linearly ramped-up in time over a 5-day period. At the ocean surface, meteorological forcing was applied via wind stresses and net heat fluxes generated by the TOGA-COARE Bulk Flux algorithm contained within ROMS. The forcing data to generate the stresses and heat flux (wind speed components, air pressure, air temperature, relative humidity, net shortwave radiation flux and downward longwave radiation flux) were provided by the 6-km resolution NAM Alaska nest model. Here too, the wind speeds were ramped-up in time linearly over a 5-day time period. The modeling set-up did not include ice dynamics or sediment dynamics and ice formation was prevented by suppressing the meteorological cooling during the winter months. The baroclinic time step employed in ROMS was 5 seconds and the baroclinic: barotropic splitting was 30:1. The computation was sped up using MPI parallelization with 384 processors used with an 8 x 48 tiling in the x-y directions.

3.3.1 Water Level Skill Assessment

Predicted water levels were evaluated against observations at Seldovia, Nikiski and Anchorage where NOS/CO-OPS continuously carries out observations. These three locations are shown as magenta triangles in Figure 1. The results for individual stations are summarized below in Figure 8 and Table 6. The water level time series was demeaned before the skill assessment. The acceptable error magnitude, X, is calculated with the formulation, $X = \max(X_0 , 10\% \text{ range})$, and criteria outlined in Section 3.1.

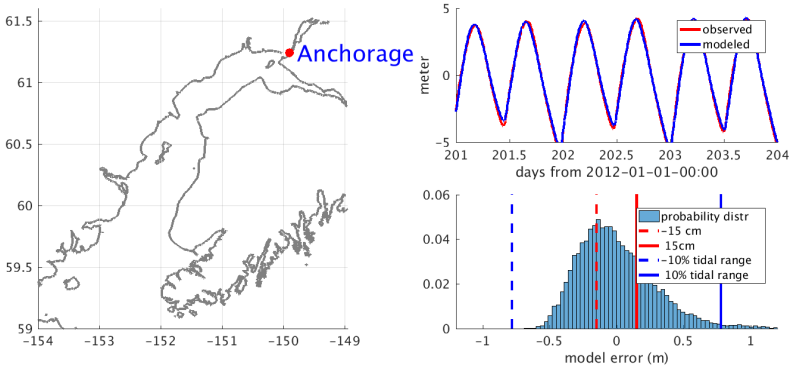


```
Station:                                  Anchorage
Observed data time period from: / 4/30/2012  to / 9/ 3/2012 with gaps of    0.00 days
Data gap is filled using SVD method
Data are not filtered
-------------------------------------------------------------------------------------------
VARIABLE     X      N    IMAX     SM     RMSE     SD      NOF   CF     POF   MDNO   MDPO  WOF   SKILL
CRITERION    -      -    -        -      -        -       <1%   >90%   <1%   <N     <N    <.5%
-------------------------------------------------------------------------------------------

     SCENARIO: HINDCAST
H                    29520   0.036
h                    29520  -0.055
H-h         78 cm 24h 29520   0.091  0.296  0.281   0.0  99.0   0.0    0.0   0.0   0.00  1.00
AHW-ahw     78 cm 24h   237   0.126  0.203  0.159   0.0 100.0   0.0    0.0   0.0
ALW-alw     78 cm 24h   238   0.203  0.253  0.152   0.0 100.0   0.0    0.0   0.0
THW-thw   0.50  h 25h   237  -0.195  0.237  0.134   0.0  99.6   0.0    0.0   0.0
TLW-tlw   0.50  h 25h   238   0.105  0.174  0.138   0.0 100.0   0.0    0.0   0.0
```

a. Anchorage

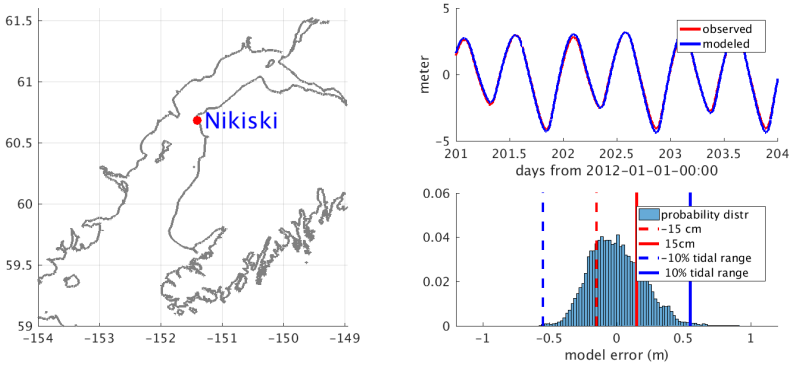


```
Station:                                  Nikiski
Observed data time period from: / 4/30/2012  to / 9/ 3/2012 with gaps of    0.00 days
Data gap is filled using SVD method
Data are not filtered
-------------------------------------------------------------------------------------------
VARIABLE     X      N    IMAX     SM     RMSE     SD      NOF   CF     POF   MDNO   MDPO  WOF   SKILL
CRITERION    -      -    -        -      -        -       <1%   >90%   <1%   <N     <N    <.5%
-------------------------------------------------------------------------------------------

     SCENARIO: HINDCAST
H                    29520   0.035
h                    29520  -0.042
H-h         55 cm 24h 29520   0.076  0.212  0.198   0.0  99.4   0.0    0.0   0.0   0.00  1.00
AHW-ahw     55 cm 24h   237   0.209  0.247  0.131   0.0 100.0   0.0    0.0   0.0
ALW-alw     55 cm 24h   238  -0.105  0.196  0.166   0.0  99.6   0.0    0.0   0.0
THW-thw   0.50  h 25h   237  -0.032  0.152  0.149   0.0  98.3   0.0    0.0   0.0
TLW-tlw   0.50  h 25h   238   0.039  0.143  0.138   0.0 100.0   0.0    0.0   0.0
```

b. Nikiski

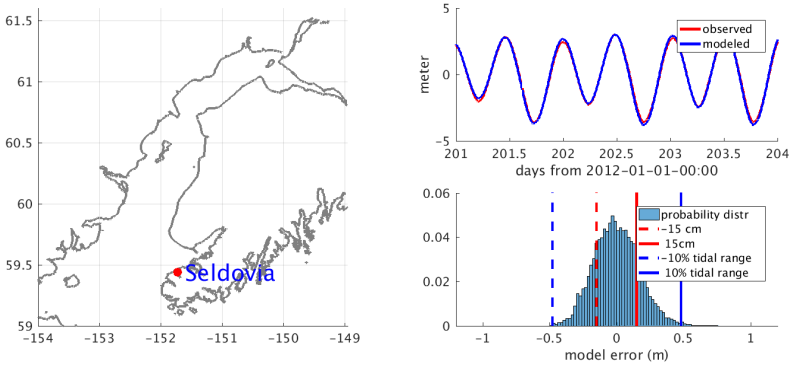


```
Station:                                Seldovia
Observed data time period from: / 4/30/2012  to / 9/ 3/2012 with gaps of    0.00 days
Data gap is filled using SVD method
Data are not filtered
-------------------------------------------------------------------------------------------------------
VARIABLE    X     N    IMAX     SM     RMSE     SD     NOF   CF    POF   MDNO  MDPO  WOF   SKILL
CRITERION   -     -     -       -       -       -     <1%  >90%   <1%    <N    <N  <.5%
-------------------------------------------------------------------------------------------------------

     SCENARIO: HINDCAST
H                    29520  -0.002
h                    29520  -0.064
H-h         48 cm 24h 29520   0.063  0.179  0.168   0.0  99.5   0.0    0.0   0.0  0.00  1.00
AHW-ahw     48 cm 24h   237   0.192  0.235  0.135   0.0  98.7   0.0    0.0   0.0
ALW-alw     48 cm 24h   237  -0.027  0.159  0.158   0.0  99.6   0.0    0.0   0.0
THW-thw  0.50  h 25h   237  -0.009  0.156  0.156   0.0 100.0   0.0    0.0   0.0
TLW-tlw  0.50  h 25h   237   0.009  0.136  0.136   0.0 100.0   0.0    0.0   0.0
```

c. Seldovia

Figure 8. (Panel clockwise from top-left) Geographic location of station, Graphic comparison between modeled and observed water level, histogram of error probability distribution, and summary of water level (demeaned) skill assessments, Hindcast 1 (4/30/2012 - 9/3/2012). The histogram is the probability distribution of the error or mismatch between the model and observation. Red dashed line and red solid line define the range of [-X_0, X_0]. Blue dashed line and blue solid line define the range of [-X, X]. The probability within the range [-X, X] is the CF (central frequency). a. Anchorage. b. Nikiski. c. Seldovia.

Table 6. Summary of water level skill assessment for water level at Anchorage, Nikiski and Seldovia, Hindcast 1 (4/30/2012 - 9/3/2012). Results from different scenarios are also presented.

Location		X_0: 15 cm	X_0: 15 cm with demeaning	X: 10% tidal range	X: 10% tidal range with demeaning
Anchorage	CF (%)	9%	35%	86%	99%
	RMSE (cm)	56.7	29.6	56.7	29.6
Nikiski	CF (%)	37%	48%	99%	99%
	RMSE (cm)	26	21.2	26	21.2
Seldovia	CF (%)	36%	59%	96%	100%
	RMSE (cm)	25.3	17.9	25.8	17.9

Overall the model water levels perform well for these three stations. Demeaning reduced the RMSE and improved the model skill. Demeaning, a post processing for the water level prediction (can be used for current prediction as well), is to remove the model local mean sea level from model time series. The model predicted water level will be demeaned water level plus the observation local mean sea level. Ideally the mean removed from the model water level time series should be a long term average of the local model water level. For both Hindcast 1 and Hindacst 2

water level skill assessments, only the local mean water level of the skill assessment period is removed when the demeaning is performed. For Anchorage station, CF is 86% without demeaning. CF improved to 99% after demeaning.

3.3.2 Current Skill Assessment

The modeled currents were compared against the NOS/CO-OPS Summer 2012 survey data which were taken by current meters at 9 locations (Table 5) in Cook Inlet. Figure 9 shows that the current meters are distributed well throughout Cook Inlet and hence provide a good picture of the nature of currents within Cook Inlet. Model current skill is assessed against the observation for the 2 month long observation period from around 6/14/2012 to 8/14/2012. Subsurface currents from both model and observation between 4 and 30 meters below the sea surface at roughly 2 meters interval are used for skill assessment. The modeled current will be extracted from the model corresponding to the depth of the observed current. Some observations are not available at some depths or rejected due to poor data quality. Due to the fact that the observed currents are very much uniformly distributed in the vertical along the water column between 4 and 30 meters below the surface, only skill assessment results from 5-6 meter below sea surface will be presented in this report. Two skill assessments are performed for the currents. Firstly, we perform the harmonic analysis to the velocity along the principal current direction (PCD) and across the PCD. A comparison is made from the harmonic analysis results. Then we made a statistical analysis and skill assessment to the raw current direction and speed data.

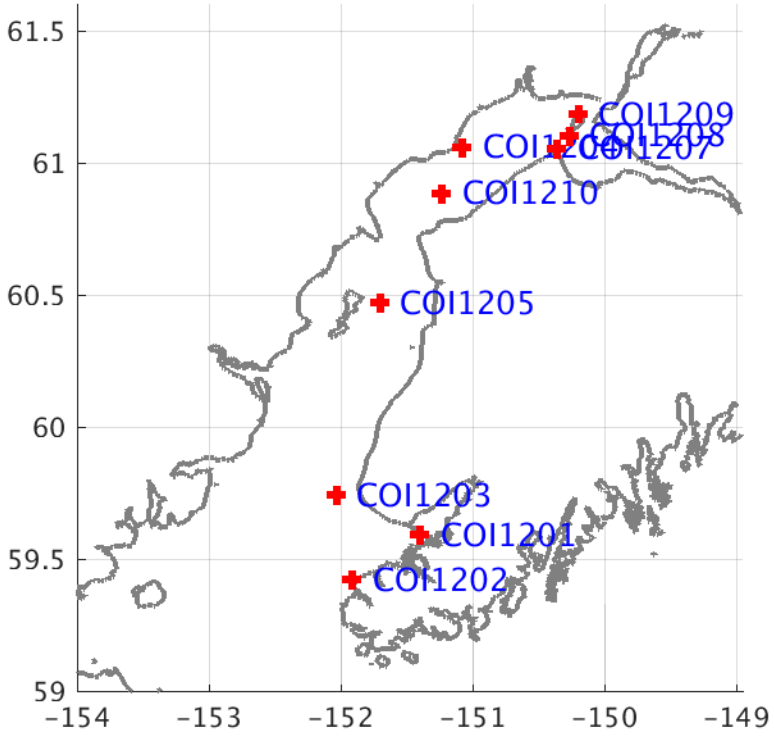

Figure 9. The distribution of the nine current stations (red crosses, COI1201, COI1202, COI1203, COI1204, COI1205, COI1207, COI1208, COI1209, COI1210) during NOS/CO-OPS summer 2012 months long field campaign in Cook Inlet.

3.3.2.1 Comparison of Currents Harmonic Constants

The standard procedure (Hess et al., 2003) of harmonic analysis of a tidal current time series, either observed or modeled, requires firstly to calculate Principal Current Direction (PCD, usually the flood and ebb currents direction). Then the velocity vectors are projected into both PCD direction and cross PCD. Lastly harmonic analysis is performed to the projected time series for both PCD and cross PCD. Two additional parameters, diurnal range of the principal currents and R (ratio of variance of cross PCD current and variance of PCD current), are computed from projected current velocity time series. The diurnal range provide a good estimate of the amplitude of the tidal current. It is used for computation of the current speed skill assessment acceptable error magnitude X= max(X_0 , 10% range). Another parameter calculated is R, ratio of variance of cross PCD current and variance of PCD current, which is the indication of the flow pattern (0<=R<=1, R=0 means a unidirection current, and R=1 is rotary current). A basic requirement for current is that the difference between observed and modeled PCD should be within 30 degrees. For all nine stations (Table 7), the RMSE of the modeled PCD is only 2.05 degree, with maximum difference less than 5 degree. Ratio R for both observed and modeled current are less than 0.25, which means currents in Cook Inlet are very much unidirection currents.

Table 7. Principal Current Direction (PCD), R of observed and modeled currents, diurnal range of observed current, PCD difference between observed and modeled currents from all 9 current stations at skill assessment depth (around 5-6 meters below sea surface).

Station	Depth (m)	Observed PCD (degree)	Observed R	Observed PCD velocity diurnal range (m/s)	Modeled PCD (degree)	Modeled R	Modeled and observed PCD difference (degree)
COI1201	6.4	31.00	0.15	0.84	33.00	0.17	2.00
COI1202	4.6	36.00	0.01	2.66	35.00	0.01	-1.00
COI1203	5.8	-1.00	0.01	3.27	-1.00	0.00	0.00
COI1204	6.0	38.00	0.00	4.38	38.00	0.00	0.00
COI1205	5.5	15.00	0.02	4.52	17.00	0.02	2.00
COI1207	5.7	-72.00	0.01	4.60	-73.00	0.01	-1.00
COI1208	6.2	-58.00	0.02	3.52	-62.00	0.01	-4.00
COI1209	5.9	76.00	0.01	4.19	74.00	0.00	-2.00
COI1210	5.2	58.00	0.01	4.39	55.00	0.01	-3.00
						RMSE	2.05

Harmonic analysis is performed to the current time series for both PCD and cross PCD. The detailed results from harmonic analysis are posted in Appendix A. In general, M_2 tidal current dominates the tidal current energy. If we estimate the kinetic energy in term of square of the current

speed, a rough calculation shows that M_2 and S_2 tides consist of 75% and 18% of total tidal momentum energy respectively. Overall the model preforms very well in terms of the amplitude and phase of major tidal current constituents. Table 8 give the M_2 tidal constituents amplitude and phase results. The RMSE for M_2 current amplitude is only 17 cm/s. The M_2 current phase RMSE is about 5.13 degree, which can be translate to an RMSE of 10.5 minutes.

The tidal current is usually very much uniform throughout the water column except close to the bottom where bottom friction has a large impact. There is no significant difference in terms of PCD, R, diurnal range, amplitude and phase for a few major tidal constituents over top 30 meter water column below the sea surface.

Table 8. Comparison of observed and modeled PCD M_2 current tidal constituent amplitudes (m/s), phase/epochs (degree), and their difference. All current stations.

Station	Depth (m)	Observed amplitude (m/s)	Observed phase (degree)	Modeled amplitude (m/s)	Modeled phase (degree)	Modeled observed amplitude difference (m/s)	Modeled observed phase difference (degree)
COI1201	6.4	0.30	254.70	0.28	247.60	-0.01	-7.10
COI1202	4.6	1.16	246.60	1.41	250.70	0.25	4.10
COI1203	5.8	1.40	119.40	1.54	121.00	-0.13	1.60
COI1204	6.0	2.02	11.10	2.11	6.60	0.09	-4.50
COI1205	5.5	1.80	357.20	2.00	355.70	0.20	-1.50
COI1207	5.7	2.09	12.60	1.99	19.00	-0.10	6.40
COI1208	6.2	1.67	22.90	1.58	23.00	-0.08	0.10
COI1209	5.9	1.95	225.00	2.32	33.90	0.37	8.90
COI1210	5.2	2.01	3.00	2.12	1.40	0.11	-1.60
					RMSE	0.17	5.13

3.3.2.2 Current Skill Assessment

Besides the harmonic analysis of tidal currents, we preformed skill assessment for currents direction and speed from raw current data (Figures 10-27).

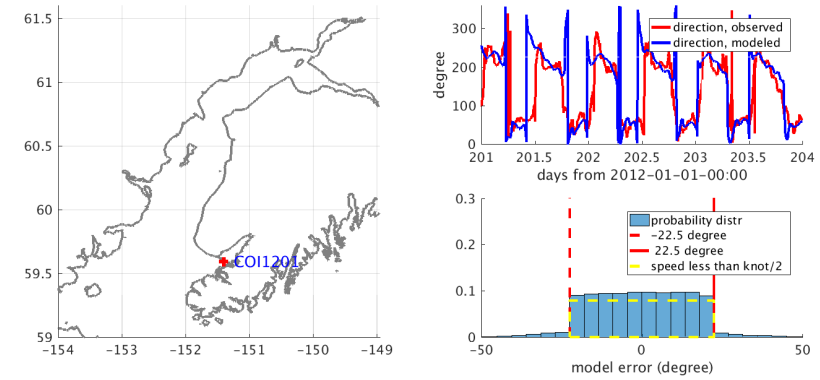


```
Station:  CMIST COI1201  6.4m, Homer Spit, bin 28
 Observed data time period from: / 6/14/2012  to / 8/14/2012with gaps of    0.00 days
 Data gap is filled by SVD method
 Data are not filtered
-------------------------------------------------------------------------------------------
 VARIABLE    X     N    IMAX    SM    RMSE    SD     NOF   CF    POF   MDNO  MDPO  WOF  SKILL
 CRITERION   -     -     -      -      -      -     <1%  >90%   <1%    <N    <N  <.5%
-------------------------------------------------------------------------------------------

     SCENARIO: HINDCAST
D                     14816 166.261
d                     14816 144.562
D-d        22.5 dg 24h 14816   0.144  8.987  8.985   0.2  94.5   0.2    0.4  0.7         0.73
DFC-dfc    22.5 dg 24h    34  -3.519 28.258 28.459   2.9  52.9   8.8    0.0  0.0
DEC-dec    22.5 dg 24h    81   0.596 21.373 21.498   3.7  77.8   4.9    0.0  0.0
```

Figure 10. Current direction (degree), station COI1201, Hindcast 1 (6/14/2012 - 8/14/2012). Note (apply to all current direction figure caption): (panel clockwise from top-left) 1) geographic location of current station, 2) graphic comparison between modeled and observed current direction, 3) histogram of error probability distribution, and 4) summary of current direction skill assessment. The histogram is the probability distribution of the error or mismatch between the model and observation. Red dashed line and red solid line define the range [-X, X]. Yellow dashed line represents evenly distributed probability when speed less than ½ knot (the current direction is computed only for current speeds above ½ knot) over the range [-X, X]. The probability within the range [-X, X] is the CF (central frequency).

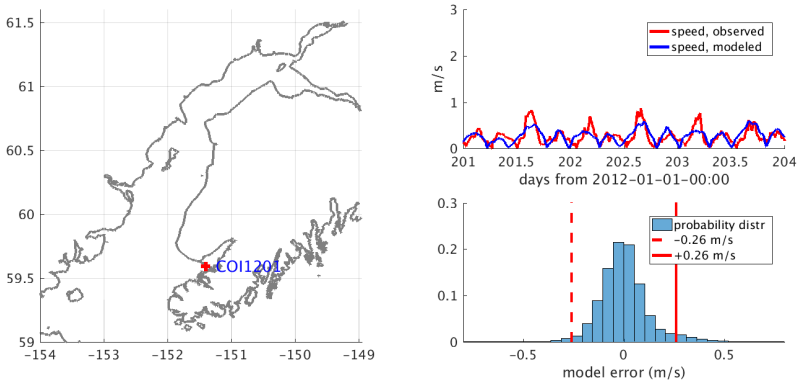

Station: CMIST COI1201 6.4m, Homer Spit, bin 28
Observed data time period from: / 6/14/2012 to / 8/14/2012 with gaps of 0.00 days
Data gap is filled by SVD method
Data are not filtered

VARIABLE	X	N	IMAX	SM	RMSE	SD	NOF	CF	POF	MDNO	MDPO	WOF	SKILL
CRITERION	-	-	-	-	-	-	<1%	>90%	<1%	<N	<N	<.5%	

SCENARIO: HINDCAST

U			14816	0.220								
u			14816	0.220								
U-u	26 cm/s	24h	14816	-0.001	0.118	0.118	0.1	95.1	0.0	0.3	0.0	0.80
AFC-afc	26 cm/s	24h	34	-0.020	0.060	0.057	0.0	100.0	0.0	0.0	0.0	
AEC-aec	26 cm/s	24h	81	-0.190	0.265	0.186	2.5	49.4	0.0	12.3	0.0	
TFC-tfc	0.50h	25h	34	-0.038	0.774	0.784	11.8	38.2	5.9	0.0	0.0	
TEC-tec	0.50h	25h	81	0.044	0.905	0.910	11.1	37.0	8.6	36.5	0.0	
TSF-tsf	0.25h	25h	21	0.254	0.867	0.850	4.8	47.6	14.3	0.0	0.0	
TEF-tef	0.25h	25h	27	-0.274	0.979	0.958	37.0	40.7	7.4	0.0	0.0	
TSE-tse	0.25h	25h	48	-0.214	0.981	0.967	10.4	56.2	8.3	0.0	12.4	
TEE-tee	0.25h	25h	60	-0.500	0.924	0.784	41.7	35.0	1.7	37.2	0.0	

Figure 11. Current speed (m/s), station COI1201, Hindcast 1 (6/14/2012 - 8/14/2012). Note (apply to all current direction figure caption): (panel clockwise from top-left) 1) geographic location of current station, 2) graphic comparison between modeled and observed current speed, 3) histogram of error probability distribution, and 4) summary of current speed skill assessment. The histogram is the probability distribution of the error or mismatch between the model and observation. Red dashed line and red solid line define the range [$-X_0$, X_0]. Blue dashed line and blue solid line define the range [-X, X] (only red line will be presented if $X=X_0$). The probability within the range [-X, X] is the CF (central frequency).

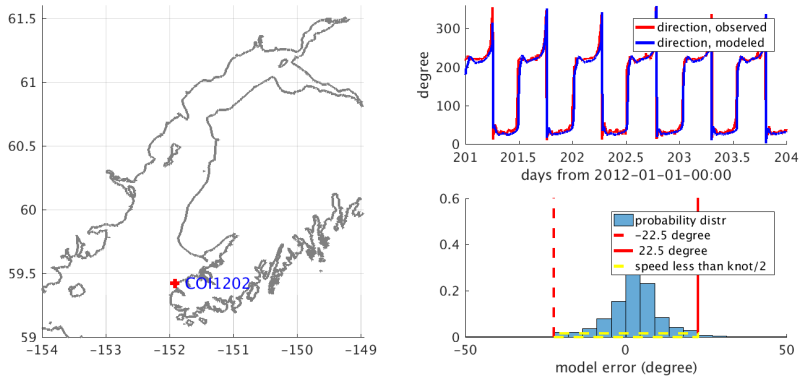

Station: CMIST COI1202 4.6m, Pt. Pogishi, SW of,
Observed data time period from: / 6/13/2012 to / 8/14/2012with gaps of 0.00 days
Data gap is filled by SVD method
Data are not filtered

VARIABLE	X	N	IMAX	SM	RMSE	SD	NOF	CF	POF	MDNO	MDPO	WOF	SKILL
CRITERION	-	-	-	-	-	-	<1%	>90%	<1%	<N	<N	<.5%	
SCENARIO: HINDCAST													
D			14884	130.350									
d			14884	134.106									
D-d	22.5	dg 24h	14884	-2.522	7.484	7.047	0.0	98.2	0.1	0.0	0.6		0.96
DFC-dfc	22.5	dg 24h	107	-2.153	3.932	3.305	0.0	100.0	0.0	0.0	0.0		
DEC-dec	22.5	dg 24h	14	1.380	7.402	7.547	0.0	100.0	0.0	0.0	0.0		

Figure 12. Current direction (degree), station COI1202, Hindcast 1 (6/13/2012 - 8/14/2012).

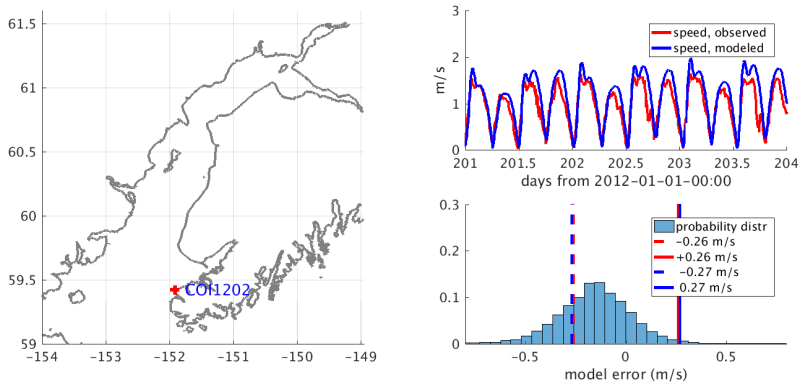

Station: CMIST COI1202 4.6m, Pt. Pogishi, SW of,
Observed data time period from: / 6/13/2012 to / 8/14/2012 with gaps of 0.00 days
Data gap is filled by SVD method
Data are not filtered

VARIABLE	X	N	IMAX	SM	RMSE	SD	NOF	CF	POF	MDNO	MDPO	WOF	SKILL
CRITERION	-	-	-	-	-	-	<1%	>90%	<1%	<N	<N	<.5%	
SCENARIO: HINDCAST													
U			14884	0.964									
u			14884	0.797									
U-u	27	cm/s 24h	14884	0.167	0.260	0.199	0.0	74.3	3.4	0.0	1.9		0.93
AFC-afc	27	cm/s 24h	107	0.119	0.154	0.098	0.0	98.1	0.0	0.0	0.0		
AEC-aec	27	cm/s 24h	14	0.154	0.198	0.129	0.0	78.6	0.0	0.0	0.0		
TFC-tfc	0.50	h 25h	107	0.283	0.682	0.623	3.7	47.7	10.3	0.0	0.0		
TEC-tec	0.50	h 25h	14	-0.336	0.692	0.628	14.3	57.1	0.0	0.0	0.0		
TSF-tsf	0.25	h 25h	87	0.150	0.274	0.231	0.0	96.6	0.0	0.0	0.0		
TEF-tef	0.25	h 25h	87	0.026	0.181	0.180	0.0	98.9	0.0	0.0	0.0		
TSE-tse	0.25	h 25h	13	-0.391	0.540	0.388	7.7	53.8	0.0	0.0	0.0		
TEE-tee	0.25	h 25h	13	-0.514	0.569	0.254	0.0	53.8	0.0	0.0	0.0		

Figure 13. Current speed (m/s), station COI1202, Hindcast 1 (6/13/2012 - 8/14/2012).

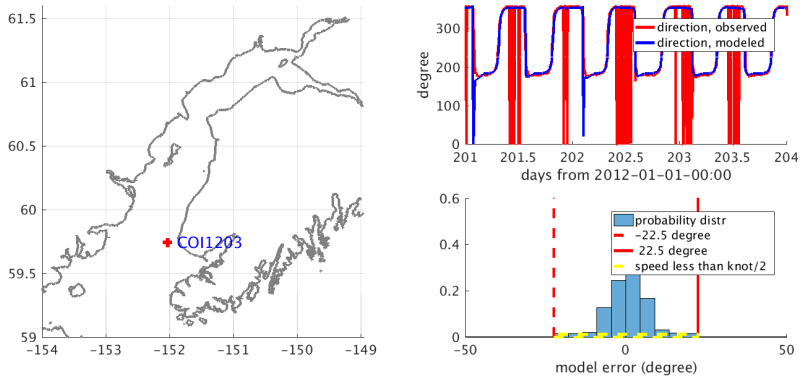

Station: CMIST COI1203 5.8m, Anchor Point, W of,
Observed data time period from: / 6/14/2012 to / 8/14/2012with gaps of 0.00 days
Data gap is filled by SVD method
Data are not filtered

VARIABLE	X	N	IMAX	SM	RMSE	SD	NOF	CF	POF	MDNO	MDPO	WOF	SKILL
CRITERION	-	-	-	-	-	-	<1%	>90%	<1%	<N	<N	<.5%	
SCENARIO: HINDCAST													
D			14674	268.180									
d			14674	255.438									
D-d	22.5 dg	24h	14674	-0.684	5.457	5.415	0.0	99.3	0.0	0.0	0.4		0.80
DFC-dfc	22.5 dg	24h	117	3.490	4.224	2.390	0.0	100.0	0.0	0.0	0.0		
DEC-dec	22.5 dg	24h	119	-3.544	3.781	1.322	0.0	100.0	0.0	0.0	0.0		

Figure 14. Current direction (degree), station COI1203, Hindcast 1 (6/14/2012 - 8/14/2012).

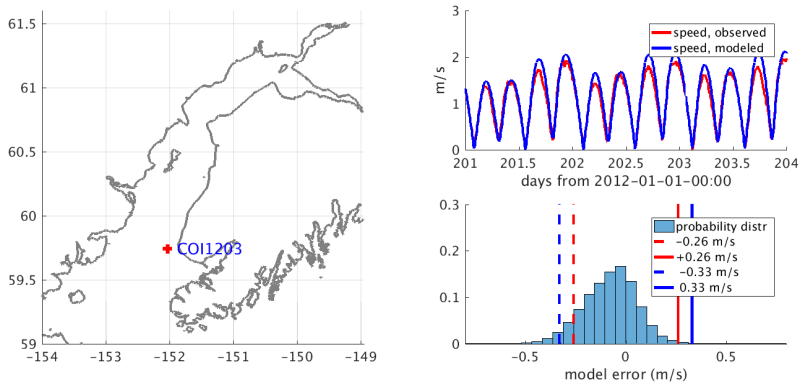

Station: CMIST COI1203 5.8m, Anchor Point, W of,
Observed data time period from: / 6/14/2012 to / 8/14/2012 with gaps of 0.00 days
Data gap is filled by SVD method
Data are not filtered

VARIABLE	X	N	IMAX	SM	RMSE	SD	NOF	CF	POF	MDNO	MDPO	WOF	SKILL
CRITERION	-	-	-	-	-	-	<1%	>90%	<1%	<N	<N	<.5%	
SCENARIO: HINDCAST													
U			14674	1.043									
u			14674	0.964									
U-u	33 cm/s	24h	14674	0.079	0.152	0.130	0.0	96.5	0.0	0.0	0.0		0.98
AFC-afc	33 cm/s	24h	117	0.179	0.207	0.105	0.0	96.6	0.0	0.0	0.0		
AEC-aec	33 cm/s	24h	119	0.045	0.088	0.076	0.0	100.0	0.0	0.0	0.0		
TFC-tfc	0.50h	25h	117	0.120	0.304	0.281	0.9	87.2	0.0	0.0	0.0		
TEC-tec	0.50h	25h	119	0.143	0.426	0.403	0.0	67.2	0.0	0.0	0.0		
TSF-tsf	0.25h	25h	116	-0.061	0.173	0.162	0.0	99.1	0.0	0.0	0.0		
TEF-tef	0.25h	25h	117	-0.063	0.169	0.157	0.0	98.3	0.0	0.0	0.0		
TSE-tse	0.25h	25h	92	0.042	0.214	0.211	1.1	97.8	0.0	0.0	0.0		
TEE-tee	0.25h	25h	98	0.066	0.203	0.193	0.0	95.9	0.0	0.0	0.0		

Figure 15. Current speed (m/s), station COI1203, Hindcast 1 (6/14/2012 - 8/14/2012).

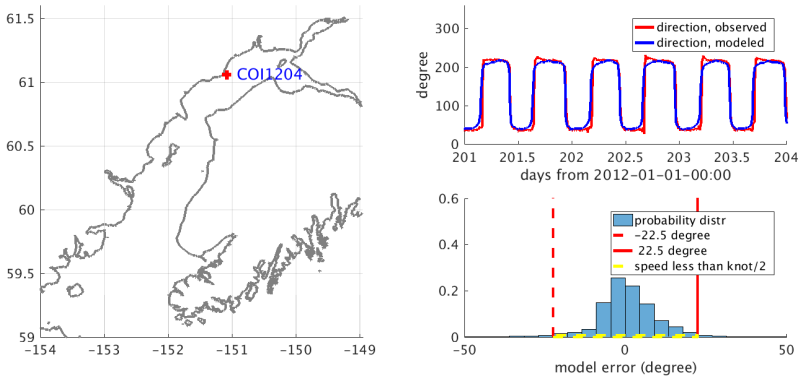


```
Station: CMIST COI1204  6.0m, North Forelands, bi
 Observed data time period from: / 6/16/2012  to / 8/17/2012with gaps of    0.00 days
 Data gap is filled by SVD method
 Data are not filtered
-------------------------------------------------------------------------------------------
 VARIABLE    X      N    IMAX     SM     RMSE     SD      NOF   CF     POF   MDNO  MDPO  WOF  SKILL
 CRITERION   -      -     -       -       -       -      <1%  >90%   <1%    <N    <N  <.5%
-------------------------------------------------------------------------------------------

     SCENARIO: HINDCAST
D                     14880 138.762
d                     14880 137.675
D-d         22.5 dg 24h 14880  -0.334 10.007 10.002   0.2  96.7   0.5    0.2   0.3         0.98
DFC-dfc     22.5 dg 24h    14   2.569  4.714  4.102   0.0 100.0   0.0    0.0   0.0
DEC-dec     22.5 dg 24h   120  -0.820  2.437  2.305   0.0 100.0   0.0    0.0   0.0
```

Figure 16. Current direction (degree), station COI1204, Hindcast 1 (6/16/2012 - 8/17/2012).

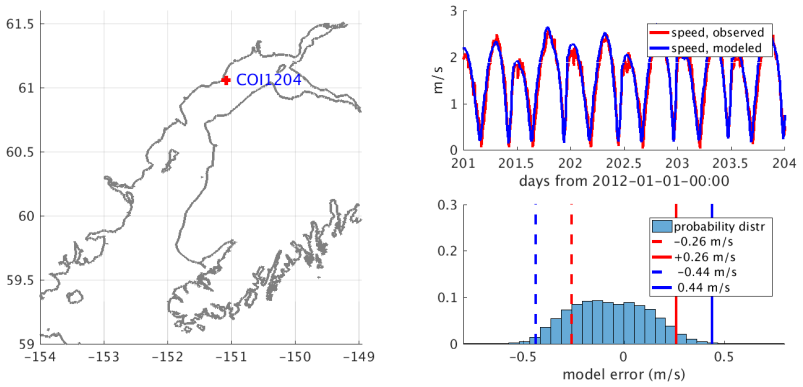


```
Station: CMIST COI1204  6.0m, North Forelands, bi
Observed data time period from: / 6/16/2012  to / 8/17/2012 with gaps of    0.00 days
Data gap is filled by SVD method
Data are not filtered
-------------------------------------------------------------------------------------------
 VARIABLE    X      N    IMAX     SM     RMSE     SD      NOF   CF     POF   MDNO  MDPO  WOF  SKILL
 CRITERION   -      -     -       -       -       -      <1%  >90%   <1%    <N    <N  <.5%
-------------------------------------------------------------------------------------------

     SCENARIO: HINDCAST
U                     14880   1.485
u                     14880   1.415
U-u         44 cm/s 24h 14880   0.070  0.204  0.191   0.0  98.5   0.0    0.0   0.0         0.98
AFC-afc     44 cm/s 24h    14  -0.052  0.104  0.093   0.0 100.0   0.0    0.0   0.0
AEC-aec     44 cm/s 24h   120   0.090  0.137  0.104   0.0 100.0   0.0    0.0   0.0
TFC-tfc     0.50h   25h    14  -0.236  0.401  0.337   0.0  64.3   0.0    0.0   0.0
TEC-tec     0.50h   25h   120  -0.398  0.539  0.365   3.3  53.3   0.0    0.0   0.0
TSF-tsf     0.25h   25h     9  -0.154  0.228  0.179   0.0  88.9   0.0    0.0   0.0
TEF-tef     0.25h   25h     9  -0.016  0.176  0.186   0.0 100.0   0.0    0.0   0.0
TSE-tse     0.25h   25h    36  -0.167  0.225  0.153   0.0  97.2   0.0    0.0   0.0
TEE-tee     0.25h   25h    39  -0.295  0.339  0.170   0.0  92.3   0.0    0.0   0.0
```

Figure 17. Current speed (m/s), station COI1204, Hindcast 1 (6/16/2012 - 8/17/2012).

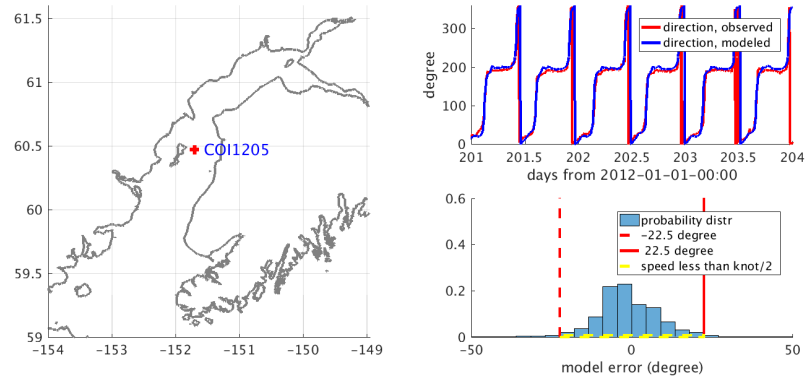

Station: CMIST COI1205 5.5m, Kalgin Island, 4nm
Observed data time period from: / 6/15/2012 to / 8/15/2012with gaps of 0.00 days
Data gap is filled by SVD method
Data are not filtered

VARIABLE	X	N	IMAX	SM	RMSE	SD	NOF	CF	POF	MDNO	MDPO	WOF	SKILL
CRITERION	-	-	-	-	-	-	<1%	>90%	<1%	<N	<N	<.5%	

SCENARIO: HINDCAST

D			14852	154.887									
d			14852	139.792									
D-d	22.5	dg 24h	14852	1.516	9.771	9.653	0.0	97.2	0.4	0.1	0.3		0.86
DFC-dfc	22.5	dg 24h	103	-4.280	6.763	5.262	0.0	100.0	0.0	0.0	0.0		
DEC-dec	22.5	dg 24h	116	4.222	5.271	3.169	0.0	100.0	0.0	0.0	0.0		

Figure 18. Current direction (degree), station COI1205, Hindcast 1 (6/15/2012 - 8/15/2012).

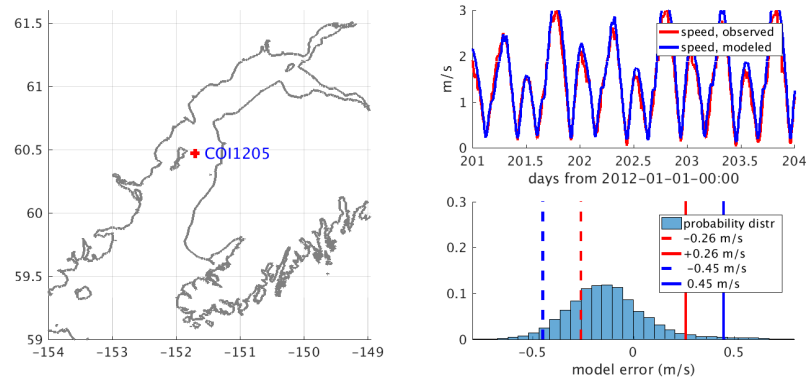

Station: CMIST COI1205 5.5m, Kalgin Island, 4nm
Observed data time period from: / 6/15/2012 to / 8/15/2012 with gaps of 0.00 days
Data gap is filled by SVD method
Data are not filtered

VARIABLE	X	N	IMAX	SM	RMSE	SD	NOF	CF	POF	MDNO	MDPO	WOF	SKILL
CRITERION	-	-	-	-	-	-	<1%	>90%	<1%	<N	<N	<.5%	

SCENARIO: HINDCAST

U			14852	1.404									
u			14852	1.273									
U-u	45	cm/s 24h	14852	0.130	0.239	0.200	0.0	94.9	0.0	0.0	0.0		0.98
AFC-afc	45	cm/s 24h	103	0.177	0.201	0.096	0.0	100.0	0.0	0.0	0.0		
AEC-aec	45	cm/s 24h	116	0.200	0.307	0.234	0.0	84.5	0.0	0.0	0.0		
TFC-tfc	0.50h	25h	103	0.016	0.336	0.337	0.0	84.5	0.0	0.0	0.0		
TEC-tec	0.50h	25h	116	-0.209	0.561	0.523	6.0	65.5	2.6	0.0	0.0		
TSF-tsf	0.25h	25h	78	-0.000	0.168	0.169	0.0	97.4	0.0	0.0	0.0		
TEF-tef	0.25h	25h	80	-0.084	0.199	0.181	0.0	97.5	0.0	0.0	0.0		
TSE-tse	0.25h	25h	68	0.011	0.194	0.195	0.0	98.5	0.0	0.0	0.0		
TEE-tee	0.25h	25h	73	-0.197	0.306	0.235	0.0	91.8	0.0	0.0	0.0		

Figure 19. Current speed (m/s), station COI1205, Hindcast 1 (6/15/2012 - 8/15/2012).

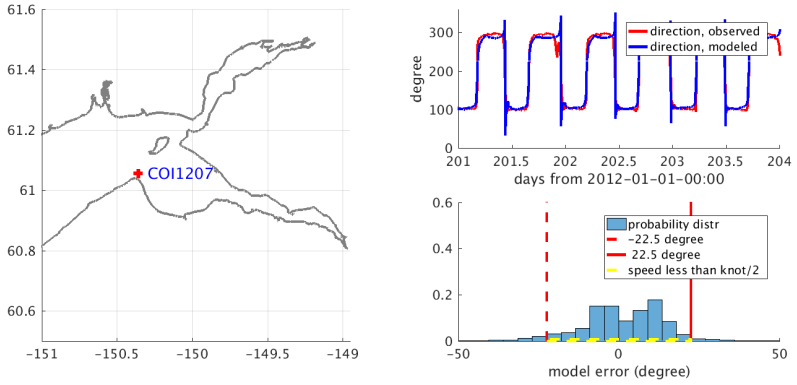

Station: CMIST COI1207 5.7m, Point Possession, b
Observed data time period from: / 6/16/2012 to / 8/17/2012with gaps of 0.00 days
Data gap is filled by SVD method
Data are not filtered

VARIABLE	X	N	IMAX	SM	RMSE	SD	NOF	CF	POF	MDNO	MDPO	WOF	SKILL
CRITERION	-	-	-	-	-	-	<1%	>90%	<1%	<N	<N	<.5%	
SCENARIO: HINDCAST													
D			14853	205.201									
d			14853	205.055									
D-d	22.5	dg 24h	14853	-1.256	13.151	13.091	0.3	92.9	0.5	0.5	0.2		0.98
DFC-dfc	22.5	dg 24h	8	1.002	2.651	2.624	0.0	100.0	0.0	0.0	0.0		
DEC-dec	22.5	dg 24h	109	-7.242	8.011	3.441	0.0	100.0	0.0	0.0	0.0		

Figure 20. Current direction (degree), station COI1207, Hindcast 1 (6/16/2012 - 8/17/2012).

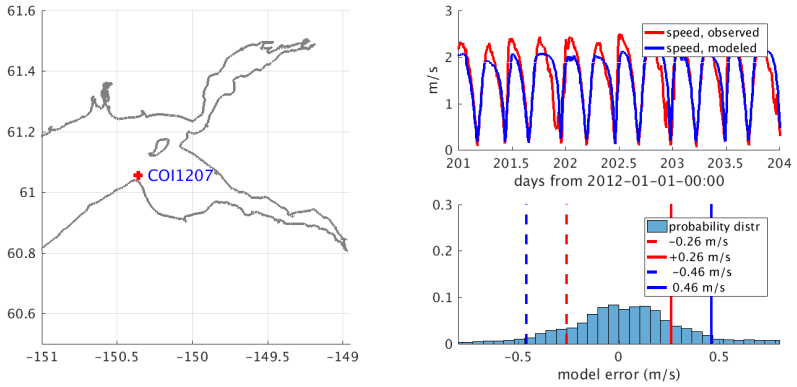

Station: CMIST COI1207 5.7m, Point Possession, b
Observed data time period from: / 6/16/2012 to / 8/17/2012 with gaps of 0.00 days
Data gap is filled by SVD method
Data are not filtered

VARIABLE	X	N	IMAX	SM	RMSE	SD	NOF	CF	POF	MDNO	MDPO	WOF	SKILL
CRITERION	-	-	-	-	-	-	<1%	>90%	<1%	<N	<N	<.5%	
SCENARIO: HINDCAST													
U			14853	1.426									
u			14853	1.459									
U-u	46	cm/s 24h	14853	-0.033	0.339	0.338	1.4	86.4	1.2	0.7	1.2		0.93
AFC-afc	46	cm/s 24h	8	-0.302	0.317	0.102	0.0	100.0	0.0	0.0	0.0		
AEC-aec	46	cm/s 24h	109	-0.242	0.296	0.171	0.0	97.2	0.0	0.0	0.0		
TFC-tfc	0.50h	25h	8	0.588	0.887	0.710	0.0	50.0	25.0	0.0	0.0		
TEC-tec	0.50h	25h	109	0.077	0.709	0.708	0.0	50.5	12.8	0.0	13.1		
TSF-tsf	0.25h	25h	5	-0.068	0.677	0.753	20.0	60.0	0.0	0.0	0.0		
TEF-tef	0.25h	25h	7	-0.091	0.107	0.061	0.0	100.0	0.0	0.0	0.0		
TSE-tse	0.25h	25h	57	0.024	0.146	0.145	0.0	98.2	0.0	0.0	0.0		
TEE-tee	0.25h	25h	61	-0.103	0.178	0.146	0.0	96.7	0.0	0.0	0.0		

Figure 21. Current speed (m/s), station COI1207, Hindcast 1 (6/16/2012 - 8/17/2012).

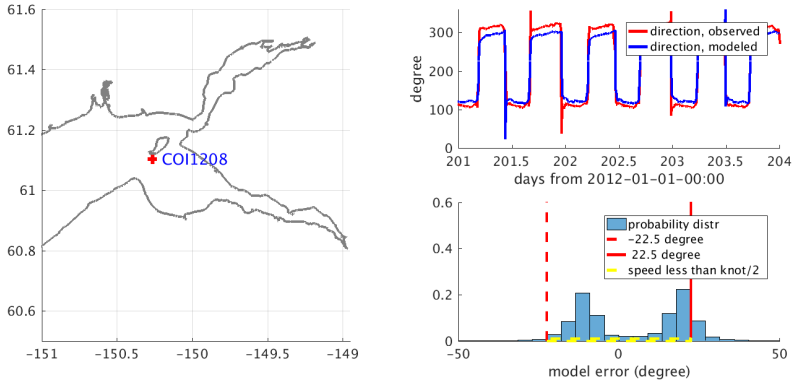

Station: CMIST COI1208 6.2m, Fire Island, South
Observed data time period from: / 6/16/2012 to / 8/17/2012with gaps of 0.00 days
Data gap is filled by SVD method
Data are not filtered

VARIABLE	X	N	IMAX	SM	RMSE	SD	NOF	CF	POF	MDNO	MDPO	WOF	SKILL
CRITERION	-	-	-	-	-	-	<1%	>90%	<1%	<N	<N	<.5%	
SCENARIO: HINDCAST													
D			14852	213.388									
d			14852	217.089									
D-d	22.5	dg 24h	14852	-4.608	16.625	15.974	0.3	87.0	0.1	0.6	0.2		0.97
DFC-dfc	22.5	dg 24h	54	10.001	10.171	1.868	0.0	100.0	0.0	0.0	0.0		
DEC-dec	22.5	dg 24h	27	-23.681	24.049	4.275	0.0	44.4	0.0	0.0	0.0		

Figure 22. Current direction (degree), station COI1208, Hindcast 1 (6/16/2012 - 8/17/2012).

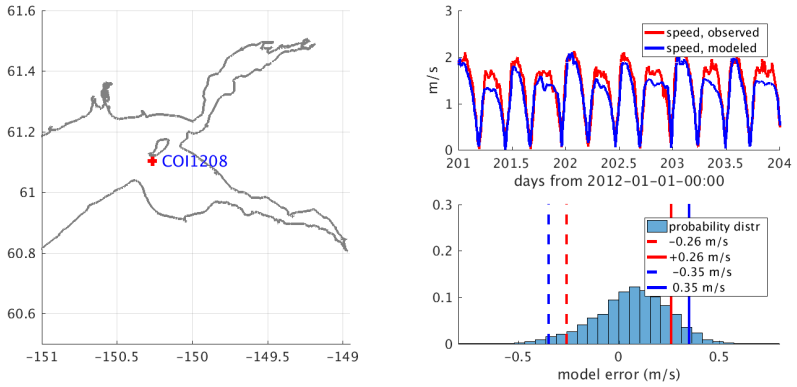

Station: CMIST COI1208 6.2m, Fire Island, South
Observed data time period from: / 6/16/2012 to / 8/17/2012 with gaps of 0.00 days
Data gap is filled by SVD method
Data are not filtered

VARIABLE	X	N	IMAX	SM	RMSE	SD	NOF	CF	POF	MDNO	MDPO	WOF	SKILL
CRITERION	-	-	-	-	-	-	<1%	>90%	<1%	<N	<N	<.5%	
SCENARIO: HINDCAST													
U			14852	1.119									
u			14852	1.186									
U-u	35	cm/s 24h	14852	-0.067	0.194	0.182	0.0	93.4	0.0	0.0	0.0		0.97
AFC-afc	35	cm/s 24h	54	-0.055	0.106	0.092	0.0	100.0	0.0	0.0	0.0		
AEC-aec	35	cm/s 24h	27	-0.246	0.258	0.079	0.0	88.9	0.0	0.0	0.0		
TFC-tfc	0.50	h 25h	54	-0.411	0.588	0.425	5.6	46.3	0.0	0.0	0.0		
TEC-tec	0.50	h 25h	27	-0.667	0.954	0.695	25.9	11.1	0.0	0.0	0.0		
TSF-tsf	0.25	h 25h	33	-0.087	0.264	0.253	0.0	90.9	0.0	0.0	0.0		
TEF-tef	0.25	h 25h	33	-0.057	0.173	0.166	0.0	100.0	0.0	0.0	0.0		
TSE-tse	0.25	h 25h	24	-0.133	0.250	0.216	0.0	95.8	0.0	0.0	0.0		
TEE-tee	0.25	h 25h	24	-0.316	0.401	0.252	0.0	70.8	0.0	0.0	0.0		

Figure 23. Current speed (m/s), station COI1208, Hindcast 1 (6/16/2012 - 8/17/2012).

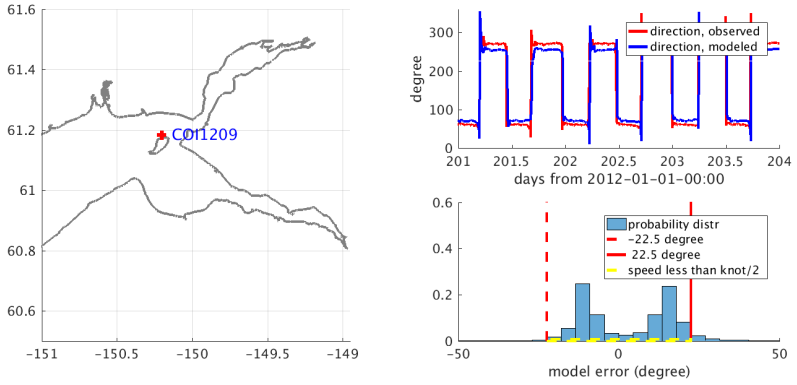

Station: CMIST COI1209 5.9m, Fire Island, North
Observed data time period from: / 6/17/2012 to / 8/17/2012with gaps of 0.00 days
Data gap is filled by SVD method
Data are not filtered

VARIABLE	X	N	IMAX	SM	RMSE	SD	NOF	CF	POF	MDNO	MDPO	WOF	SKILL
CRITERION	-	-	-	-	-	-	<1%	>90%	<1%	<N	<N	<.5%	
SCENARIO: HINDCAST													
D			14667	169.017									
d			14667	171.487									
D-d	22.5	dg 24h	14667	-3.374	16.309	15.957	0.4	95.2	0.1	0.3	0.0		0.96
DFC-dfc	22.5	dg 24h	30	10.180	10.419	2.255	0.0	100.0	0.0	0.0	0.0		
DEC-dec	22.5	dg 24h	72	-18.308	18.442	2.229	0.0	95.8	0.0	0.0	0.0		

Figure 24. Current direction (degree), station COI1209, Hindcast 1 (6/17/2012 - 8/17/2012).

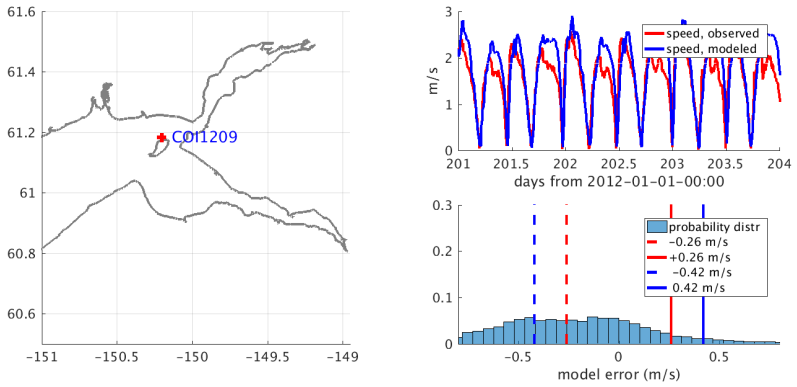

Station: CMIST COI1209 5.9m, Fire Island, North
Observed data time period from: / 6/17/2012 to / 8/17/2012 with gaps of 0.00 days
Data gap is filled by SVD method
Data are not filtered

VARIABLE	X	N	IMAX	SM	RMSE	SD	NOF	CF	POF	MDNO	MDPO	WOF	SKILL
CRITERION	-	-	-	-	-	-	<1%	>90%	<1%	<N	<N	<.5%	
SCENARIO: HINDCAST													
U			14667	1.622									
u			14667	1.428									
U-u	42	cm/s 24h	14667	0.194	0.401	0.350	0.5	65.2	0.6	0.5	0.4		0.91
AFC-afc	42	cm/s 24h	30	0.203	0.251	0.150	0.0	93.3	0.0	0.0	0.0		
AEC-aec	42	cm/s 24h	72	0.331	0.341	0.086	0.0	83.3	0.0	0.0	0.0		
TFC-tfc	0.50h	25h	30	0.443	0.616	0.435	0.0	50.0	6.7	0.0	0.0		
TEC-tec	0.50h	25h	72	0.536	0.747	0.523	0.0	37.5	9.7	0.0	0.0		
TSF-tsf	0.25h	25h	17	0.120	0.259	0.237	0.0	82.4	0.0	0.0	0.0		
TEF-tef	0.25h	25h	19	0.124	0.200	0.162	0.0	100.0	0.0	0.0	0.0		
TSE-tse	0.25h	25h	60	0.112	0.173	0.132	0.0	100.0	0.0	0.0	0.0		
TEE-tee	0.25h	25h	60	0.074	0.156	0.139	0.0	100.0	0.0	0.0	0.0		

Figure 25. Current speed (m/s), station COI1209, Hindcast 1 (6/17/2012 - 8/17/2012).

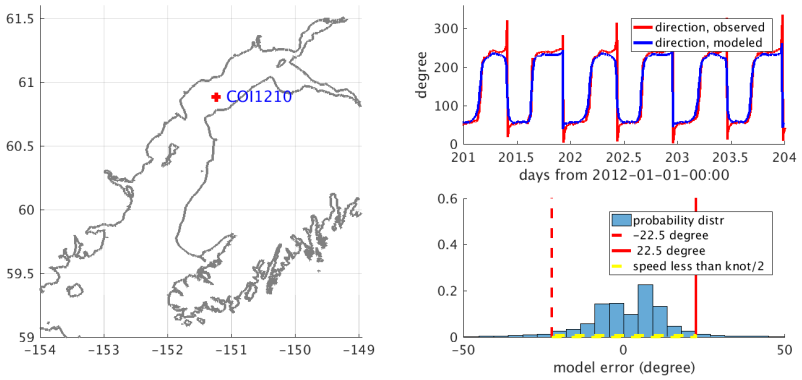

Station: CMIST COI1210 5.2m, Middle Ground Shoal
Observed data time period from: / 6/15/2012 to / 8/16/2012with gaps of 0.00 days
Data gap is filled by SVD method
Data are not filtered

VARIABLE	X	N	IMAX	SM	RMSE	SD	NOF	CF	POF	MDNO	MDPO	WOF	SKILL
CRITERION	-	-	-	-	-	-	<1%	>90%	<1%	<N	<N	<.5%	
SCENARIO: HINDCAST													
D			14894	152.388									
d			14894	154.574									
D-d	22.5	dg 24h	14894	-1.149	13.093	13.043	0.5	92.7	0.7	0.3	0.4		0.97
DFC-dfc	22.5	dg 24h	69	5.161	6.015	3.111	0.0	100.0	0.0	0.0	0.0		
DEC-dec	22.5	dg 24h	120	-6.747	7.241	2.639	0.0	100.0	0.0	0.0	0.0		

Figure 26. Current direction (degree), station COI1210, Hindcast 1 (6/15/2012 - 8/16/2012).

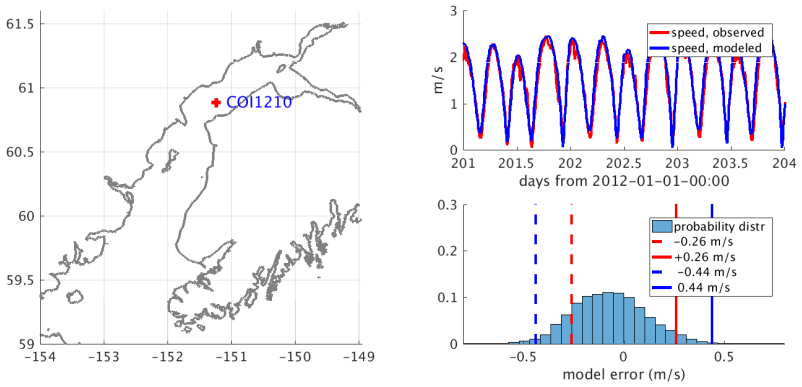

Station: CMIST COI1210 5.2m, Middle Ground Shoal
Observed data time period from: / 6/15/2012 to / 8/16/2012 with gaps of 0.00 days
Data gap is filled by SVD method
Data are not filtered

VARIABLE	X	N	IMAX	SM	RMSE	SD	NOF	CF	POF	MDNO	MDPO	WOF	SKILL
CRITERION	-	-	-	-	-	-	<1%	>90%	<1%	<N	<N	<.5%	
SCENARIO: HINDCAST													
U			14894	1.468									
u			14894	1.394									
U-u	44	cm/s 24h	14894	0.074	0.194	0.180	0.0	98.2	0.0	0.0	0.1		0.98
AFC-afc	44	cm/s 24h	69	-0.023	0.146	0.145	0.0	100.0	0.0	0.0	0.0		
AEC-aec	44	cm/s 24h	120	0.093	0.155	0.125	0.0	100.0	0.0	0.0	0.0		
TFC-tfc	0.50	h 25h	69	0.106	0.429	0.419	0.0	65.2	0.0	0.0	0.0		
TEC-tec	0.50	h 25h	120	-0.055	0.363	0.360	0.0	78.3	0.8	0.0	0.0		
TSF-tsf	0.25	h 25h	57	-0.070	0.179	0.166	0.0	96.5	0.0	0.0	0.0		
TEF-tef	0.25	h 25h	61	0.097	0.171	0.142	0.0	98.4	0.0	0.0	0.0		
TSE-tse	0.25	h 25h	34	-0.105	0.192	0.163	0.0	100.0	0.0	0.0	0.0		
TEE-tee	0.25	h 25h	37	-0.243	0.328	0.225	0.0	91.9	0.0	0.0	0.0		

Figure 27. Current speed (m/s), station COI1210, Hindcast 1 (6/15/2012 - 8/16/2012).

Table 9. Summary for current skill assessment, Hindcast 1 (around 6/14/2012 - 8/14/2012).

Station	Longitude	Latitude	Direction, X: 22.5 degree. CF (%)	Speed, X_0: 26 cm/s. CF (%)	Speed, X: 10% speed range. CF (%)
COI1201	-151.40	59.59	94.5%	95.1%	95.1%
COI1202	-151.92	59.42	98.2%	72.3%	74.3%
COI1203	-152.03	59.74	99.3%	90.7%	96.5%
COI1204	-151.08	62.06	96.7%	78.0%	98.5%
COI1205	-151.71	60.47	97.2%	71.7%	94.9%
COI1207	-150.36	61.06	92.9%	66.0%	86.4%
COI1208	-150.26	61.10	87.0%	81.0%	93.4%
COI1209	-150.20	61.18	95.2%	44.9%	65.2%
COI1210	-151.23	60.89	92.7%	81.8%	98.2%

Overall, the model predicted the current direction very well (Table 9); all current stations have a central frequency of >90%, except station COI1208. That particular station COI1208, where CF is 87.0%, is very close to southern tip of Fire Island which is located near the entrances of the Knik Arm and Turnagain Arm. This area is characterized by the vast muddy tidal flat off the shipping channel. That mud flat is relatively difficult to survey and to model as well. Also, mud flats are very much subject to sedimentation morphology. Subtle changes of the flat and the water channel will change the flow pattern greatly during flood and ebb.

The prediction of the current speed was not as accurate as the flow direction (Table 9). Of 6 out of 9 current stations, CF was above 90%. At station COI1202 (CF=74.2%, Southwest of Pt. Pogishi) near Seldovia, the model overestimated the current. At station COI1207 (Point Possession), CF of model current was 86.4%. At station COI1209 (CF=65.2%) near North Fire Island, histogram probability distribution shift toward negative, and the error had a negative bias. The model overestimated the current speed at COI1209 as well as at COI1202. Overall the timing of the current direction switch from the ebb to flood or flood to ebb is quite accurate from current speed plot and current direction plot (Figures 10-27), which can be further indicated by the small phase error of the dominant tidal current constituent M_2 (Appendix A).

Besides the skill assessment for currents near the sea surface, we also performed skill assessment for depth along the water column from 4-30 depth range in 2 meters interval. The velocity distribution along water column from 4-30 meter is quite uniform without much variation. The maximum velocity slightly decreases from near sea surface to 30 meters depth. The central frequency for both current direction and speed is very close to 5-6 meter depth results. In other words, 5-6 meter skill assessment has a very good representation of the water column in term of model current skill. We did not present the results at all depth except 5-6 meter depth in this report due to the redundancy.

3.3.3 Temperature Skill Assessment

There are continuous sea surface temperature measurements at the three CO-OPS stations of Anchorage, Nikiski, and Seldovia. Model skill is assessed for the period from 5/1/2012 to 9/3/2012 (Figure 28).

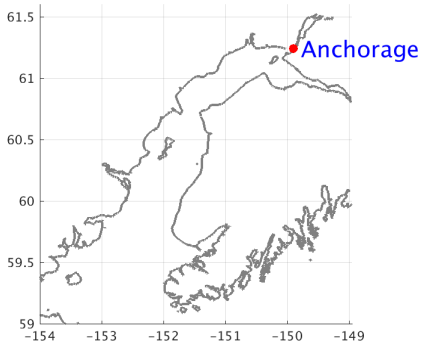

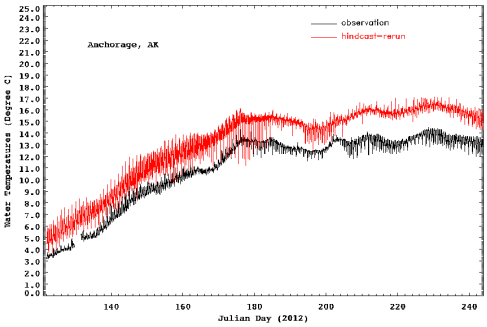


```
Station:                                Anchorage
Observed data time period from: / 5/ 1/2012  to / 9/ 3/2012 with gaps of    1.84 days
Data gap is filled using SVD method
Data are not filtered
-------------------------------------------------------------------------------------------------
VARIABLE    X     N   IMAX    SM    RMSE    SD     NOF   CF    POF   MONO  MDPO  WOF   SKILL
CRITERION   -     -    -      -      -      -     <1%  >90%   <1%    <N    <N  <.5%
-------------------------------------------------------------------------------------------------

     SCENARIO: HINDCAST
T                   29081  13.270
t                   29081  11.080
T-t        3.0 c 24h 29081   2.190  2.239  0.463   0.0  97.8   0.0    0.0  0.0          0.89
```

a. Anchorage.

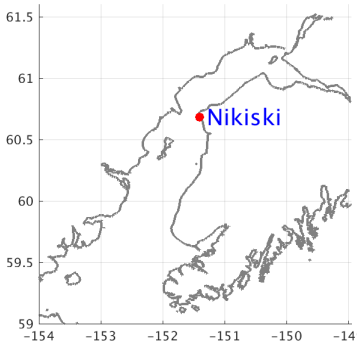

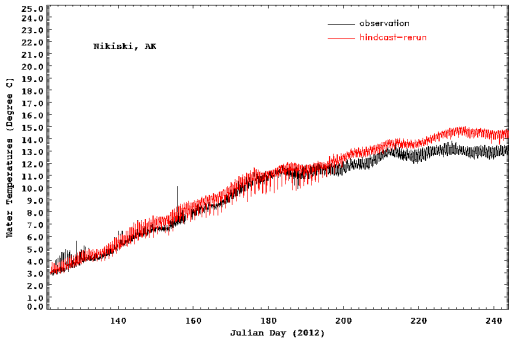


```
Station:                                Nikiski
Observed data time period from: / 5/ 1/2012  to / 9/ 3/2012 with gaps of    1.62 days
Data gap is filled using SVD method
Data are not filtered
-------------------------------------------------------------------------------------------------
VARIABLE    X     N   IMAX    SM    RMSE    SD     NOF   CF    POF   MONO  MDPO  WOF   SKILL
CRITERION   -     -    -      -      -      -     <1%  >90%   <1%    <N    <N  <.5%
-------------------------------------------------------------------------------------------------

     SCENARIO: HINDCAST
T                   29134  10.325
t                   29134   9.707
T-t        3.0 c 24h 29134   0.618  0.852  0.586   0.0 100.0   0.0    0.0  0.0          0.98
```

b. Nikiski.

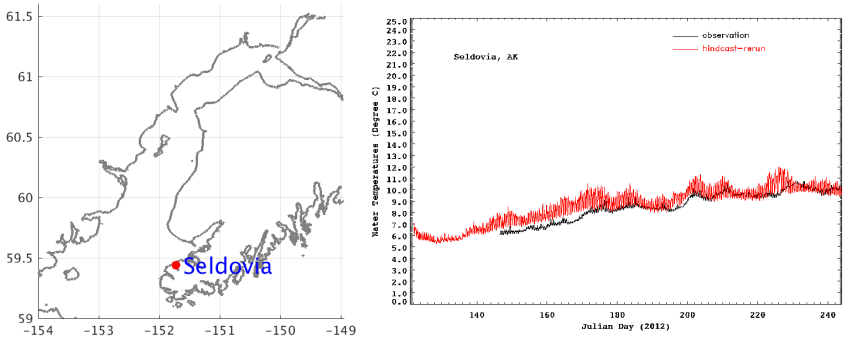


```
Station:                                  Seldovia
Observed data time period from: / 5/25/2012  to / 9/ 3/2012 with gaps of    0.00 days
Data gap is filled using SVD method
Data are not filtered
-------------------------------------------------------------------------------------------------
VARIABLE    X     N    IMAX    SM    RMSE    SD     NOF   CF    POF   MDNO  MDPO  WOF  SKILL
CRITERION   -     -     -      -      -      -     <1%  >90%   <1%    <N    <N  <.5%
-------------------------------------------------------------------------------------------------

     SCENARIO: HINDCAST
T                    23628   9.250
t                    23628   8.625
T-t        3.0 c 24h 23628   0.624  0.883  0.625   0.0 100.0   0.0    0.0   0.0        0.86
```

c. Seldovia

Figure 28. (Panel clockwise from top-left) Geographic location of stations, Graphic comparison between modeled and observed water temperature, and summary of sea surface temperature skill assessments, Hindcast 1 (5/1/2012 - 9/3/2012). a. Anchorage. b. Nikiski. c. Seldovia.

Table 10. Model temperature skill assessment at Anchorage, Nikiski, and Seldovia, Hindcast 1 (5/1/2012 - 9/3/2012).

Location	CF (%)	RMSE (degree)
Anchorage	98 %	2.24
Nikiski	100 %	0.85
Seldovia	100 %	0.88

The RMSE for both Nikiski and Seldovia was less than 1 degree Celsius, and their CF was 100% (Table 10). In the upper Cook Inlet, Anchorage station, the RMSE was 2.24 degree Celsius, much higher than Nikiski and Seldovia (Table 10), and CF was 98%. The figure shows an almost constant error (or bias) in the Anchorage. Another item about the sea surface temperature results is that the model daily variation of temperature is higher than the observed sea surface temperature.

3.4 Synoptic Hindcast 2 (2013-2015) Simulation and Skill Assessment

The Summer 2012 synoptic hindcast simulation only tested the CIOFS configuration for a single season. Therefore, in order to examine the performance of CIOFS over the four seasons and its behavior during the extreme conditions over the winter when the ice suppression algorithm will be active, a longer, multi-seasonal simulation was designed. Furthermore, as the fully operational set-up will be using G-RTOFS products for open ocean boundary forcing (temperature, salinity and sub-tidal water levels) it was decided to use this product for this second synoptic hindcast too. It was hoped that the simulation will contain at least two spring, summer, fall and winter seasons to ensure robustness and reliability. Furthermore, successful recovery of the model from the winter season's cooling effects needed to be tested.

A model simulation covering August 15, 2013 – September 15, 2015 was therefore planned and executed. The two main differences between this simulation and the summer 2012 simulation were: (i) the initial conditions were from the re-run (with convergent initial conditions) of the summer 2012 simulation assuming that August 2012 and August 2013 were similar and (ii) the use of G-RTOFS products for open boundary conditions as opposed to using climatological temperature and salinity fields. Initial attempts at running the simulation with a 5 second baroclinic timestep failed in numerical instabilities and so a reduction of the time step by 50% was performed to ensure the completion of the full 25-month simulation without any numerical instabilities. Hence, this is the recommended time step for the fully operational setup also. The horizontal current CFL numbers are plotted as histograms (Figure 29) and their small numbers attest to the numerical stability associated with using 2.5s as the baroclinic timestep. The vertical current CFL number has less meaning in these simulations due to the wetting-drying taking place.

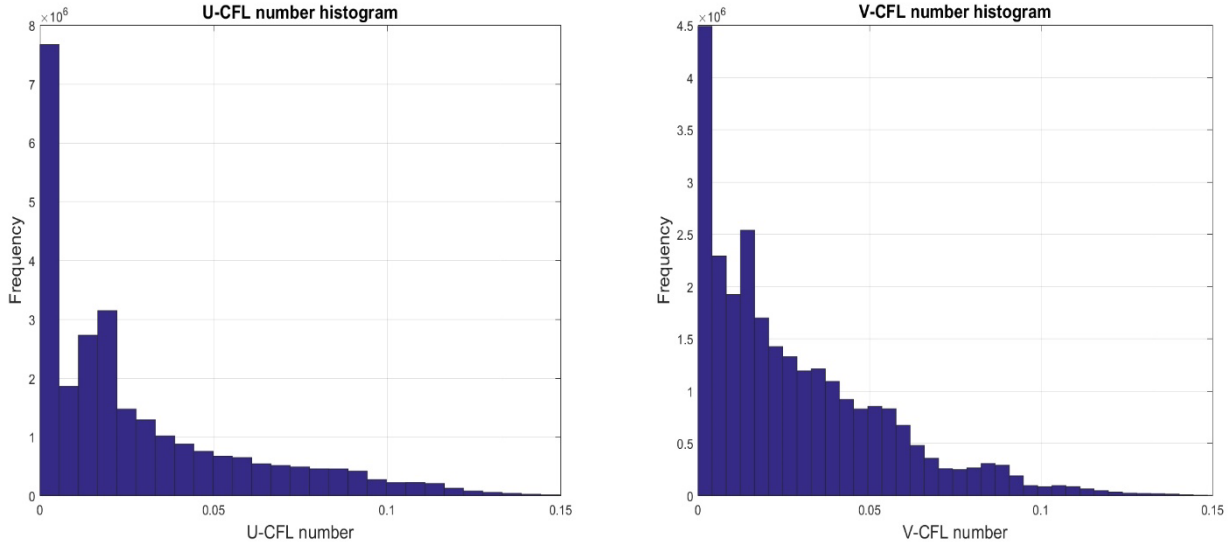

Figure 29. The CFL number distributions associated with the horizontal model currents.

We conducted skill assessment using the water level and temperature station data from CO-OPS tidal gauges. No salinity skill assessment was performed since there are no salinity data available at these stations.

3.4.1 Water Level Skill Assessment

Hindcast 2 water level skill assessment results were very similar to the Hindcast 1 skill assessment (Figure 30; Table 11). After demeaning the water level time series, the RMSE for Anchorage, Nikiski, and Seldovia was 29.5, 25.7 and 22.3 centimeters respectively. The RMSE had a trend of increase from lower Cook Inlet upstream towards upper Cook Inlet. Even with an increase of RMSE towards Anchorage, the CF was relatively high, all above 97%. That is consistent with the fact that the tidal range increased from the lower Cook Inlet upstream towards upper Cook Inlet, and the acceptable error magnitude X would increase as well. If we use the default acceptable error magnitude X_0, the skill deteriorates towards upper Cook Inlet (Table 11).

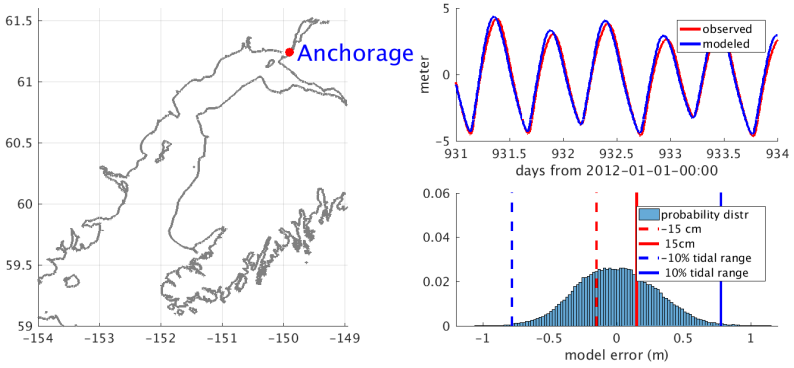

Station: Anchorage
Observed data time period from: /12/31/2013 to / 9/ 2/2015 with gaps of 0.00 days
Data gap is filled using SVD method
Data are not filtered

VARIABLE	X	N	IMAX	SM	RMSE	SD	NOF	CF	POF	MDNO	MDPO	WOF	SKILL
CRITERION	-	-	-	-	-	-	<1%	>90%	<1%	<N	<N	<.5%	
SCENARIO: HINDCAST													
H			145620	0.000									
h			145620	-0.026									
H-h	78	cm 24h	145620	0.026	0.295	0.293	0.0	99.5	0.0	0.0	0.0	0.00	1.00
AHW-ahw	78	cm 24h	1173	0.064	0.209	0.199	0.0	100.0	0.0	0.0	0.0		
ALW-alw	78	cm 24h	1172	0.158	0.268	0.217	0.0	99.9	0.0	0.0	0.0		
THW-thw	0.50	h 25h	1173	-0.265	0.315	0.172	0.0	89.4	0.0	0.0	0.0		
TLW-tlw	0.50	h 25h	1172	0.024	0.125	0.123	0.0	99.7	0.0	0.0	0.0		

a. Anchorage.

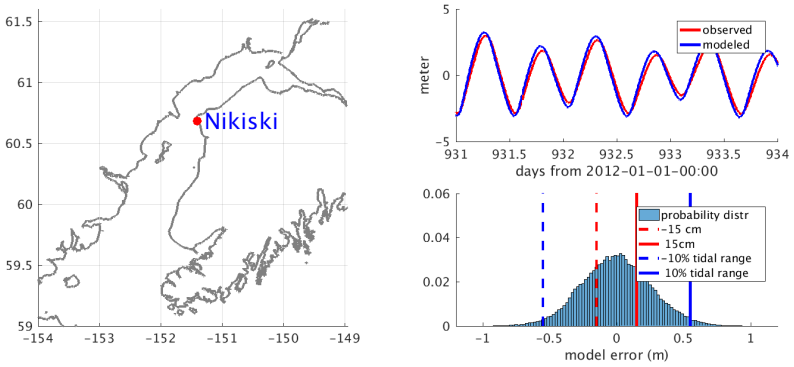

Station: Nikiski
Observed data time period from: /12/31/2013 to / 9/ 2/2015 with gaps of 0.00 days
Data gap is filled using SVD method
Data are not filtered

VARIABLE	X	N	IMAX	SM	RMSE	SD	NOF	CF	POF	MDNO	MDPO	WOF	SKILL
CRITERION	-	-	-	-	-	-	<1%	>90%	<1%	<N	<N	<.5%	
SCENARIO: HINDCAST													
H			145620	0.002									
h			145620	-0.045									
H-h	55 cm	24h	145620	0.047	0.257	0.253	0.0	97.0	0.0	0.0	0.0	0.00	1.00
AHW-ahw	55 cm	24h	1172	0.195	0.262	0.176	0.0	99.1	0.0	0.0	0.0		
ALW-alw	55 cm	24h	1172	-0.156	0.249	0.194	0.0	97.1	0.0	0.0	0.0		
THW-thw	0.50	h	25h	1172	-0.146	0.215	0.157	0.0	95.8	0.0	0.0	0.0	
TLW-tlw	0.50	h	25h	1172	-0.031	0.137	0.133	0.0	99.8	0.0	0.0	0.0	

b. Nikiski.

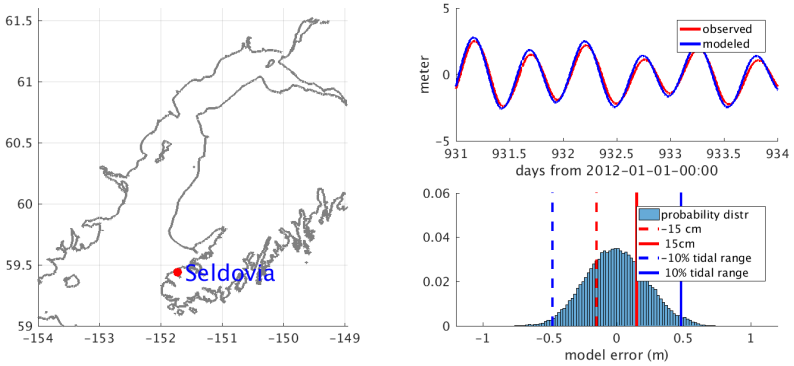

Station: Seldovia
Observed data time period from: /12/31/2013 to / 9/ 2/2015 with gaps of 0.00 days
Data gap is filled using SVD method
Data are not filtered

VARIABLE	X	N	IMAX	SM	RMSE	SD	NOF	CF	POF	MDNO	MDPO	WOF	SKILL
CRITERION	-	-	-	-	-	-	<1%	>90%	<1%	<N	<N	<.5%	
SCENARIO: HINDCAST													
H			145620	0.000									
h			145620	0.016									
H-h	48 cm	24h	145620	-0.015	0.223	0.222	0.0	97.1	0.0	0.0	0.0	0.00	1.00
AHW-ahw	48 cm	24h	1172	0.121	0.219	0.183	0.0	98.7	0.0	0.0	0.0		
ALW-alw	48 cm	24h	1172	-0.106	0.220	0.193	0.0	97.0	0.0	0.0	0.0		
THW-thw	0.50	h	25h	1172	-0.101	0.178	0.147	0.0	98.7	0.0	0.0	0.0	
TLW-tlw	0.50	h	25h	1172	-0.054	0.149	0.139	0.0	99.3	0.0	0.0	0.0	

c. Seldovia.

Figure 30. (Panel clockwise from top-left) Geographic location of stations, graphic comparison between modeled and observed water level, histogram of error probability distribution, and summary of water level (demeaned) skill assessments, Hindcast 2 (12/31/2013 - 9/2/2015). The histogram is the probability distribution of the error or mismatch between the model and observation. Red dashed line and red solid line define the range of [-X_0, X_0]., Blue dashed line and

blue solid line define the range of [-X, X]. , the probability within the range [-X, X] is the CF (central frequency). a. Anchorage. b. Nikiski. c. Seldovia.

Table 11. Summary of water level skill assessment, Hindcast 2 (12/31/2013 - 9/2/2015).

Location		X_0: 15cm	X_0: 15 cm with demeaning	X: 10% tidal range	X: 10% tidal range with demeaning
Anchorage	CF (%)	15%	37%	89%	100%
	RMSE (cm)	51.9	29.5	51.9	29.5
Nikiski	CF (%)	39%	44%	95%	97%
	RMSE (cm)	28.9	25.7	28.9	25.7
Seldovia	CF (%)	43%	49%	95%	97%
	RMSE (cm)	25.1	22.3	25.1	22.3

3.4.2 Temperature Skill Assessment

The sea surface temperature skill assessment was performed at three CO-OPS stations from 1/1/2014 to 7/28/2015, a period lasting about one and half years (Figure 31). While two stations have a CF of 100%, the temperature CF for Anchorage was 88.3%, and RMSE was 1.9 ºC (Table 12). There was a large discrepancy between the model temperature and observed temperature during the summer. The temperature bias in Anchorage area could be caused by a variety of factors, for example, net short-wave radiation, sensible and latent heat exchange, etc. From previous modeling experiences in high latitude, the summer differences in SST are often associated with the net short-wave radiation which dominated the sea surface heat flux budget. Since sea surface temperature is a tracer in a hydrodynamic model that would follow closely to the ambient air temperature, it is also very possible that the cause of the SST discrepancy is the biased forcing air temperature in Anchorage area. The temperature skill in the winter time was much better, with all stations 100% of the time within 3 degrees of the observed sea surface temperature. The summer temperature is something to follow closely in the operational setting.

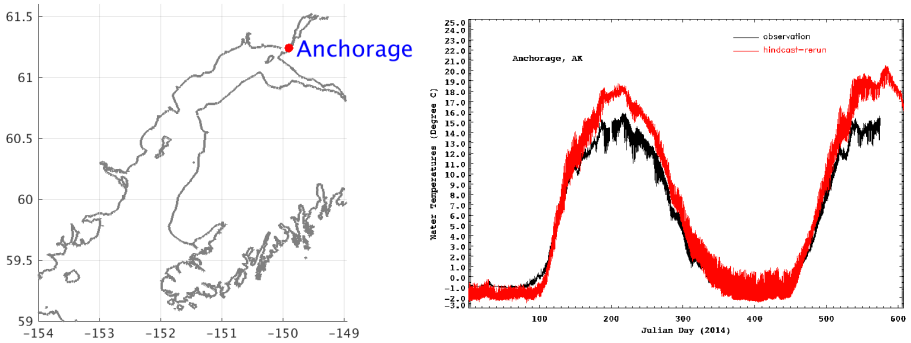


```
Station:                                    Anchorage
Observed data time period from: / 1/ 1/2014  to / 7/28/2015 with gaps of    3.63 days
Data gap is filled using SVD method
Data are not filtered
-------------------------------------------------------------------------------------------
VARIABLE    X     N   IMAX    SM    RMSE    SD     NOF   CF    POF   MDNO  MDPO  WOF  SKILL
CRITERION   -     -   -       -     -       -      <1%   >90%  <1%   <N    <N    <.5%
-------------------------------------------------------------------------------------------

     SCENARIO: HINDCAST
T                  136850   6.152
t                  136850   5.311
T-t       3.0 c 24h136850   0.841  1.901  1.705   0.0   88.3   0.1    0.0   0.9        0.98
```

a. Anchorage.

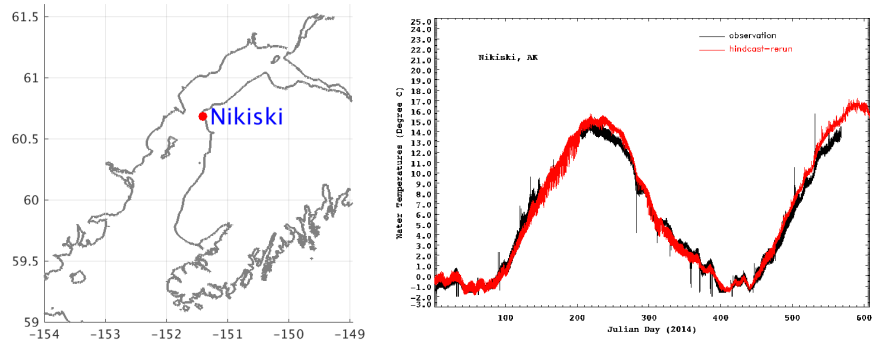


```
Station:                                    Nikiski
Observed data time period from: / 1/ 1/2014  to / 7/22/2015 with gaps of   21.78 days
Data gap is filled using SVD method
Data are not filtered
-------------------------------------------------------------------------------------------
VARIABLE    X     N   IMAX    SM    RMSE    SD     NOF   CF    POF   MDNO  MDPO  WOF  SKILL
CRITERION   -     -   -       -     -       -      <1%   >90%  <1%   <N    <N    <.5%
-------------------------------------------------------------------------------------------

     SCENARIO: HINDCAST
T                  130875   5.301
t                  130875   5.056
T-t       3.0 c 24h130875   0.245  0.689  0.645   0.0  100.0   0.0    0.0   0.0        1.00
```

b. Nikiski.

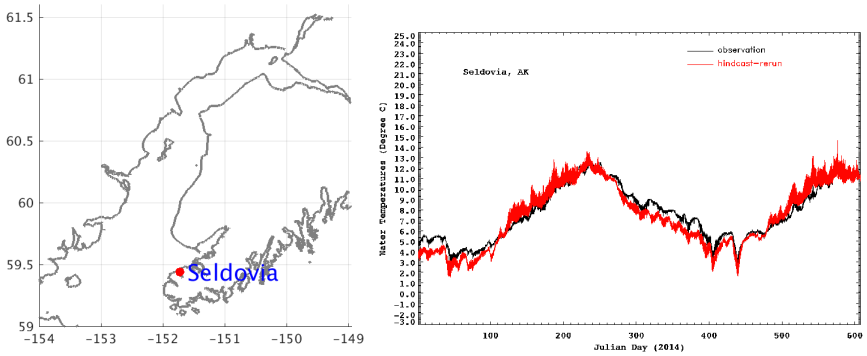


```
Station:                                  Seldovia
Observed data time period from: / 1/ 1/2014  to / 7/23/2015 with gaps of    1.71 days
Data gap is filled using SVD method
Data are not filtered
-------------------------------------------------------------------------------------------
VARIABLE     X      N    IMAX     SM     RMSE     SD      NOF   CF     POF   MDNO  MDPO  WOF  SKILL
CRITERION    -      -      -      -       -       -      <1%  >90%   <1%    <N    <N  <.5%
-------------------------------------------------------------------------------------------

     SCENARIO: HINDCAST
T                   136088   7.169
t                   136088   7.431
T-t        3.0 c 24h136088  -0.262  0.946  0.909   0.0   99.9   0.0    0.0   0.0        0.97
```

c. Seldovia.

Figure 31. (Panel clockwise from top-left) Geographic location of stations, Graphic comparison between modeled and observed water temperature, and summary of sea surface temperature skill assessments, Hindcast 2 (1/1/2014 - 7/28/2015). a. Anchorage. b. Nikiski. c. Seldovia.

Table 12. Model temperature skill assessment at Anchorage, Nikiski, and Seldovia, Hindcast 2 (1/1/2014 - 7/28/2015).

Location\criteria	Entire period		Winter (December, January, February) only	
	CF (%)	RMSE (degree)	CF (%)	RMSE (degree)
Anchorage	88.3 %	1.90	100 %	0.88
Nikiski	100 %	0.69	100 %	0.45
Seldovia	99.9 %	0.95	100 %	1.16

There are no current measurements data available during the 2013-2015 synoptic hindcast simulation time period. Therefore, a visual comparison of the currents from this hindcast with those from the summer 2012 hindcast was carried out. It was found that they were very similar in nature thereby confirming that the two simulations were similar in nature and the use of different open boundary data sources (G-RTOFS versus monthly climatology) or a 50% reduction in the baroclinic time step does not adversely affect the quality of the model predictions.

One of the main aims of this second synoptic hindcast was to examine what happens to the model predictions during the winter months and the effectiveness of the ice suppression algorithm in ROMS. An inspection of the temperature and salinity fields during the winter months showed no abnormal values over most of the grid points with isolated locations having abnormally low/high temperature and salinity values from time to time. These locations occurred on topography (that

experience wetting-drying periodically) during drying period with no continuous wet-point connection to the open water. There were no abnormal temperature or salinity values over the locations where bathymetry was present (relative to an MSL datum and where the water surface elevation was zero).

4. CONCLUSION AND FUTURE WORK

The Cook Inlet Operational Forecast System (CIOFS) has been developed using the state-of-art hydrodynamic ocean model ROMS. The model covers the entire Cook Inlet and waters leading to Cook Inlet around the Kodiak Archipelago (including Shelikof Strait, Stevenson Entrance, Kennedy Entrance and Chugach Passage). The major purpose of CIOFS is to provide water level and current guidance to the mariner in and out of the ports in the Cook Inlet. CIOFS also provides a platform for future particle tracking, water quality and ecosystem modelling work in the Cook Inlet region.

The observed data used for the model validation and skill assessment include 1) observed water level and surface water temperature from long-term CO-OPS stations in Seldovia, Nikiski, and Anchorage, and 2) two month-long current observations deployed in the summer of 2012.

Three numerical simulations have been performed based on availability of observed data sets. One tidal only simulation and two hindcast simulations were conducted. Of the two hindcast simulations, the first hindcast simulated from 1/1/2012 to 9/15/2012, which coincided with summer 2012 current meter deployments in Cook Inlet. The second hindcast simulation lasted two years from 8/15/2013 to 9/15/2015. The skill assessments based on the observations were performed. The water level prediction performed very well for both hindcasts. Central Frequency (CF) was more than 95% from all water level stations. The major finding of the water level skill assessment is that the RMSE was higher in the upper Cook Inlet (Anchorage) where it is shallow, muddy, and the tidal range can be 8-9 meters high.

At two stations in the lower and middle Cook Inlet, Soldovia and Nikiski, for temperature skill assessment, the CF was always more than 99.9%, mostly approaching 100%. In the upper Cook Inlet (Anchorage), the model temperature, especially during the summer, usually had a warm bias. Since the sea surface temperature field usually is a very passive state variable, sea surface temperature bias is most likely due to bias of the meteorological temperature field. With gradual improvement of weather models, the surface forcing bias should be able to be reduced along with the hydrodynamic model results. The CF of temperature skill assessment at Anchorage are 98% for Hindacast 1 (assessment period: 5/1/2012 - 9/3/2012) and 88.3% for Hindcast 2 (assessment period: 1/1/2014 - 7/28/2015) respectively.

For current skill assessment, the current direction was simulated well. At 8 out of 9 current observation locations, CF of current direction was above 90%. One station near South Fire Island had a low CF value (87.0). For current magnitude, 7 out of 9 stations had a CF value above 85%. One of the low CF value stations was near the north coast of Fire Island, and another station was near Seldovia. Both stations overpredicted current speed.

Cook Inlet has qualities that make it challenging to develop an OFS, for example: extreme diurnal/semidiurnal high water level change, extensive mudflats in the upper Cook Inlet region, lack of accurate bathymetry data in the upper Cook Inlet region, and lack of observation data for all the state variables. Overall, CIOFS fulfilled its original task to provide water level and currents guidance, as well as temperature.

There are a few issues that may point to a direction to improve the performance of CIOFS. The first item is to improve the tides and tidal currents of CIOFS. There are regular occurrences of tidal bores in the Turnagain Arm of upper Cook Inlet. Since tidal bores produce a discontinuity like a shock wave, simulation of tidal bores would be impossible using conventional hydrodynamic ocean models. How to cope with a nonlinearity like a tidal bore to improve the water level and current prediction in upper Cook Inlet would be a key for future improvement.

In Cook Inlet, there are vast areas of tidal mud flats which are dried out during low water and submerged during high water. Tidal flats are difficult to survey and the bottom topography is under constant change especially when there are strong currents and large sediment discharges from the river. Better bathymetry survey data, and even a coupled sediment transport and morphological model would be useful.

One of the most significant developments relevant to OFSs recently is the development of the National Water Model (NWM), which would provide a nation-wide forecast of the over-land ground runoff from rivers. The Alaska part of the NWM is expected to be implemented in the next couple of years. Once the NWM for Alaska is available, CIOFS should have a much more accurate and more complete river input file that should also include forecast information.

Another issue of CIOFS is that currently the river input in the model is in a fixed location that will never be dried out during low water. An improvement of the hydrodynamic model would be to allow the river injection in the model be far more upstream at higher elevation, which would be a better representation of reality. Considering that the CIOFS mesh grid is up to 15 meters above MSL, a more realistic dynamic interaction between water from inland and coastal/estuarine water will further improve the model.

Data availability greatly hindered the development of CIOFS. Because of this, we did not try to validate the salinity output. In the future, salinity would be one variable to be validate against.

The last item regarding improvements in the model is the ice in Cook Inlet. Although Cook Inlet is free of ice most times of the year, there is ice in Cook Inlet during the winter, especially in the upper Cook Inlet. Surely, ice will have some impact on navigation in the Cook Inlet. Ice should be the priority in the future development/refinement of CIOFS.

ACKNOWLEDGEMENTS

The authors would like to thank Dr. Christopher Paternostro and his group's work for the tidal current observation field campaign in Cook Inlet in 2012, and for providing the data from the survey.

REFERENCES

Brabets, T.P., G.L. Nelson, J.M. Dorava, and A.M. Milner, 1999. Water-quality assessment of the Cook Inlet basin, Alaska : environmental setting. U.S. Geological Survey Water-Resources Investigations Report 99-4025 National Water-Quality Assessment Program U.S. Dept. of the Interior, U.S. Geological Survey ; U.S. Geological Survey, Branch of Information Services.

Deltares, 2014. RGFGRID User Manual: generation and manipulation of curvilinear grids for Delft3D-FLOW and Delft3D-Wave. Deltares, Delft, The Netherlands.

DiMego, G., 2012. Mesoscale Modeling Branch (NAM Mostly). Proceedings, 2012 NCEP Product Review, NOAA/NWS/National Centers for Environmental Prediction, Environmental Modeling Center, NCWCP, Riverdale, MD (Available at http://www.emc.ncep.noaa.gov/mmb/mmbpll/misc/MMB.ProdSuiteRev.Dec2012.pptx).

Fairall, C.W., E.F. Bradley, D.P. Rogers, J.B. Edson, and G.S. Young, 1996. Bulk parameterization of air–sea fluxes in TOGA COARE. J. Geophys. Res., 101, 3747–3767.

Fairall, C.W., E.F. Bradley, J.E. Hare, A.A. Grachev, and J.B. Edson, 2003. Bulk parameterization of air–sea fluxes: updates and verification for the COARE algorithm. J. Climate, 16, 571-591.

Hess, K., T. Gross, R. Schmalz, J. Kelley, F. Aikman III, E. Wei, and M. Vincent, 2003. NOS Standards for Evaluating Operational Nowcast and Forecast Hydrodynamic Model Systems. NOAA Tech Report NOS CS 17, Silver Spring, Maryland. 47 pp.

Haidvogel, D.B., H.G. Arango, K.S. Hedstrom, A. Beckmann, P. Malanotte-Rizzoli, and A.F. Shchepetkin, 2000. Model evaluation experiments in the North Atlantic Basin simulations in nonlinear terrain-following coordinates. Dynamics of Atmospheres and Oceans, 32, 239–281.

Lanerolle, L., R.C. Patchen, and F. Aikman III, 2011. The second generation Chesapeake Bay Operational Forecast System (CBOFS2): model development and skill assessment. NOAA Technical Report NOS CS29, Silver Spring, Maryland; 91p.

Lanerolle, L., C. Paternostro, G. Dusek, L. McLaughlin, and S. Skaling, 2012. An assessment of the renewable hydrokinetic energy potential in Cook Inlet, Alaska. In Proceedings of the OCEANS Conference, Virginia Beach, VA, USA, 14–19 October 2012.

Mellor, G.L., T. Yamada, 1982. Development of a turbulence closure model for geophysical fluid problems. Reviews of Geophysics and Space Physics, 20, 851–875.

Preisendorfer, R. W., 1988. Principal Component Analysis in Meteorology and Oceanography. Developments in Atmospheric Science, v. 17. Elsevier, Amsterdam. pp 425.

Shchepetkin, A.F., J.C. McWilliams, 2003. A method for computing horizontal pressure-gradient force in an oceanic model with a nonaligned vertical coordinate. Journal of Geophysical Research, 108 (C3), 3090-.

Shchepetkin, A.F., J.C. McWilliams, 2005. The regional oceanic modeling system (ROMS) a split-explicit, free-surface, topography following-coordinate oceanic model. Ocean Modelling, 9 (4), 347–404.

Spargo, E., J. Westerink, R. Luettich, and D. Mark, 2003. ENPAC 2003: A Tidal Constituent Database for Eastern North Pacific Ocean. Technical Report ERDC/CHL TR-04-12, U.S. Army Engineer Research and Development Center, Coastal and Hydraulics Laboratory, Vicksburg, MS, USA, 2004; Available online:

http://www.unc.edu/ims/ccats/tides/ENPAC_2003_report.pdf (accessed on 18 September 2018).

Umlauf, L., H. Burchard, 2003. A generic length-scale equation for geophysical turbulence models. J. Marine Res., 61, 235–265.

Warner, J.C., C.R. Sherwood, H.G. Arango, and R.P. Signell, 2005. Performance of Four Turbulence Closure Methods Implemented Using a Generic Length Scale Method. Journal: Ocean Modelling, 8 (1-2), 81-113.

Zhang, A., K.W. Hess and F. Aikman III, 2010. User-based Skill Assessment Techniques for Operational Hydrodynamic Forecast Systems. Journal of Operational Oceanography, Volume 3 (2), 11-24.

APPENDIX A. COMPARISON OF OBSERVED AND MODELED CURRENTS TIDAL HARMONIC ANALYSIS RESULTS

Table A-1. Comparison of tidal constituent amplitudes (m/s) and epochs (degree) for tidal currents. Station: COI1201, depth: 6.4m.

```
Station: "CMIST COI1201  6.4m, Homer Spit, bin 28
Observation: Least Squares H.A.  Beginning  6-20-2012  at Hour  9.90
Model: Least Squares H.A.  Beginning  6-12-2012  at Hour  0.00
 Amplitudes are in m/s, and Phase is in degrees (GMT)
```

N	Constituent	Observed(R= 0.147) Amplitude	Epoch	Modeled(R= 0.169) Amplitude	Epoch	Difference Amplitude	Epoch
CURRENT ALONG PCD		DIR= 31		DIR= 33			
1	M(2)	0.297	254.7	0.283	247.6	-0.014	-7.1
2	S(2)	0.106	289.3	0.141	302.0	0.035	12.7
3	N(2)	0.063	226.5	0.064	218.6	0.001	-7.9
4	K(1)	0.200	149.6	0.059	209.1	-0.141	59.5
5	M(4)	0.050	354.9	0.023	75.1	-0.027	80.2
6	O(1)	0.016	156.0	0.034	216.6	0.018	60.6
7	M(6)	0.024	84.3	0.014	133.6	-0.010	49.3
8	MK(3)	0.012	352.9	0.020	51.6	0.008	58.7
9	S(4)	0.006	26.5	0.004	254.4	-0.002	132.1
10	MN(4)	0.000	0.0	0.014	63.9	0.000	0.0
11	NU(2)	0.000	0.0	0.011	98.2	0.000	0.0
12	S(6)	0.003	156.0	0.001	314.4	-0.002	158.4
13	MU(2)	0.000	0.0	0.010	129.9	0.000	0.0
14	2N(2)	0.024	57.9	0.006	149.2	-0.018	91.3
15	OO(1)	0.000	0.0	0.006	68.7	0.000	0.0
16	LAMBDA(2)	0.000	0.0	0.009	106.2	0.000	0.0
17	S(1)	0.346	285.9	0.000	0.0	-0.346	74.1
18	M(1)	0.011	16.8	0.004	102.3	-0.007	85.5
19	J(1)	0.006	243.8	0.007	183.3	0.001	-60.5
20	MM	0.000	0.0	0.013	13.4	0.000	0.0
21	SSA	0.000	0.0	1.341	234.6	0.000	0.0
22	SA	0.000	0.0	5.257	297.3	0.000	0.0
23	MSF	0.000	0.0	0.015	111.5	0.000	0.0
24	MF	0.000	0.0	0.024	170.6	0.000	0.0
25	RHO(1)	0.000	0.0	0.005	71.5	0.000	0.0
26	Q(1)	0.004	49.5	0.005	180.3	0.001	130.8
27	T(2)	0.000	0.0	0.041	329.6	0.000	0.0
28	R(2)	0.000	0.0	0.000	0.0	0.000	0.0
29	2Q(1)	0.009	209.2	0.008	297.3	-0.001	88.1
30	P(1)	0.153	83.2	0.019	232.2	-0.134	149.0
31	2SM(2)	0.000	0.0	0.004	156.8	0.000	0.0
32	M(3)	0.000	0.0	0.004	174.6	0.000	0.0
33	L(2)	0.008	16.2	0.014	33.2	0.006	17.0
34	2MK(3)	0.000	0.0	0.018	27.8	0.000	0.0
35	K(2)	0.033	293.7	0.021	317.7	-0.012	24.0
36	M(8)	0.008	167.8	0.004	307.6	-0.004	139.8
37	MS(4)	0.031	50.9	0.020	133.7	-0.011	82.8
CURRENT ACROSS PCD		DIR= 121		DIR= 123			
1	M(2)	0.048	191.3	0.075	172.9	0.027	-18.4
2	S(2)	0.000	0.0	0.075	124.3	0.000	0.0
3	N(2)	0.014	176.2	0.021	190.5	0.007	14.3
4	K(1)	0.079	58.7	0.023	181.3	-0.056	122.6
5	M(4)	0.035	216.7	0.033	209.2	-0.002	-7.5
6	O(1)	0.005	156.4	0.018	45.0	0.013	-111.4

7	M(6)	0.012	231.9	0.021	357.0	0.009	125.1
8	MK(3)	0.021	173.6	0.033	195.3	0.012	21.7
9	S(4)	0.006	215.6	0.011	326.0	0.005	110.4
10	MN(4)	0.000	0.0	0.015	205.3	0.000	0.0
11	NU(2)	0.000	0.0	0.017	187.4	0.000	0.0
12	S(6)	0.007	326.5	0.002	57.9	-0.005	91.4
13	MU(2)	0.000	0.0	0.006	227.2	0.000	0.0
14	2N(2)	0.016	214.0	0.002	48.1	-0.014	-165.9
15	OO(1)	0.000	0.0	0.001	309.9	0.000	0.0
16	LAMBDA(2)	0.000	0.0	0.007	100.0	0.000	0.0
17	S(1)	0.129	197.3	0.054	345.7	-0.075	148.4
18	M(1)	0.006	197.4	0.002	161.2	-0.004	-36.2
19	J(1)	0.007	311.9	0.005	342.5	-0.002	30.6
20	MM	0.000	0.0	0.011	298.6	0.000	0.0
21	SSA	0.000	0.0	0.000	0.0	0.000	0.0
22	SA	0.000	0.0	0.136	120.1	0.000	0.0
23	MSF	0.000	0.0	0.001	317.6	0.000	0.0
24	MF	0.000	0.0	0.007	304.9	0.000	0.0
25	RHO(1)	0.000	0.0	0.002	261.9	0.000	0.0
26	Q(1)	0.004	219.0	0.004	18.0	0.000	159.0
27	T(2)	0.037	142.6	0.057	95.2	0.020	-47.4
28	R(2)	0.107	186.0	0.000	0.0	-0.107	174.0
29	2Q(1)	0.002	254.8	0.002	286.0	0.000	31.2
30	P(1)	0.057	351.6	0.031	111.9	-0.026	120.3
31	2SM(2)	0.000	0.0	0.003	38.6	0.000	0.0
32	M(3)	0.000	0.0	0.006	24.7	0.000	0.0
33	L(2)	0.013	279.8	0.006	18.4	-0.007	98.6
34	2MK(3)	0.000	0.0	0.021	177.5	0.000	0.0
35	K(2)	0.075	234.9	0.036	170.1	-0.039	-64.8
36	M(8)	0.010	344.0	0.006	63.6	-0.004	79.6
37	MS(4)	0.025	252.7	0.029	265.4	0.004	12.7

Table A-2. Comparison of tidal constituent amplitudes (m/s) and epochs (degree) for tidal currents. Station: COI1202, depth: 4.6m.

Station: "CMIST COI1202 4.6m, Pt. Pogishi, SW of
Observation: Least Squares H.A. Beginning 6-13-2012 at Hour 20.20
Model: Least Squares H.A. Beginning 6-12-2012 at Hour 0.00
Amplitudes are in m/s, and Phase is in degrees (GMT)

N	Constituent	Observed(R= 0.013) Amplitude	Epoch	Modeled(R= 0.012) Amplitude	Epoch	Difference Amplitude	Epoch
CURRENT ALONG PCD		DIR= 36		DIR= 35			
1	M(2)	1.156	246.6	1.409	250.7	0.253	4.1
2	S(2)	0.737	287.9	0.490	275.3	-0.247	-12.6
3	N(2)	0.224	202.2	0.278	214.6	0.054	12.4
4	K(1)	0.043	151.4	0.144	159.4	0.101	8.0
5	M(4)	0.022	205.8	0.029	225.5	0.007	19.7
6	O(1)	0.030	177.7	0.064	171.7	0.034	-6.0
7	M(6)	0.053	269.2	0.061	241.3	0.008	-27.9
8	MK(3)	0.019	240.2	0.036	15.8	0.017	135.6
9	S(4)	0.014	291.6	0.002	322.2	-0.012	30.6
10	MN(4)	0.000	0.0	0.015	185.9	0.000	0.0
11	NU(2)	0.000	0.0	0.019	306.6	0.000	0.0
12	S(6)	0.005	249.6	0.010	251.0	0.005	1.4
13	MU(2)	0.000	0.0	0.103	117.4	0.000	0.0
14	2N(2)	0.110	336.6	0.037	258.6	-0.073	-78.0
15	OO(1)	0.000	0.0	0.023	294.6	0.000	0.0
16	LAMBDA(2)	0.000	0.0	0.036	291.4	0.000	0.0
17	S(1)	0.084	120.3	0.000	0.0	-0.084	-120.3
18	M(1)	0.021	323.6	0.020	302.5	-0.001	-21.1
19	J(1)	0.016	70.0	0.018	350.0	0.002	80.0
20	MM	0.000	0.0	0.031	203.3	0.000	0.0
21	SSA	0.000	0.0	0.017	218.4	0.000	0.0
22	SA	0.000	0.0	0.000	0.0	0.000	0.0
23	MSF	0.000	0.0	0.050	216.4	0.000	0.0
24	MF	0.000	0.0	0.006	186.8	0.000	0.0
25	RHO(1)	0.000	0.0	0.022	145.7	0.000	0.0
26	Q(1)	0.002	297.4	0.021	212.7	0.019	-84.7
27	T(2)	0.274	300.4	0.000	0.0	-0.274	59.6
28	R(2)	0.000	0.0	0.000	0.0	0.000	0.0
29	2Q(1)	0.011	189.3	0.005	146.2	-0.006	-43.1
30	P(1)	0.000	0.0	0.023	121.5	0.000	0.0
31	2SM(2)	0.000	0.0	0.016	217.4	0.000	0.0
32	M(3)	0.000	0.0	0.003	159.8	0.000	0.0
33	L(2)	0.077	353.7	0.040	340.6	-0.037	-13.1
34	2MK(3)	0.000	0.0	0.006	300.4	0.000	0.0
35	K(2)	0.154	333.2	0.146	275.7	-0.008	-57.5
36	M(8)	0.012	275.6	0.034	274.3	0.022	-1.3
37	MS(4)	0.024	265.9	0.018	251.4	-0.006	-14.5
CURRENT ACROSS PCD		DIR= 126		DIR= 125			
1	M(2)	0.062	341.6	0.055	353.5	-0.007	11.9
2	S(2)	0.000	0.0	0.032	63.1	0.000	0.0
3	N(2)	0.012	297.5	0.012	296.3	0.000	-1.2
4	K(1)	0.052	290.4	0.000	0.0	-0.052	69.6
5	M(4)	0.020	37.8	0.024	19.6	0.004	-18.2
6	O(1)	0.017	259.8	0.016	243.7	-0.001	-16.1
7	M(6)	0.026	216.2	0.046	210.7	0.020	-5.5
8	MK(3)	0.006	119.7	0.010	46.0	0.004	-73.7
9	S(4)	0.002	347.7	0.004	109.2	0.002	121.5
10	MN(4)	0.000	0.0	0.008	353.9	0.000	0.0

11	NU(2)	0.000	0.0	0.010	46.5	0.000	0.0
12	S(6)	0.001	108.8	0.004	181.9	0.003	73.1
13	MU(2)	0.000	0.0	0.014	235.8	0.000	0.0
14	2N(2)	0.012	51.7	0.007	53.8	-0.005	2.1
15	OO(1)	0.000	0.0	0.004	94.4	0.000	0.0
16	LAMBDA(2)	0.000	0.0	0.003	21.6	0.000	0.0
17	S(1)	0.083	88.7	0.023	200.4	-0.060	111.7
18	M(1)	0.004	79.8	0.007	95.8	0.003	16.0
19	J(1)	0.005	115.4	0.009	163.6	0.004	48.2
20	MM	0.000	0.0	0.028	206.2	0.000	0.0
21	SSA	0.000	0.0	0.531	215.7	0.000	0.0
22	SA	0.000	0.0	1.901	287.5	0.000	0.0
23	MSF	0.000	0.0	0.037	225.3	0.000	0.0
24	MF	0.000	0.0	0.014	211.2	0.000	0.0
25	RHO(1)	0.000	0.0	0.004	314.9	0.000	0.0
26	Q(1)	0.002	99.0	0.001	304.8	-0.001	154.2
27	T(2)	0.033	15.8	0.024	112.4	-0.009	96.6
28	R(2)	0.125	19.3	0.000	0.0	-0.125	-19.3
29	2Q(1)	0.006	172.3	0.004	266.2	-0.002	93.9
30	P(1)	0.042	237.5	0.007	249.4	-0.035	11.9
31	2SM(2)	0.000	0.0	0.006	329.9	0.000	0.0
32	M(3)	0.000	0.0	0.002	151.7	0.000	0.0
33	L(2)	0.005	113.7	0.010	132.3	0.005	18.6
34	2MK(3)	0.000	0.0	0.017	37.8	0.000	0.0
35	K(2)	0.085	63.6	0.006	187.2	-0.079	123.6
36	M(8)	0.006	45.7	0.012	292.5	0.006	113.2
37	MS(4)	0.005	29.9	0.010	64.3	0.005	34.4

Table A-3. Comparison of tidal constituent amplitudes (m/s) and epochs (degree) for tidal currents. Station: COI1203, depth: 5.8m.

Station: "CMIST COI1201 6.4m, Homer Spit, bin 28
Observation: Least Squares H.A. Beginning 6-20-2012 at Hour 9.90
Model: Least Squares H.A. Beginning 6-12-2012 at Hour 0.00
 Amplitudes are in m/s, and Phase is in degrees (GMT)

N	Constituent	Observed(R= 0.147) Amplitude	Epoch	Modeled(R= 0.169) Amplitude	Epoch	Difference Amplitude	Epoch
CURRENT ALONG PCD		DIR= 31		DIR= 33			
1	M(2)	0.297	254.7	0.283	247.6	-0.014	-7.1
2	S(2)	0.106	289.3	0.141	302.0	0.035	12.7
3	N(2)	0.063	226.5	0.064	218.6	0.001	-7.9
4	K(1)	0.200	149.6	0.059	209.1	-0.141	59.5
5	M(4)	0.050	354.9	0.023	75.1	-0.027	80.2
6	O(1)	0.016	156.0	0.034	216.6	0.018	60.6
7	M(6)	0.024	84.3	0.014	133.6	-0.010	49.3
8	MK(3)	0.012	352.9	0.020	51.6	0.008	58.7
9	S(4)	0.006	26.5	0.004	254.4	-0.002	132.1
10	MN(4)	0.000	0.0	0.014	63.9	0.000	0.0
11	NU(2)	0.000	0.0	0.011	98.2	0.000	0.0
12	S(6)	0.003	156.0	0.001	314.4	-0.002	158.4
13	MU(2)	0.000	0.0	0.010	129.9	0.000	0.0
14	2N(2)	0.024	57.9	0.006	149.2	-0.018	91.3
15	OO(1)	0.000	0.0	0.006	68.7	0.000	0.0
16	LAMBDA(2)	0.000	0.0	0.009	106.2	0.000	0.0
17	S(1)	0.346	285.9	0.000	0.0	-0.346	74.1
18	M(1)	0.011	16.8	0.004	102.3	-0.007	85.5
19	J(1)	0.006	243.8	0.007	183.3	0.001	-60.5
20	MM	0.000	0.0	0.013	13.4	0.000	0.0
21	SSA	0.000	0.0	1.341	234.6	0.000	0.0
22	SA	0.000	0.0	5.257	297.3	0.000	0.0
23	MSF	0.000	0.0	0.015	111.5	0.000	0.0
24	MF	0.000	0.0	0.024	170.6	0.000	0.0
25	RHO(1)	0.000	0.0	0.005	71.5	0.000	0.0
26	Q(1)	0.004	49.5	0.005	180.3	0.001	130.8
27	T(2)	0.000	0.0	0.041	329.6	0.000	0.0
28	R(2)	0.000	0.0	0.000	0.0	0.000	0.0
29	2Q(1)	0.009	209.2	0.008	297.3	-0.001	88.1
30	P(1)	0.153	83.2	0.019	232.2	-0.134	149.0
31	2SM(2)	0.000	0.0	0.004	156.8	0.000	0.0
32	M(3)	0.000	0.0	0.004	174.6	0.000	0.0
33	L(2)	0.008	16.2	0.014	33.2	0.006	17.0
34	2MK(3)	0.000	0.0	0.018	27.8	0.000	0.0
35	K(2)	0.033	293.7	0.021	317.7	-0.012	24.0
36	M(8)	0.008	167.8	0.004	307.6	-0.004	139.8
37	MS(4)	0.031	50.9	0.020	133.7	-0.011	82.8
CURRENT ACROSS PCD		DIR= 121		DIR= 123			
1	M(2)	0.048	191.3	0.075	172.9	0.027	-18.4
2	S(2)	0.000	0.0	0.075	124.3	0.000	0.0
3	N(2)	0.014	176.2	0.021	190.5	0.007	14.3
4	K(1)	0.079	58.7	0.023	181.3	-0.056	122.6
5	M(4)	0.035	216.7	0.033	209.2	-0.002	-7.5
6	O(1)	0.005	156.4	0.018	45.0	0.013	-111.4
7	M(6)	0.012	231.9	0.021	357.0	0.009	125.1
8	MK(3)	0.021	173.6	0.033	195.3	0.012	21.7
9	S(4)	0.006	215.6	0.011	326.0	0.005	110.4
10	MN(4)	0.000	0.0	0.015	205.3	0.000	0.0

11	NU(2)	0.000	0.0	0.017	187.4	0.000	0.0
12	S(6)	0.007	326.5	0.002	57.9	-0.005	91.4
13	MU(2)	0.000	0.0	0.006	227.2	0.000	0.0
14	2N(2)	0.016	214.0	0.002	48.1	-0.014	-165.9
15	OO(1)	0.000	0.0	0.001	309.9	0.000	0.0
16	LAMBDA(2)	0.000	0.0	0.007	100.0	0.000	0.0
17	S(1)	0.129	197.3	0.054	345.7	-0.075	148.4
18	M(1)	0.006	197.4	0.002	161.2	-0.004	-36.2
19	J(1)	0.007	311.9	0.005	342.5	-0.002	30.6
20	MM	0.000	0.0	0.011	298.6	0.000	0.0
21	SSA	0.000	0.0	0.000	0.0	0.000	0.0
22	SA	0.000	0.0	0.136	120.1	0.000	0.0
23	MSF	0.000	0.0	0.001	317.6	0.000	0.0
24	MF	0.000	0.0	0.007	304.9	0.000	0.0
25	RHO(1)	0.000	0.0	0.002	261.9	0.000	0.0
26	Q(1)	0.004	219.0	0.004	18.0	0.000	159.0
27	T(2)	0.037	142.6	0.057	95.2	0.020	-47.4
28	R(2)	0.107	186.0	0.000	0.0	-0.107	174.0
29	2Q(1)	0.002	254.8	0.002	286.0	0.000	31.2
30	P(1)	0.057	351.6	0.031	111.9	-0.026	120.3
31	2SM(2)	0.000	0.0	0.003	38.6	0.000	0.0
32	M(3)	0.000	0.0	0.006	24.7	0.000	0.0
33	L(2)	0.013	279.8	0.006	18.4	-0.007	98.6
34	2MK(3)	0.000	0.0	0.021	177.5	0.000	0.0
35	K(2)	0.075	234.9	0.036	170.1	-0.039	-64.8
36	M(8)	0.010	344.0	0.006	63.6	-0.004	79.6
37	MS(4)	0.025	252.7	0.029	265.4	0.004	12.7

Table A-4. Comparison of tidal constituent amplitudes (m/s) and epochs (degree) for tidal currents. Station: COI1202, depth: 4.6m.

Station: "CMIST COI1202 4.6m, Pt. Pogishi, SW of
Observation: Least Squares H.A. Beginning 6-13-2012 at Hour 20.20
Model: Least Squares H.A. Beginning 6-12-2012 at Hour 0.00
Amplitudes are in m/s, and Phase is in degrees (GMT)

N	Constituent	Observed(R= 0.013) Amplitude	Epoch	Modeled(R= 0.012) Amplitude	Epoch	Difference Amplitude	Epoch
CURRENT ALONG PCD		DIR= 36		DIR= 35			
1	M(2)	1.156	246.6	1.409	250.7	0.253	4.1
2	S(2)	0.737	287.9	0.490	275.3	-0.247	-12.6
3	N(2)	0.224	202.2	0.278	214.6	0.054	12.4
4	K(1)	0.043	151.4	0.144	159.4	0.101	8.0
5	M(4)	0.022	205.8	0.029	225.5	0.007	19.7
6	O(1)	0.030	177.7	0.064	171.7	0.034	-6.0
7	M(6)	0.053	269.2	0.061	241.3	0.008	-27.9
8	MK(3)	0.019	240.2	0.036	15.8	0.017	135.6
9	S(4)	0.014	291.6	0.002	322.2	-0.012	30.6
10	MN(4)	0.000	0.0	0.015	185.9	0.000	0.0
11	NU(2)	0.000	0.0	0.019	306.6	0.000	0.0
12	S(6)	0.005	249.6	0.010	251.0	0.005	1.4
13	MU(2)	0.000	0.0	0.103	117.4	0.000	0.0
14	2N(2)	0.110	336.6	0.037	258.6	-0.073	-78.0
15	OO(1)	0.000	0.0	0.023	294.6	0.000	0.0
16	LAMBDA(2)	0.000	0.0	0.036	291.4	0.000	0.0
17	S(1)	0.084	120.3	0.000	0.0	-0.084	-120.3
18	M(1)	0.021	323.6	0.020	302.5	-0.001	-21.1
19	J(1)	0.016	70.0	0.018	350.0	0.002	80.0
20	MM	0.000	0.0	0.031	203.3	0.000	0.0
21	SSA	0.000	0.0	0.017	218.4	0.000	0.0
22	SA	0.000	0.0	0.000	0.0	0.000	0.0
23	MSF	0.000	0.0	0.050	216.4	0.000	0.0
24	MF	0.000	0.0	0.006	186.8	0.000	0.0
25	RHO(1)	0.000	0.0	0.022	145.7	0.000	0.0
26	Q(1)	0.002	297.4	0.021	212.7	0.019	-84.7
27	T(2)	0.274	300.4	0.000	0.0	-0.274	59.6
28	R(2)	0.000	0.0	0.000	0.0	0.000	0.0
29	2Q(1)	0.011	189.3	0.005	146.2	-0.006	-43.1
30	P(1)	0.000	0.0	0.023	121.5	0.000	0.0
31	2SM(2)	0.000	0.0	0.016	217.4	0.000	0.0
32	M(3)	0.000	0.0	0.003	159.8	0.000	0.0
33	L(2)	0.077	353.7	0.040	340.6	-0.037	-13.1
34	2MK(3)	0.000	0.0	0.006	300.4	0.000	0.0
35	K(2)	0.154	333.2	0.146	275.7	-0.008	-57.5
36	M(8)	0.012	275.6	0.034	274.3	0.022	-1.3
37	MS(4)	0.024	265.9	0.018	251.4	-0.006	-14.5
CURRENT ACROSS PCD		DIR= 126		DIR= 125			
1	M(2)	0.062	341.6	0.055	353.5	-0.007	11.9
2	S(2)	0.000	0.0	0.032	63.1	0.000	0.0
3	N(2)	0.012	297.5	0.012	296.3	0.000	-1.2
4	K(1)	0.052	290.4	0.000	0.0	-0.052	69.6
5	M(4)	0.020	37.8	0.024	19.6	0.004	-18.2
6	O(1)	0.017	259.8	0.016	243.7	-0.001	-16.1
7	M(6)	0.026	216.2	0.046	210.7	0.020	-5.5
8	MK(3)	0.006	119.7	0.010	46.0	0.004	-73.7
9	S(4)	0.002	347.7	0.004	109.2	0.002	121.5
10	MN(4)	0.000	0.0	0.008	353.9	0.000	0.0

11	NU(2)	0.000	0.0	0.010	46.5	0.000	0.0
12	S(6)	0.001	108.8	0.004	181.9	0.003	73.1
13	MU(2)	0.000	0.0	0.014	235.8	0.000	0.0
14	2N(2)	0.012	51.7	0.007	53.8	-0.005	2.1
15	OO(1)	0.000	0.0	0.004	94.4	0.000	0.0
16	LAMBDA(2)	0.000	0.0	0.003	21.6	0.000	0.0
17	S(1)	0.083	88.7	0.023	200.4	-0.060	111.7
18	M(1)	0.004	79.8	0.007	95.8	0.003	16.0
19	J(1)	0.005	115.4	0.009	163.6	0.004	48.2
20	MM	0.000	0.0	0.028	206.2	0.000	0.0
21	SSA	0.000	0.0	0.531	215.7	0.000	0.0
22	SA	0.000	0.0	1.901	287.5	0.000	0.0
23	MSF	0.000	0.0	0.037	225.3	0.000	0.0
24	MF	0.000	0.0	0.014	211.2	0.000	0.0
25	RHO(1)	0.000	0.0	0.004	314.9	0.000	0.0
26	Q(1)	0.002	99.0	0.001	304.8	-0.001	154.2
27	T(2)	0.033	15.8	0.024	112.4	-0.009	96.6
28	R(2)	0.125	19.3	0.000	0.0	-0.125	-19.3
29	2Q(1)	0.006	172.3	0.004	266.2	-0.002	93.9
30	P(1)	0.042	237.5	0.007	249.4	-0.035	11.9
31	2SM(2)	0.000	0.0	0.006	329.9	0.000	0.0
32	M(3)	0.000	0.0	0.002	151.7	0.000	0.0
33	L(2)	0.005	113.7	0.010	132.3	0.005	18.6
34	2MK(3)	0.000	0.0	0.017	37.8	0.000	0.0
35	K(2)	0.085	63.6	0.006	187.2	-0.079	123.6
36	M(8)	0.006	45.7	0.012	292.5	0.006	113.2
37	MS(4)	0.005	29.9	0.010	64.3	0.005	34.4

Table A-5. Comparison of tidal constituent amplitudes (m/s) and epochs (degree) for tidal currents. Station: COI1203, depth: 5.8m.

Station: "CMIST COI1203 5.8m, Anchor Point, W of
Observation: Least Squares H.A. Beginning 6-14-2012 at Hour 18.70
Model: Least Squares H.A. Beginning 6-12-2012 at Hour 0.00
Amplitudes are in m/s, and Phase is in degrees (GMT)

N	Constituent	Observed(R= 0.005) Amplitude	Epoch	Modeled(R= 0.004) Amplitude	Epoch	Difference Amplitude	Epoch
CURRENT ALONG PCD		DIR= 179		DIR= 179			
1	M(2)	1.404	119.4	1.538	121.0	0.134	1.6
2	S(2)	0.622	159.2	0.502	148.5	-0.120	-10.7
3	N(2)	0.278	73.0	0.280	86.7	0.002	13.7
4	K(1)	0.192	15.8	0.229	19.8	0.037	4.0
5	M(4)	0.059	297.3	0.072	295.4	0.013	-1.9
6	O(1)	0.125	358.9	0.145	3.2	0.020	4.3
7	M(6)	0.042	247.0	0.024	290.3	-0.018	43.3
8	MK(3)	0.031	164.2	0.046	185.5	0.015	21.3
9	S(4)	0.008	321.2	0.004	352.8	-0.004	31.6
10	MN(4)	0.000	0.0	0.026	262.2	0.000	0.0
11	NU(2)	0.000	0.0	0.033	156.6	0.000	0.0
12	S(6)	0.007	189.9	0.000	0.0	-0.007	170.1
13	MU(2)	0.000	0.0	0.097	329.9	0.000	0.0
14	2N(2)	0.083	198.7	0.033	112.3	-0.050	-86.4
15	OO(1)	0.000	0.0	0.015	162.9	0.000	0.0
16	LAMBDA(2)	0.000	0.0	0.020	210.9	0.000	0.0
17	S(1)	0.000	0.0	0.000	0.0	0.000	0.0
18	M(1)	0.009	148.8	0.014	157.3	0.005	8.5
19	J(1)	0.004	323.2	0.015	227.0	0.011	-96.2
20	MM	0.000	0.0	0.005	176.8	0.000	0.0
21	SSA	0.000	0.0	0.099	40.5	0.000	0.0
22	SA	0.000	0.0	0.000	0.0	0.000	0.0
23	MSF	0.000	0.0	0.015	140.0	0.000	0.0
24	MF	0.000	0.0	0.024	194.4	0.000	0.0
25	RHO(1)	0.000	0.0	0.016	332.8	0.000	0.0
26	Q(1)	0.012	330.9	0.027	19.2	0.015	48.3
27	T(2)	0.166	181.4	0.000	0.0	-0.166	178.6
28	R(2)	0.000	0.0	0.000	0.0	0.000	0.0
29	2Q(1)	0.013	334.9	0.010	327.4	-0.003	-7.5
30	P(1)	0.053	11.0	0.051	14.7	-0.002	3.7
31	2SM(2)	0.000	0.0	0.013	84.5	0.000	0.0
32	M(3)	0.000	0.0	0.005	230.4	0.000	0.0
33	L(2)	0.063	208.9	0.057	200.0	-0.006	-8.9
34	2MK(3)	0.000	0.0	0.026	163.3	0.000	0.0
35	K(2)	0.092	172.7	0.141	149.3	0.049	-23.4
36	M(8)	0.011	76.6	0.005	82.6	-0.006	6.0
37	MS(4)	0.047	336.0	0.046	341.1	-0.001	5.1
CURRENT ACROSS PCD		DIR= 269		DIR= 269			
1	M(2)	0.070	210.1	0.068	215.9	-0.002	5.8
2	S(2)	0.000	0.0	0.000	0.0	0.000	0.0
3	N(2)	0.010	137.5	0.003	10.4	-0.007	-127.1
4	K(1)	0.057	109.7	0.029	250.7	-0.028	141.0
5	M(4)	0.040	61.1	0.018	297.5	-0.022	123.6
6	O(1)	0.006	229.6	0.027	96.2	0.021	-133.4
7	M(6)	0.011	294.9	0.009	307.8	-0.002	12.9
8	MK(3)	0.005	18.6	0.010	170.9	0.005	152.3
9	S(4)	0.001	325.9	0.005	338.4	0.004	12.5
10	MN(4)	0.000	0.0	0.010	239.2	0.000	0.0

11	NU(2)	0.000	0.0	0.014	241.5	0.000	0.0
12	S(6)	0.000	0.0	0.001	346.5	0.000	0.0
13	MU(2)	0.000	0.0	0.021	23.4	0.000	0.0
14	2N(2)	0.008	230.2	0.012	142.1	0.004	-88.1
15	OO(1)	0.000	0.0	0.002	307.9	0.000	0.0
16	LAMBDA(2)	0.000	0.0	0.006	36.1	0.000	0.0
17	S(1)	0.103	261.7	0.089	55.3	-0.014	153.6
18	M(1)	0.002	94.5	0.002	271.8	0.000	177.3
19	J(1)	0.001	242.4	0.002	10.3	0.001	127.9
20	MM	0.000	0.0	0.014	47.2	0.000	0.0
21	SSA	0.000	0.0	0.186	125.2	0.000	0.0
22	SA	0.000	0.0	0.487	156.0	0.000	0.0
23	MSF	0.000	0.0	0.030	42.9	0.000	0.0
24	MF	0.000	0.0	0.015	71.6	0.000	0.0
25	RHO(1)	0.000	0.0	0.008	83.5	0.000	0.0
26	Q(1)	0.004	189.0	0.007	141.0	0.003	-48.0
27	T(2)	0.017	189.3	0.005	105.4	-0.012	-83.9
28	R(2)	0.056	212.8	0.033	198.0	-0.023	-14.8
29	2Q(1)	0.003	287.1	0.004	97.6	0.001	170.5
30	P(1)	0.055	66.5	0.044	205.2	-0.011	138.7
31	2SM(2)	0.000	0.0	0.002	127.2	0.000	0.0
32	M(3)	0.000	0.0	0.003	231.9	0.000	0.0
33	L(2)	0.006	236.8	0.013	286.9	0.007	50.1
34	2MK(3)	0.000	0.0	0.006	170.8	0.000	0.0
35	K(2)	0.044	257.1	0.022	234.8	-0.022	-22.3
36	M(8)	0.008	137.8	0.003	118.0	-0.005	-19.8
37	MS(4)	0.019	89.5	0.014	325.4	-0.005	124.1

Table A-6. Comparison of tidal constituent amplitudes (m/s) and epochs (degree) for tidal currents. Station: COI1204, depth: 6.0m.

Station: "CMIST COI1204 6.0m, North Forelands, b
Observation: Least Squares H.A. Beginning 6-16-2012 at Hour 1.10
Model: Least Squares H.A. Beginning 6-12-2012 at Hour 0.00
Amplitudes are in m/s, and Phase is in degrees (GMT)

N	Constituent	Observed(R= 0.004) Amplitude	Epoch	Modeled(R= 0.003) Amplitude	Epoch	Difference Amplitude	Epoch
CURRENT ALONG PCD		DIR= 38		DIR= 38			
1	M(2)	2.016	11.1	2.110	6.6	0.094	-4.5
2	S(2)	0.872	51.6	0.588	44.6	-0.284	-7.0
3	N(2)	0.309	331.5	0.334	336.7	0.025	5.2
4	K(1)	0.198	252.3	0.222	244.0	0.024	-8.3
5	M(4)	0.195	308.8	0.200	318.8	0.005	10.0
6	O(1)	0.121	244.9	0.134	241.4	0.013	-3.5
7	M(6)	0.095	242.0	0.098	251.6	0.003	9.6
8	MK(3)	0.033	347.1	0.031	290.0	-0.002	-57.1
9	S(4)	0.012	102.6	0.008	84.4	-0.004	-18.2
10	MN(4)	0.000	0.0	0.062	285.1	0.000	0.0
11	NU(2)	0.000	0.0	0.029	343.6	0.000	0.0
12	S(6)	0.010	213.6	0.008	241.6	-0.002	28.0
13	MU(2)	0.000	0.0	0.164	157.2	0.000	0.0
14	2N(2)	0.128	7.6	0.037	290.8	-0.091	76.8
15	OO(1)	0.000	0.0	0.024	349.9	0.000	0.0
16	LAMBDA(2)	0.000	0.0	0.033	7.0	0.000	0.0
17	S(1)	0.000	0.0	0.000	0.0	0.000	0.0
18	M(1)	0.012	358.6	0.025	0.0	0.013	1.4
19	J(1)	0.010	48.0	0.022	60.0	0.012	12.0
20	MM	0.000	0.0	0.033	200.4	0.000	0.0
21	SSA	0.000	0.0	0.000	0.0	0.000	0.0
22	SA	0.000	0.0	0.058	130.1	0.000	0.0
23	MSF	0.000	0.0	0.036	231.6	0.000	0.0
24	MF	0.000	0.0	0.000	0.0	0.000	0.0
25	RHO(1)	0.000	0.0	0.027	185.9	0.000	0.0
26	Q(1)	0.009	227.6	0.040	242.9	0.031	15.3
27	T(2)	0.249	46.6	0.000	0.0	-0.249	-46.6
28	R(2)	0.000	0.0	0.000	0.0	0.000	0.0
29	2Q(1)	0.008	232.2	0.008	161.6	0.000	-70.6
30	P(1)	0.043	230.4	0.043	245.3	0.000	14.9
31	2SM(2)	0.000	0.0	0.036	279.5	0.000	0.0
32	M(3)	0.000	0.0	0.014	92.0	0.000	0.0
33	L(2)	0.103	54.6	0.071	31.9	-0.032	-22.7
34	2MK(3)	0.000	0.0	0.067	291.3	0.000	0.0
35	K(2)	0.212	74.0	0.182	44.2	-0.030	-29.8
36	M(8)	0.035	216.5	0.046	205.2	0.011	-11.3
37	MS(4)	0.116	353.0	0.119	2.7	0.003	9.7
CURRENT ACROSS PCD		DIR= 128		DIR= 128			
1	M(2)	0.038	280.9	0.033	101.3	-0.005	-179.6
2	S(2)	0.067	319.9	0.000	0.0	-0.067	40.1
3	N(2)	0.018	252.2	0.009	193.2	-0.009	-59.0
4	K(1)	0.067	86.8	0.051	264.1	-0.016	177.3
5	M(4)	0.042	188.6	0.052	224.1	0.010	35.5
6	O(1)	0.024	157.4	0.020	203.9	-0.004	46.5
7	M(6)	0.024	181.1	0.013	56.5	-0.011	-124.6
8	MK(3)	0.019	61.4	0.020	45.0	0.001	-16.4
9	S(4)	0.004	172.1	0.005	160.8	0.001	-11.3
10	MN(4)	0.000	0.0	0.023	173.9	0.000	0.0

11	NU(2)	0.000	0.0	0.010	36.8	0.000	0.0
12	S(6)	0.003	84.7	0.003	188.3	0.000	103.6
13	MU(2)	0.000	0.0	0.029	207.1	0.000	0.0
14	2N(2)	0.021	50.6	0.013	332.6	-0.008	78.0
15	OO(1)	0.000	0.0	0.005	237.5	0.000	0.0
16	LAMBDA(2)	0.000	0.0	0.007	287.7	0.000	0.0
17	S(1)	0.094	225.4	0.102	49.4	0.008	-176.0
18	M(1)	0.001	124.4	0.007	335.7	0.006	148.7
19	J(1)	0.007	117.3	0.002	6.2	-0.005	-111.1
20	MM	0.000	0.0	0.017	21.5	0.000	0.0
21	SSA	0.000	0.0	0.017	219.8	0.000	0.0
22	SA	0.000	0.0	0.000	0.0	0.000	0.0
23	MSF	0.000	0.0	0.027	52.9	0.000	0.0
24	MF	0.000	0.0	0.016	42.6	0.000	0.0
25	RHO(1)	0.000	0.0	0.005	127.5	0.000	0.0
26	Q(1)	0.009	161.4	0.004	159.3	-0.005	-2.1
27	T(2)	0.025	323.5	0.008	124.0	-0.017	160.5
28	R(2)	0.000	0.0	0.033	220.1	0.000	0.0
29	2Q(1)	0.005	164.0	0.009	207.5	0.004	43.5
30	P(1)	0.045	31.6	0.054	191.4	0.009	159.8
31	2SM(2)	0.000	0.0	0.005	176.1	0.000	0.0
32	M(3)	0.000	0.0	0.013	127.2	0.000	0.0
33	L(2)	0.011	74.7	0.008	68.3	-0.003	-6.4
34	2MK(3)	0.000	0.0	0.009	111.4	0.000	0.0
35	K(2)	0.016	4.6	0.036	274.3	0.020	90.3
36	M(8)	0.008	66.6	0.007	192.4	-0.001	125.8
37	MS(4)	0.025	259.5	0.025	288.5	0.000	29.0

Table A-7. Comparison of tidal constituent amplitudes (m/s) and epochs (degree) for tidal currents. Station: COI1205, depth: 5.5m.

Station: "CMIST COI1205 5.5m, Kalgin Island, 4nm
Observation: Least Squares H.A. Beginning 6-15-2012 at Hour 1.80
Model: Least Squares H.A. Beginning 6-12-2012 at Hour 0.00
Amplitudes are in m/s, and Phase is in degrees (GMT)

N	Constituent	Observed(R= 0.015) Amplitude	Epoch	Modeled(R= 0.016) Amplitude	Epoch	Difference Amplitude	Epoch
CURRENT ALONG PCD		DIR= 15		DIR= 17			
1	M(2)	1.798	357.2	1.996	355.7	0.198	-1.5
2	S(2)	0.789	45.5	0.606	41.5	-0.183	-4.0
3	N(2)	0.322	310.5	0.356	323.0	0.034	12.5
4	K(1)	0.000	0.0	0.193	223.3	0.000	0.0
5	M(4)	0.126	268.3	0.136	281.6	0.010	13.3
6	O(1)	0.132	243.0	0.167	249.3	0.035	6.3
7	M(6)	0.043	333.2	0.053	5.5	0.010	32.3
8	MK(3)	0.040	118.3	0.051	134.3	0.011	16.0
9	S(4)	0.015	312.7	0.018	308.4	0.003	-4.3
10	MN(4)	0.000	0.0	0.069	229.7	0.000	0.0
11	NU(2)	0.000	0.0	0.036	0.7	0.000	0.0
12	S(6)	0.003	12.2	0.009	335.0	0.006	37.2
13	MU(2)	0.000	0.0	0.122	179.0	0.000	0.0
14	2N(2)	0.086	44.4	0.026	314.6	-0.060	89.8
15	OO(1)	0.000	0.0	0.032	63.3	0.000	0.0
16	LAMBDA(2)	0.000	0.0	0.013	15.9	0.000	0.0
17	S(1)	0.415	212.9	0.231	245.1	-0.184	32.2
18	M(1)	0.036	127.4	0.038	92.0	0.002	-35.4
19	J(1)	0.034	177.5	0.039	129.3	0.005	-48.2
20	MM	0.000	0.0	0.036	194.1	0.000	0.0
21	SSA	0.000	0.0	0.000	0.0	0.000	0.0
22	SA	0.000	0.0	0.218	311.7	0.000	0.0
23	MSF	0.000	0.0	0.057	214.9	0.000	0.0
24	MF	0.000	0.0	0.026	160.1	0.000	0.0
25	RHO(1)	0.000	0.0	0.062	319.6	0.000	0.0
26	Q(1)	0.060	188.7	0.018	101.3	-0.042	-87.4
27	T(2)	0.274	71.4	0.124	117.5	-0.150	46.1
28	R(2)	0.000	0.0	0.000	0.0	0.000	0.0
29	2Q(1)	0.034	323.4	0.032	303.5	-0.002	-19.9
30	P(1)	0.111	337.2	0.000	0.0	-0.111	22.8
31	2SM(2)	0.000	0.0	0.021	325.2	0.000	0.0
32	M(3)	0.000	0.0	0.018	265.5	0.000	0.0
33	L(2)	0.096	68.8	0.057	56.4	-0.039	-12.4
34	2MK(3)	0.000	0.0	0.028	36.4	0.000	0.0
35	K(2)	0.121	77.4	0.126	41.4	0.005	-36.0
36	M(8)	0.020	202.3	0.018	203.2	-0.002	0.9
37	MS(4)	0.093	301.8	0.104	319.0	0.011	17.2
CURRENT ACROSS PCD		DIR= 105		DIR= 107			
1	M(2)	0.137	83.5	0.152	79.0	0.015	-4.5
2	S(2)	0.065	104.1	0.000	0.0	-0.065	-104.1
3	N(2)	0.005	144.1	0.016	104.0	0.011	-40.1
4	K(1)	0.029	67.4	0.105	331.1	0.076	96.3
5	M(4)	0.104	52.5	0.136	83.5	0.032	31.0
6	O(1)	0.044	74.2	0.018	128.7	-0.026	54.5
7	M(6)	0.027	354.1	0.017	29.7	-0.010	35.6
8	MK(3)	0.047	307.2	0.038	328.0	-0.009	20.8
9	S(4)	0.009	248.9	0.002	351.9	-0.007	103.0
10	MN(4)	0.000	0.0	0.055	47.3	0.000	0.0

11	NU(2)	0.000	0.0	0.015	52.6	0.000	0.0
12	S(6)	0.001	7.2	0.004	72.8	0.003	65.6
13	MU(2)	0.000	0.0	0.041	203.2	0.000	0.0
14	2N(2)	0.044	40.8	0.021	318.2	-0.023	82.6
15	OO(1)	0.000	0.0	0.004	62.5	0.000	0.0
16	LAMBDA(2)	0.000	0.0	0.002	139.7	0.000	0.0
17	S(1)	0.000	0.0	0.150	95.4	0.000	0.0
18	M(1)	0.005	85.4	0.005	113.2	0.000	27.8
19	J(1)	0.008	110.5	0.009	77.6	0.001	-32.9
20	MM	0.000	0.0	0.005	306.1	0.000	0.0
21	SSA	0.000	0.0	0.012	293.0	0.000	0.0
22	SA	0.000	0.0	0.000	0.0	0.000	0.0
23	MSF	0.000	0.0	0.013	54.1	0.000	0.0
24	MF	0.000	0.0	0.012	246.6	0.000	0.0
25	RHO(1)	0.000	0.0	0.014	6.4	0.000	0.0
26	Q(1)	0.012	111.9	0.020	84.8	0.008	-27.1
27	T(2)	0.049	83.6	0.026	255.3	-0.023	171.7
28	R(2)	0.000	0.0	0.042	223.1	0.000	0.0
29	2Q(1)	0.006	128.2	0.006	165.2	0.000	37.0
30	P(1)	0.012	180.1	0.078	241.1	0.066	61.0
31	2SM(2)	0.000	0.0	0.006	348.1	0.000	0.0
32	M(3)	0.000	0.0	0.019	66.1	0.000	0.0
33	L(2)	0.015	98.1	0.016	93.1	0.001	-5.0
34	2MK(3)	0.000	0.0	0.040	339.9	0.000	0.0
35	K(2)	0.020	168.5	0.019	281.2	-0.001	112.7
36	M(8)	0.005	276.8	0.023	15.7	0.018	98.9
37	MS(4)	0.037	114.3	0.075	133.3	0.038	19.0

Table A-8. Comparison of tidal constituent amplitudes (m/s) and epochs (degree) for tidal currents. Station: COI1207, depth: 5.7m.

Station: "CMIST COI1207 5.7m, Point Possession,
Observation: Least Squares H.A. Beginning 6-16-2012 at Hour 20.20
Model: Least Squares H.A. Beginning 6-12-2012 at Hour 0.00
 Amplitudes are in m/s, and Phase is in degrees (GMT)

N	Constituent	Observed(R= 0.010) Amplitude	Epoch	Modeled(R= 0.007) Amplitude	Epoch	Difference Amplitude	Epoch
CURRENT ALONG PCD		DIR= 108		DIR= 107			
1	M(2)	2.090	12.6	1.989	19.0	-0.101	6.4
2	S(2)	0.919	52.5	0.545	59.7	-0.374	7.2
3	N(2)	0.318	334.3	0.314	353.7	-0.004	19.4
4	K(1)	0.185	255.0	0.204	257.7	0.019	2.7
5	M(4)	0.129	13.4	0.197	20.0	0.068	6.6
6	O(1)	0.101	243.6	0.139	251.5	0.038	7.9
7	M(6)	0.156	289.7	0.159	270.1	0.003	-19.6
8	MK(3)	0.125	359.0	0.077	327.1	-0.048	-31.9
9	S(4)	0.017	166.9	0.010	156.7	-0.007	-10.2
10	MN(4)	0.000	0.0	0.069	355.6	0.000	0.0
11	NU(2)	0.000	0.0	0.037	355.4	0.000	0.0
12	S(6)	0.009	286.2	0.007	258.2	-0.002	-28.0
13	MU(2)	0.000	0.0	0.163	162.8	0.000	0.0
14	2N(2)	0.135	4.1	0.040	295.2	-0.095	68.9
15	OO(1)	0.000	0.0	0.023	349.0	0.000	0.0
16	LAMBDA(2)	0.000	0.0	0.030	22.5	0.000	0.0
17	S(1)	0.000	0.0	0.000	0.0	0.000	0.0
18	M(1)	0.011	309.8	0.018	354.8	0.007	45.0
19	J(1)	0.010	16.0	0.018	87.3	0.008	71.3
20	MM	0.000	0.0	0.030	220.2	0.000	0.0
21	SSA	0.000	0.0	0.000	0.0	0.000	0.0
22	SA	0.000	0.0	0.077	343.0	0.000	0.0
23	MSF	0.000	0.0	0.049	252.2	0.000	0.0
24	MF	0.000	0.0	0.012	257.9	0.000	0.0
25	RHO(1)	0.000	0.0	0.025	202.6	0.000	0.0
26	Q(1)	0.011	248.8	0.045	261.4	0.034	12.6
27	T(2)	0.269	43.3	0.000	0.0	-0.269	-43.3
28	R(2)	0.000	0.0	0.000	0.0	0.000	0.0
29	2Q(1)	0.003	175.8	0.014	192.4	0.011	16.6
30	P(1)	0.036	233.1	0.051	266.2	0.015	33.1
31	2SM(2)	0.000	0.0	0.032	296.8	0.000	0.0
32	M(3)	0.000	0.0	0.008	155.2	0.000	0.0
33	L(2)	0.111	49.6	0.085	36.8	-0.026	-12.8
34	2MK(3)	0.000	0.0	0.109	313.9	0.000	0.0
35	K(2)	0.261	72.8	0.175	66.2	-0.086	-6.6
36	M(8)	0.048	263.3	0.030	240.1	-0.018	-23.2
37	MS(4)	0.088	80.9	0.106	65.0	0.018	-15.9
CURRENT ACROSS PCD		DIR= 198		DIR= 197			
1	M(2)	0.024	15.0	0.022	111.8	-0.002	96.8
2	S(2)	0.072	180.4	0.048	357.3	-0.024	176.9
3	N(2)	0.002	42.4	0.022	111.1	0.020	68.7
4	K(1)	0.000	0.0	0.009	241.1	0.000	0.0
5	M(4)	0.121	209.0	0.059	244.7	-0.062	35.7
6	O(1)	0.013	165.6	0.003	41.4	-0.010	-124.2
7	M(6)	0.023	165.4	0.050	298.8	0.027	133.4
8	MK(3)	0.035	112.4	0.021	151.5	-0.014	39.1
9	S(4)	0.002	255.6	0.004	235.1	0.002	-20.5
10	MN(4)	0.000	0.0	0.012	167.1	0.000	0.0

11	NU(2)	0.000	0.0	0.018	42.9	0.000	0.0
12	S(6)	0.003	19.7	0.004	343.9	0.001	35.8
13	MU(2)	0.000	0.0	0.020	169.8	0.000	0.0
14	2N(2)	0.002	178.7	0.014	226.9	0.012	48.2
15	OO(1)	0.000	0.0	0.003	231.5	0.000	0.0
16	LAMBDA(2)	0.000	0.0	0.020	225.5	0.000	0.0
17	S(1)	0.038	131.9	0.000	0.0	-0.038	-131.9
18	M(1)	0.004	97.4	0.002	37.9	-0.002	-59.5
19	J(1)	0.008	156.3	0.005	302.9	-0.003	146.6
20	MM	0.000	0.0	0.012	175.8	0.000	0.0
21	SSA	0.000	0.0	1.311	57.7	0.000	0.0
22	SA	0.000	0.0	4.826	118.6	0.000	0.0
23	MSF	0.000	0.0	0.026	201.6	0.000	0.0
24	MF	0.000	0.0	0.009	131.8	0.000	0.0
25	RHO(1)	0.000	0.0	0.008	228.8	0.000	0.0
26	Q(1)	0.011	168.2	0.007	317.8	-0.004	149.6
27	T(2)	0.055	167.7	0.053	331.6	-0.002	163.9
28	R(2)	0.000	0.0	0.000	0.0	0.000	0.0
29	2Q(1)	0.001	21.7	0.001	290.5	0.000	91.2
30	P(1)	0.018	239.4	0.001	289.5	-0.017	50.1
31	2SM(2)	0.000	0.0	0.011	123.4	0.000	0.0
32	M(3)	0.000	0.0	0.004	29.6	0.000	0.0
33	L(2)	0.002	138.5	0.010	218.4	0.008	79.9
34	2MK(3)	0.000	0.0	0.014	193.6	0.000	0.0
35	K(2)	0.034	243.5	0.028	92.7	-0.006	-150.8
36	M(8)	0.031	73.2	0.012	164.6	-0.019	91.4
37	MS(4)	0.057	277.5	0.023	248.1	-0.034	-29.4

Table A-9. Comparison of tidal constituent amplitudes (m/s) and epochs (degree) for tidal currents. Station: COI1208, depth: 6.2m.

Station: "CMIST COI1208 6.2m, Fire Island, South
Observation: Least Squares H.A. Beginning 6-16-2012 at Hour 21.30
Model: Least Squares H.A. Beginning 6-12-2012 at Hour 0.00
Amplitudes are in m/s, and Phase is in degrees (GMT)

N	Constituent	Observed(R= 0.015) Amplitude	Epoch	Modeled(R= 0.005) Amplitude	Epoch	Difference Amplitude	Epoch
CURRENT ALONG PCD		DIR= 122		DIR= 118			
1	M(2)	1.665	22.9	1.581	23.0	-0.084	0.1
2	S(2)	0.650	59.9	0.582	68.4	-0.068	8.5
3	N(2)	0.255	342.7	0.277	355.6	0.022	12.9
4	K(1)	0.157	253.6	0.177	262.7	0.020	9.1
5	M(4)	0.153	30.3	0.235	41.1	0.082	10.8
6	O(1)	0.093	238.3	0.108	250.0	0.015	11.7
7	M(6)	0.107	294.1	0.128	294.3	0.021	0.2
8	MK(3)	0.073	350.7	0.090	314.5	0.017	-36.2
9	S(4)	0.009	109.6	0.017	118.7	0.008	9.1
10	MN(4)	0.000	0.0	0.081	9.0	0.000	0.0
11	NU(2)	0.000	0.0	0.036	336.9	0.000	0.0
12	S(6)	0.009	300.8	0.004	340.0	-0.005	39.2
13	MU(2)	0.000	0.0	0.107	165.2	0.000	0.0
14	2N(2)	0.106	28.2	0.035	300.2	-0.071	88.0
15	OO(1)	0.000	0.0	0.019	347.7	0.000	0.0
16	LAMBDA(2)	0.000	0.0	0.044	341.9	0.000	0.0
17	S(1)	0.000	0.0	0.000	0.0	0.000	0.0
18	M(1)	0.013	357.2	0.013	14.8	0.000	17.6
19	J(1)	0.005	61.1	0.012	30.1	0.007	-31.0
20	MM	0.000	0.0	0.005	193.9	0.000	0.0
21	SSA	0.000	0.0	0.015	189.5	0.000	0.0
22	SA	0.000	0.0	0.000	0.0	0.000	0.0
23	MSF	0.000	0.0	0.023	256.8	0.000	0.0
24	MF	0.000	0.0	0.020	354.9	0.000	0.0
25	RHO(1)	0.000	0.0	0.012	192.6	0.000	0.0
26	Q(1)	0.014	243.6	0.019	267.8	0.005	24.2
27	T(2)	0.140	55.1	0.104	69.4	-0.036	14.3
28	R(2)	0.000	0.0	0.000	0.0	0.000	0.0
29	2Q(1)	0.012	227.4	0.003	111.6	-0.009	-115.8
30	P(1)	0.039	240.7	0.025	259.5	-0.014	18.8
31	2SM(2)	0.000	0.0	0.028	276.6	0.000	0.0
32	M(3)	0.000	0.0	0.006	138.9	0.000	0.0
33	L(2)	0.089	70.6	0.040	12.7	-0.049	-57.9
34	2MK(3)	0.000	0.0	0.085	305.4	0.000	0.0
35	K(2)	0.187	71.7	0.160	81.0	-0.027	9.3
36	M(8)	0.016	331.8	0.024	324.9	0.008	-6.9
37	MS(4)	0.093	82.8	0.118	85.5	0.025	2.7
CURRENT ACROSS PCD		DIR= 212		DIR= 208			
1	M(2)	0.032	94.6	0.032	127.0	0.000	32.4
2	S(2)	0.033	46.7	0.008	153.6	-0.025	106.9
3	N(2)	0.006	33.0	0.004	12.2	-0.002	-20.8
4	K(1)	0.017	329.1	0.048	291.2	0.031	-37.9
5	M(4)	0.138	246.7	0.070	322.5	-0.068	75.8
6	O(1)	0.016	293.1	0.013	207.9	-0.003	-85.2
7	M(6)	0.018	250.0	0.007	292.5	-0.011	42.5
8	MK(3)	0.030	130.5	0.022	193.6	-0.008	63.1
9	S(4)	0.005	29.4	0.004	311.8	-0.001	77.6
10	MN(4)	0.000	0.0	0.021	280.6	0.000	0.0

11	NU(2)	0.000	0.0	0.006	215.3	0.000	0.0
12	S(6)	0.005	278.5	0.000	107.6	-0.005	-170.9
13	MU(2)	0.000	0.0	0.014	2.2	0.000	0.0
14	2N(2)	0.009	326.7	0.007	143.5	-0.002	176.8
15	OO(1)	0.000	0.0	0.004	251.9	0.000	0.0
16	LAMBDA(2)	0.000	0.0	0.006	49.1	0.000	0.0
17	S(1)	0.000	0.0	0.063	88.0	0.000	0.0
18	M(1)	0.002	172.6	0.001	214.2	-0.001	41.6
19	J(1)	0.006	301.5	0.003	323.5	-0.003	22.0
20	MM	0.000	0.0	0.009	78.2	0.000	0.0
21	SSA	0.000	0.0	0.922	236.1	0.000	0.0
22	SA	0.000	0.0	3.325	297.3	0.000	0.0
23	MSF	0.000	0.0	0.009	357.1	0.000	0.0
24	MF	0.000	0.0	0.013	3.5	0.000	0.0
25	RHO(1)	0.000	0.0	0.007	146.2	0.000	0.0
26	Q(1)	0.002	337.5	0.009	192.6	0.007	-144.9
27	T(2)	0.017	4.9	0.009	218.8	-0.008	146.1
28	R(2)	0.000	0.0	0.000	0.0	0.000	0.0
29	2Q(1)	0.002	40.0	0.002	339.6	0.000	60.4
30	P(1)	0.003	344.5	0.035	248.9	0.032	-95.6
31	2SM(2)	0.000	0.0	0.001	299.8	0.000	0.0
32	M(3)	0.000	0.0	0.006	110.9	0.000	0.0
33	L(2)	0.008	54.2	0.003	228.8	-0.005	174.6
34	2MK(3)	0.000	0.0	0.021	171.1	0.000	0.0
35	K(2)	0.029	103.6	0.006	345.8	-0.023	117.8
36	M(8)	0.018	109.9	0.012	231.7	-0.006	121.8
37	MS(4)	0.066	301.4	0.028	16.9	-0.038	75.5

Table A-10. Comparison of tidal constituent amplitudes (m/s) and epochs (degree) for tidal currents. Station: COI1209, depth: 5.9m.

Station: "CMIST COI1209 5.9m, Fire Island, North
Observation: Least Squares H.A. Beginning 6-17-2012 at Hour 2.90
Model: Least Squares H.A. Beginning 6-12-2012 at Hour 0.00
Amplitudes are in m/s, and Phase is in degrees (GMT)

N	Constituent	Observed(R= 0.012) Amplitude	Epoch	Modeled(R= 0.002) Amplitude	Epoch	Difference Amplitude	Epoch
CURRENT ALONG PCD		DIR= 76		DIR= 74			
1	M(2)	1.950	25.0	2.317	33.9	0.367	8.9
2	S(2)	0.746	70.8	0.630	75.7	-0.116	4.9
3	N(2)	0.285	345.6	0.370	7.9	0.085	22.3
4	K(1)	0.191	261.5	0.262	260.4	0.071	-1.1
5	M(4)	0.192	7.6	0.282	14.9	0.090	7.3
6	O(1)	0.121	250.1	0.158	253.6	0.037	3.5
7	M(6)	0.212	303.3	0.165	324.4	-0.047	21.1
8	MK(3)	0.063	352.1	0.060	314.6	-0.003	-37.5
9	S(4)	0.012	166.8	0.018	158.3	0.006	-8.5
10	MN(4)	0.000	0.0	0.084	359.0	0.000	0.0
11	NU(2)	0.000	0.0	0.052	347.1	0.000	0.0
12	S(6)	0.014	289.3	0.005	348.5	-0.009	59.2
13	MU(2)	0.000	0.0	0.201	170.7	0.000	0.0
14	2N(2)	0.144	17.2	0.051	295.7	-0.093	81.5
15	OO(1)	0.000	0.0	0.034	0.1	0.000	0.0
16	LAMBDA(2)	0.000	0.0	0.034	13.2	0.000	0.0
17	S(1)	0.000	0.0	0.000	0.0	0.000	0.0
18	M(1)	0.013	341.9	0.025	1.8	0.012	19.9
19	J(1)	0.011	343.6	0.020	55.2	0.009	71.6
20	MM	0.000	0.0	0.044	205.5	0.000	0.0
21	SSA	0.000	0.0	0.029	244.0	0.000	0.0
22	SA	0.000	0.0	0.000	0.0	0.000	0.0
23	MSF	0.000	0.0	0.066	239.6	0.000	0.0
24	MF	0.000	0.0	0.000	0.0	0.000	0.0
25	RHO(1)	0.000	0.0	0.028	201.8	0.000	0.0
26	Q(1)	0.015	263.7	0.048	272.0	0.033	8.3
27	T(2)	0.192	72.5	0.000	0.0	-0.192	-72.5
28	R(2)	0.000	0.0	0.000	0.0	0.000	0.0
29	2Q(1)	0.010	176.0	0.007	190.2	-0.003	14.2
30	P(1)	0.036	267.3	0.053	272.1	0.017	4.8
31	2SM(2)	0.000	0.0	0.043	309.0	0.000	0.0
32	M(3)	0.000	0.0	0.011	120.7	0.000	0.0
33	L(2)	0.100	60.4	0.077	51.0	-0.023	-9.4
34	2MK(3)	0.000	0.0	0.093	328.7	0.000	0.0
35	K(2)	0.182	78.8	0.197	80.2	0.015	1.4
36	M(8)	0.035	278.1	0.044	257.2	0.009	-20.9
37	MS(4)	0.119	71.9	0.159	72.6	0.040	0.7
CURRENT ACROSS PCD		DIR= 166		DIR= 164			
1	M(2)	0.021	89.4	0.007	268.1	-0.014	178.7
2	S(2)	0.032	275.7	0.039	1.2	0.007	85.5
3	N(2)	0.006	173.6	0.009	303.0	0.003	129.4
4	K(1)	0.014	342.4	0.007	118.6	-0.007	136.2
5	M(4)	0.137	228.1	0.020	260.4	-0.117	32.3
6	O(1)	0.020	246.4	0.008	320.5	-0.012	74.1
7	M(6)	0.028	261.4	0.020	288.8	-0.008	27.4
8	MK(3)	0.016	94.2	0.008	214.1	-0.008	119.9
9	S(4)	0.004	92.8	0.002	132.9	-0.002	40.1
10	MN(4)	0.000	0.0	0.008	297.3	0.000	0.0

11	NU(2)	0.000	0.0	0.011	284.6	0.000	0.0
12	S(6)	0.003	175.7	0.002	275.8	-0.001	100.1
13	MU(2)	0.000	0.0	0.012	192.1	0.000	0.0
14	2N(2)	0.013	357.1	0.014	216.4	0.001	-140.7
15	OO(1)	0.000	0.0	0.005	194.8	0.000	0.0
16	LAMBDA(2)	0.000	0.0	0.020	166.2	0.000	0.0
17	S(1)	0.000	0.0	0.000	0.0	0.000	0.0
18	M(1)	0.002	126.6	0.007	177.3	0.005	50.7
19	J(1)	0.004	77.6	0.007	214.3	0.003	136.7
20	MM	0.000	0.0	0.016	207.8	0.000	0.0
21	SSA	0.000	0.0	0.665	56.3	0.000	0.0
22	SA	0.000	0.0	2.477	117.6	0.000	0.0
23	MSF	0.000	0.0	0.030	235.9	0.000	0.0
24	MF	0.000	0.0	0.006	247.8	0.000	0.0
25	RHO(1)	0.000	0.0	0.009	357.3	0.000	0.0
26	Q(1)	0.005	163.4	0.005	120.2	0.000	-43.2
27	T(2)	0.023	292.1	0.023	341.4	0.000	49.3
28	R(2)	0.000	0.0	0.000	0.0	0.000	0.0
29	2Q(1)	0.005	296.3	0.008	328.9	0.003	32.6
30	P(1)	0.006	39.6	0.007	239.4	0.001	160.2
31	2SM(2)	0.000	0.0	0.005	124.9	0.000	0.0
32	M(3)	0.000	0.0	0.004	67.8	0.000	0.0
33	L(2)	0.009	27.3	0.008	104.5	-0.001	77.2
34	2MK(3)	0.000	0.0	0.007	111.5	0.000	0.0
35	K(2)	0.008	2.7	0.017	67.9	0.009	65.2
36	M(8)	0.030	129.2	0.010	137.6	-0.020	8.4
37	MS(4)	0.055	280.9	0.007	355.2	-0.048	74.3

Table A-11. Comparison of tidal constituent amplitudes (m/s) and epochs (degree) for tidal currents. Station: COI1210, depth: 5.2m.

Station: "CMIST COI1210 5.2m, Middle Ground Shoa
Observation: Least Squares H.A. Beginning 6-15-2012 at Hour 22.20
Model: Least Squares H.A. Beginning 6-12-2012 at Hour 0.00
 Amplitudes are in m/s, and Phase is in degrees (GMT)

N	Constituent	Observed(R= 0.011) Amplitude	Epoch	Modeled(R= 0.007) Amplitude	Epoch	Difference Amplitude	Epoch
CURRENT ALONG PCD		DIR= 58		DIR= 55			
1	M(2)	2.009	3.0	2.119	1.4	0.110	-1.6
2	S(2)	0.813	43.3	0.607	39.6	-0.206	-3.7
3	N(2)	0.316	322.4	0.347	330.7	0.031	8.3
4	K(1)	0.218	248.6	0.209	243.7	-0.009	-4.9
5	M(4)	0.119	296.2	0.126	326.2	0.007	30.0
6	O(1)	0.121	232.0	0.135	226.8	0.014	-5.2
7	M(6)	0.084	246.5	0.080	250.2	-0.004	3.7
8	MK(3)	0.052	324.2	0.052	289.0	0.000	-35.2
9	S(4)	0.013	94.6	0.013	73.7	0.000	-20.9
10	MN(4)	0.000	0.0	0.040	289.7	0.000	0.0
11	NU(2)	0.000	0.0	0.028	346.4	0.000	0.0
12	S(6)	0.007	197.6	0.005	269.3	-0.002	71.7
13	MU(2)	0.000	0.0	0.149	151.5	0.000	0.0
14	2N(2)	0.122	0.4	0.029	314.5	-0.093	45.9
15	OO(1)	0.000	0.0	0.024	329.5	0.000	0.0
16	LAMBDA(2)	0.000	0.0	0.042	353.9	0.000	0.0
17	S(1)	0.000	0.0	0.000	0.0	0.000	0.0
18	M(1)	0.013	322.5	0.027	338.9	0.014	16.4
19	J(1)	0.015	315.0	0.016	40.4	0.001	85.4
20	MM	0.000	0.0	0.018	218.0	0.000	0.0
21	SSA	0.000	0.0	0.013	63.1	0.000	0.0
22	SA	0.000	0.0	0.000	0.0	0.000	0.0
23	MSF	0.000	0.0	0.035	231.4	0.000	0.0
24	MF	0.000	0.0	0.013	279.3	0.000	0.0
25	RHO(1)	0.000	0.0	0.010	90.8	0.000	0.0
26	Q(1)	0.014	250.3	0.020	246.2	0.006	-4.1
27	T(2)	0.230	35.4	0.000	0.0	-0.230	-35.4
28	R(2)	0.000	0.0	0.000	0.0	0.000	0.0
29	2Q(1)	0.010	217.2	0.017	141.9	0.007	-75.3
30	P(1)	0.032	252.2	0.046	236.5	0.014	-15.7
31	2SM(2)	0.000	0.0	0.030	268.5	0.000	0.0
32	M(3)	0.000	0.0	0.012	100.2	0.000	0.0
33	L(2)	0.104	41.0	0.058	23.3	-0.046	-17.7
34	2MK(3)	0.000	0.0	0.077	276.7	0.000	0.0
35	K(2)	0.198	63.4	0.183	39.3	-0.015	-24.1
36	M(8)	0.017	159.7	0.003	203.9	-0.014	44.2
37	MS(4)	0.071	342.2	0.075	356.8	0.004	14.6
CURRENT ACROSS PCD		DIR= 148		DIR= 145			
1	M(2)	0.166	92.8	0.117	92.1	-0.049	-0.7
2	S(2)	0.030	289.4	0.049	168.9	0.019	-120.5
3	N(2)	0.026	33.2	0.013	63.3	-0.013	30.1
4	K(1)	0.014	309.1	0.077	359.8	0.063	50.7
5	M(4)	0.028	181.2	0.042	208.5	0.014	27.3
6	O(1)	0.011	225.4	0.034	211.5	0.023	-13.9
7	M(6)	0.033	330.4	0.031	341.3	-0.002	10.9
8	MK(3)	0.028	14.7	0.028	357.5	0.000	17.2
9	S(4)	0.003	294.6	0.008	189.5	0.005	-105.1
10	MN(4)	0.000	0.0	0.023	169.5	0.000	0.0

11	NU(2)	0.000	0.0	0.013	71.2	0.000	0.0
12	S(6)	0.001	36.0	0.002	73.3	0.001	37.3
13	MU(2)	0.000	0.0	0.028	260.1	0.000	0.0
14	2N(2)	0.030	95.5	0.013	20.2	-0.017	-75.3
15	OO(1)	0.000	0.0	0.009	284.6	0.000	0.0
16	LAMBDA(2)	0.000	0.0	0.015	299.7	0.000	0.0
17	S(1)	0.000	0.0	0.146	141.0	0.000	0.0
18	M(1)	0.006	64.7	0.006	336.4	0.000	88.3
19	J(1)	0.004	137.0	0.004	147.9	0.000	10.9
20	MM	0.000	0.0	0.019	50.2	0.000	0.0
21	SSA	0.000	0.0	0.019	180.7	0.000	0.0
22	SA	0.000	0.0	0.000	0.0	0.000	0.0
23	MSF	0.000	0.0	0.023	77.7	0.000	0.0
24	MF	0.000	0.0	0.016	55.6	0.000	0.0
25	RHO(1)	0.000	0.0	0.007	13.2	0.000	0.0
26	Q(1)	0.003	97.5	0.002	191.9	-0.001	94.4
27	T(2)	0.034	317.3	0.022	193.3	-0.012	-124.0
28	R(2)	0.000	0.0	0.000	0.0	0.000	0.0
29	2Q(1)	0.004	211.9	0.006	150.4	0.002	-61.5
30	P(1)	0.005	285.1	0.078	282.6	0.073	-2.5
31	2SM(2)	0.000	0.0	0.008	215.7	0.000	0.0
32	M(3)	0.000	0.0	0.010	76.9	0.000	0.0
33	L(2)	0.010	89.2	0.007	234.3	-0.003	145.1
34	2MK(3)	0.000	0.0	0.008	49.8	0.000	0.0
35	K(2)	0.028	26.4	0.011	190.1	-0.017	163.7
36	M(8)	0.006	129.5	0.006	190.6	0.000	61.1
37	MS(4)	0.026	236.1	0.026	259.4	0.000	23.3